A KINETIC STUDY OF THE HARDENING REACTION OF A MODEL UNSATURATED POLYESTER RESIN.

by

IAN D. McMILLAN, B.Sc., A.R.I.C.

A thesis submitted to the University of Glasgow in fulfilment of the requirements for the degree of Doctor of Philosophy in the Faculty of Science.

The Royal College of Science and Technology,

Glasgow. February, 1957.

ProQuest LLC.
789 East Eisenhower Parkway
P.O. Box 1346
Ann Arbor, MI 48106 – 1346

ACKNOWLEDGEMENTS.

The author thanks Professor P.D. Ritchie for the interest he has displayed in this topic, and Dr. Manfred Gordon for his encouragement and advice on both practical and theoretical considerations throughout the course of this work.

Acknowledgement is made to the Senate of the University of Glasgow for permission to carry out the third year of this research at the College of Science and Technology, Manchester.

The author thanks Dr. A.C. Syme for performing a number of microhydrogenation determinations and Mr. Brian M. Grieveson for the ball rebound absorption experiments.

LIST OF PUBLICATIONS.

The bulk of the work in Sections 1 - 3 has been published in the following papers.

"Monomer Reactivity Ratios in a Model Unsaturated Polyester System". Gordon, Grieveson and McMillan, Journal of Polymer Science, volume 18, page 497, (1955).

"Classical Gelation in a Model Unsaturated Polyester Cross Polymerisation". Gordon, Grieveson and McMillan, Transactions of the Faraday Society, volume 52, page 1012, (1955).

TABLE OF CONTENTS.

Page

Section 4.

Kinetic Investigation of the Post-Gelation Rate Plot.

Section 5.

The Final State in the Polymerisation of MMA/PEF.

APPENDIX.

SUMMARY

The hardening mechanism of polyester "contact" resins is investigated with reference to a model system, methyl methacrylate/polyethylene fumarate (MMA/PEF). These two reagents are completely compatible without the addition of any complicating factors. The preparation and characterisation of the PEF resin are described.

The gelling characteristics of this system are investigated using a new viscometer-dilatometer (visco-dilatometer) technique for following polymer reactions The gel time and rate of polymerisation are investigated over a range of monomer feed ratio (PEF/MMA), catalyst concentration, temperature and degree of polymerisation of the initial polyester. Experimental points for the dependence of the gel time on the feed ratio and initial chain length are compared with theoretical curves for the gel time derived from classical gelation theory. The gel time is found constant regardless of the catalyst concentration because, on the classical gelation behaviour, an increase in polymerisation chain length cancels out the effect of the increase in rate on gelation. This constancy of the gel time confirms that the reaction is a simple copolymerisation. The effect of temperature on both the rate and gel time is in accordance with the classical gelation theory.

The direct determination of the main kinetic parameters, namely the reactivity ratios of the two monomers (MMA and PEF) is accomplished roughly by a technique of extracting the cross-copolymer

formed by solvent extraction of the gel. The "network" polymer obtained is analysed by a density technique, microanalysis and micro-hydrogenation to evaluate the monomer reactivity ratios. These techniques allow the bracketing of the values of r_M and r_F within a range which lies close to the values demanded by the theoretical treatment of the gel point.

The investigation is extended beyond the gel point where a sudden increase in the polymerisation rate is observed. This gel effect is explained by the assumption of a model where the initial reaction constants remain constant but changes in the effective radical concentrations due to diffusion control lead to a decrease in the termination reaction. This Trommsdorf effect at the gel point is only observed in systems where the primary polymerisation chain is sufficiently large.

Complete rate curves for the system, obtained by a combined dilatometer density tube technique are presented, showing the transition to the third stage of the reaction when both the initiation and propagation steps become subject to diffusion control. The polymerisation stops at approximately the same degree of cure or mobility irrespective of the feed ratio. A preliminary theory for the state of cure is put forward in terms of three parameters: the concentration of crosslinks, the concentration of residual methyl methocrylate, and the concentration of residual free polyethylene fumarate chains.

INTRODUCTION.

Unsaturated polyester resins have recently become established as constructional materials in the form of laminates, for such diverse purposes as the manufacture of car-bodies, ships up to the size of medium launches, and particularly in the aeroplane industry, where they are almost the only materials suitable for radome housings. Resins of this type consist, essentially, of an unsaturated polyester and an unsaturated monomer such as styrene or methyl methacrylate, in conjunction with a filling material of glass-fibre, cloth, paper or the like. The laminates formed in this way are strong, light, and have a high resistance to corrosion but their greatest advantage is the ease of fabrication. High pressure and elaborate moulding machines are not required. Laminates are prepared by spreading the filling material on a mould of the desired shape and spreading the materials on in successive layers at low temperatures and pressures.

Though resins of this type are now widely used, little is known about the mechanism of the hardening reaction. Their commercial development has not been fully exploited because of this lack of fundamental theoretical knowledge.

The polymerisation of these systems is characterised by an increase in viscosity of the solution, the point where the original solution first becomes solid being known as the gel point. Much of the fundamental work on the gelation and crosslinking of polymer systems is due to Flory, Stockmayer and Walling. Flory[1] first

postulated that the gel point in polyfunctional reactions occurs when the weight average molecular weight (and hence the viscosity) becomes infinite, i.e., when in an infinite sample of the reaction mixture the weight fraction of infinite networks first exceeds zero. Flory derived a statistical theory for this critical condition for polycondensations, in terms of the fraction of functionalities reacted. This thoery was extended by Stockmayer,[2] who showed that the equation could be applied to polyaddition chain reactions. Walling[3] abandoned the simple classical theory for polyadditions and postulated a diffusion control theory of gelation to obtain agreement for the gel points predicted from the classical theory with his experimental values.

The present work is an attempt to bring fundamental kinetic theories to bear on the polymerisation of polyester resins, by investigating the gelling behaviour with increase of viscosity and finding what effect the viscosity has on the kinetic steps as the reaction proceeds.

In order to investigate a complicated system of this type the relatively simple model system, methyl methacrylate/polyethylene fumarate has been chosen. These two reagents are compatible with each other in all proportions so that no additional solvents or conditioners have to be added as in commercial resins (e.g. styrene and fumarate are not wholly compatible and a solvent or other comonomer has to be added), so additional complicating factors are avoided. Though very little fundamental work on the reaction mechanism of this type of system has been published, a short introductory investigation

of the topic by the writer[4] showed that the gel point was independent of the catalyst concentration. This was interpreted in terms of a copolymerisation chain reaction between the methacrylate and fumarate unsaturation.

Experimental work involving the investigation and measurement of kinetic parameters should, ideally, be carried out in high vacuum on materials of a high state of purity. The attainment of this ideal in the present case is not possible since the polyester is a solid at room temperature and is not homogeneous. All starting meterials were purified as well as possible and the reasonable reproducibility of the results obtained justifies the treatment by classical kinetic theories.

SECTION 1.

Preparation and Characterisation of Polyethylene Fumarate.

1.1. Introduction. In order that the results of polymerisations with polyethylene fumarate can be interpreted and verified it is necessary to give a full description of the preparation and characterisation of the resin, discussing the possible presence and magnitude of various complicating factors.

The method of preparing polyethylene fumarate (PEF) was developed, before its usefulness as a crosslinker in polymerisations was realised, mainly through the work of Carothers and Arvin[5] during their investigation of the fibre forming properties of various polycondensates from acid anhydrides and glycols. e.g.,

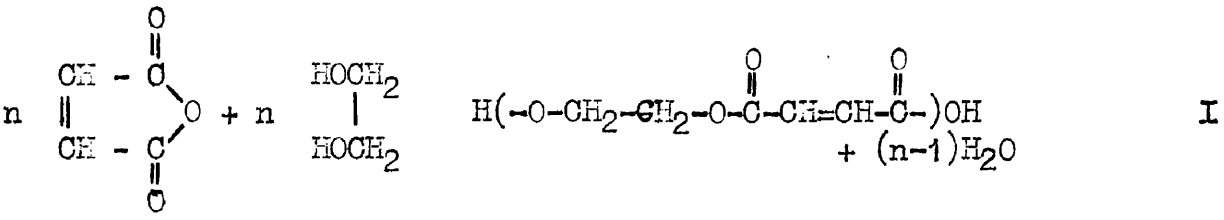

I

These and subsequent workers did not realise that the isomerisation of maleic to fumaric unsaturation may occur during the polycondensation reaction and it was only comparatively recently that Batzer and Mohr[6] detected this isomerisation and evolved a laboratory method for avoiding it.

Apart from the question of geometrical isomerisation the characterisation of polyethylene fumarate is centred on the correct weight-average number DP_w of fumarate double bonds per PEF molecule.

Provided that the resin is prepared from an equimolar mixture of glycol and anhydride, and consists of linear molecules only as illustrated by I, the distribution law of chain lengths may be taken to follow Flory's statistical equation for a random bifunctional condensation[7]:

$$w_n = n(1-p)^2 p^{n-1} \qquad (1)$$

where p is the fraction of carboxyls esterified and w_n is the weight fraction of n-mer. For this distribution, the weight-average DP_w and the number-average DP_n are given by:

$$DP_w = (1+p)/(1-p) = 2DP_n - 1 \qquad (2)$$

Three complicating factors that may cause deviations of the structure of the condensation polymer from the state defined in eqn.(1) must be taken into account. These are, departures from strictly equimolar composition, the presence of cyclic species in the resin, and the presence of crosslinked molecules arising from the latent functionalities, i.e., the fumarate unsaturation, in the condensation polymer. The extent to which these possible deviations occur is discussed.

1.2. Preparation of polyethylene fumarate - polycondensation reaction.

The polyester was prepared from a mixture of maleic anhydride, purified by two recrystallisations from chloroform, and a 5% molar excess of ethylene glycol purified by distillation in a

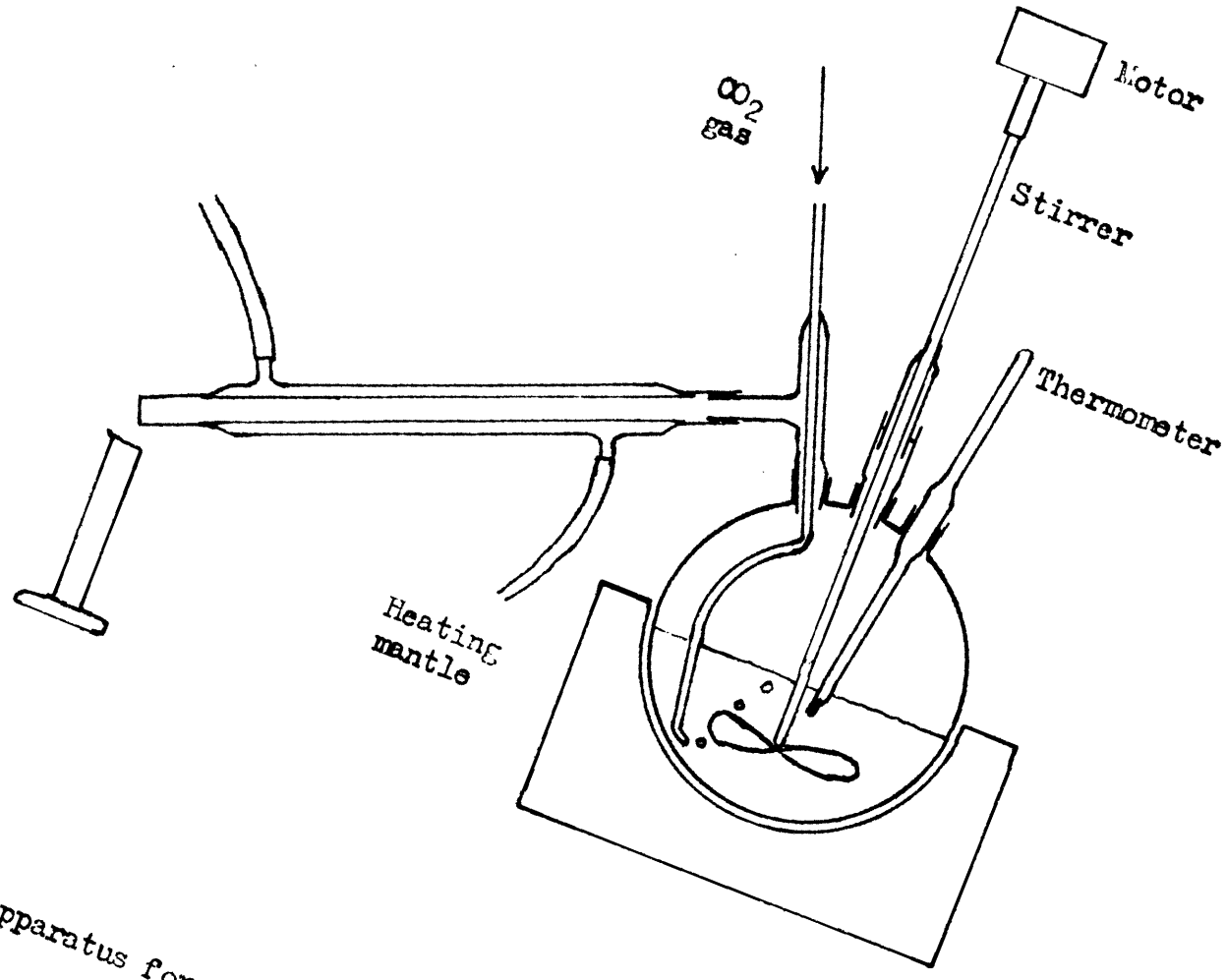

Fig. 1.

Apparatus for preparation of polyethylene fumarate.

current of carbon dioxide at approximately 20mm. H_g. pressure.

The two compounds, typically 3.23 moles of maleic anhydride and 3.39 moles of ethylene glycol, were mixed thoroughly in a beaker to a viscous paste then transferred to the reaction vessel (see fig.1). This consisted of a two litre round-bottomed flask with three necks. A mercury seal stirrer was placed in the centre neck with a thermometer and a still-head plus condenser in the side necks. A glass bubbler tube connected to a reservoir of solid carbon dioxide was introduced down the inside of the still-head allowing the CO_2 gas to bubble through the reaction mixture, the cold bubble tube also acting as an auxiliary condenser.

The flask was heated in an electric mantle, the temperature of the mixture being rapidly raised to and maintained at $195 \pm 5^{\circ}C$.

The extent of polymerisation was followed by determining the acid number of small test samples, stock samples being withdrawn from the reaction vessel as required and stored in brown bottles. In later condensation runs the reaction was followed using the rough rate curve in fig.2.

Under the storage conditions employed (in brown bottles in a refrigerator) it was found that over a 12-month period, no measurable change in the DP had occurred.

1.3. Physical properties of polyethylene fumarate resins. The resin samples prepared were glass clear, almost colourless, and ranged from a syrupy consistency ($DP_{ne} = 3$) to pitch-like consistency ($DP_{ne} = 9$).

Materials of a sticky syrupy nature like this present difficulties in handling since they can neither be poured like a liquid nor handled as a solid. It was found that the best method for handling these resins was to freeze them to the glassy state with solid CO_2 when they could be chipped or powdered.

1.3.1. Molecular weight determination.

a) End-group analysis. The acid number of each resin was found by titrating an ice-cold solution of about 0.2gm. resin in 10ml. of A.R. dioxan with decinormal sodium hydroxide which had been freed from carbonate by precipitation with barium chloride. The indicator used was phenolphthalein. The procedure adopted was to run in alkali, till near the end point, the addition of one drop gave a colouration lasting about one second. The end point was adjudged to have been reached when the addition of one further drop of alkali gave a red colouration lasting for at least 5 seconds. Subsequent addition of alkali gave a red colouration lasting for about 20 seconds. Refluxing of the dioxan solution before titration to expel any dissolved CO_2 did not alter the end point. The acid number found by this method was reproducible to $\pm$ 2%, as satisfactory as by the alternative method of titrating a chloroform solution with alcholic potash.

The end-group molecular weight and the number average degree of polymerisation DP_{ne} were calculated from the acid number according to the relation:

$$142\ DP_{ne} = \left(\frac{5600}{\text{acid number}} \right) - 18 \qquad (3)$$

All DP_{ne} values quoted are calculated from the average of three titrations.

b.) Cyroscopic molecular weight determinations were made using A.R. dioxan as solvent in a standard Beckmann apparatus. The freezing point depression constant k for dioxan was determined using two reference compounds, benzoic acid (k found = 4.565°C l.mole^{-1}) and p - toluidine (k found = 4.670°C l.mole^{-1}). Both these reference compounds were purified by two recrystallisations and the mean value k = 4.617°C l.mole^{-1} (± 1.5 %) was used to calculate all cryoscopic molecular weights and hence DP_n values. All the DP_n values quoted are averages of three determinations.

1.3.2. Specific volume determinations at 300°K. The densities of the resins were determined in a pyknometer of about 2.25 ml. capacity. The pyknometer was filled with frozen powdered resin and degassed under approximately 20mm. Hg. pressure at 100°C. Since the very high viscosity made complete filling difficult, only sufficient resin to fill the pyknometer about three-quarters full was used, together with distilled water as a confining liquid.

Results are graphed in fig.3. Owing to the difficulty of the procedure, only resin F was done in duplicate (1.3478 and 1.3472 gm/ml).

1.3.3. Refractive index measurement. Refractive indices of the resins were measured with an Abbé refractometer thermostatted at 300°K. The refractive index for the sodium D line for distilled water was

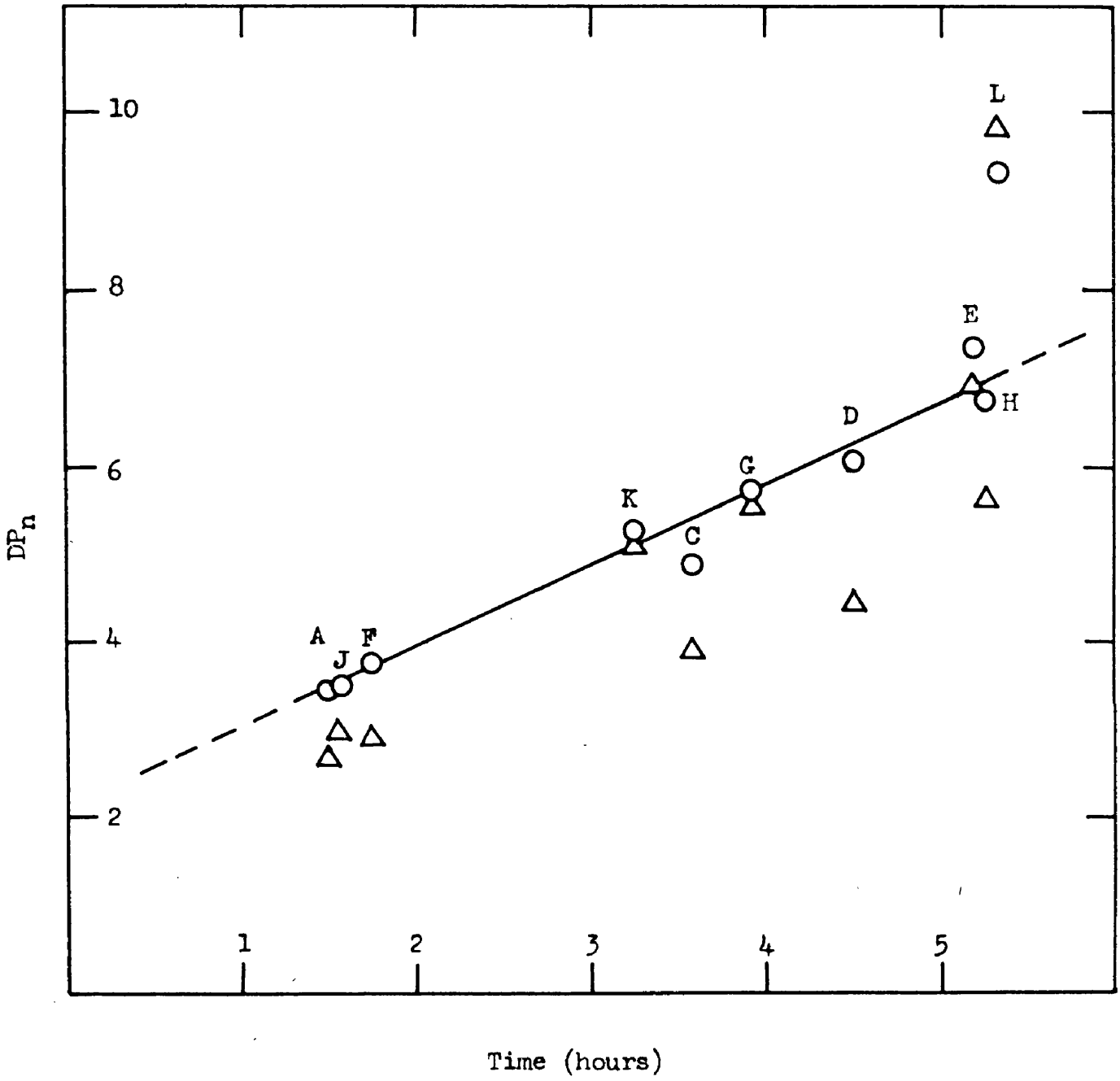

Figure 2. Rough rate curve for polyethylene fumarate condensation at 195°C.

The results shown were obtained from four different runs; A, C-E, F-H, and J-L.

End group DP_n ○ Cryoscopic DP_n △

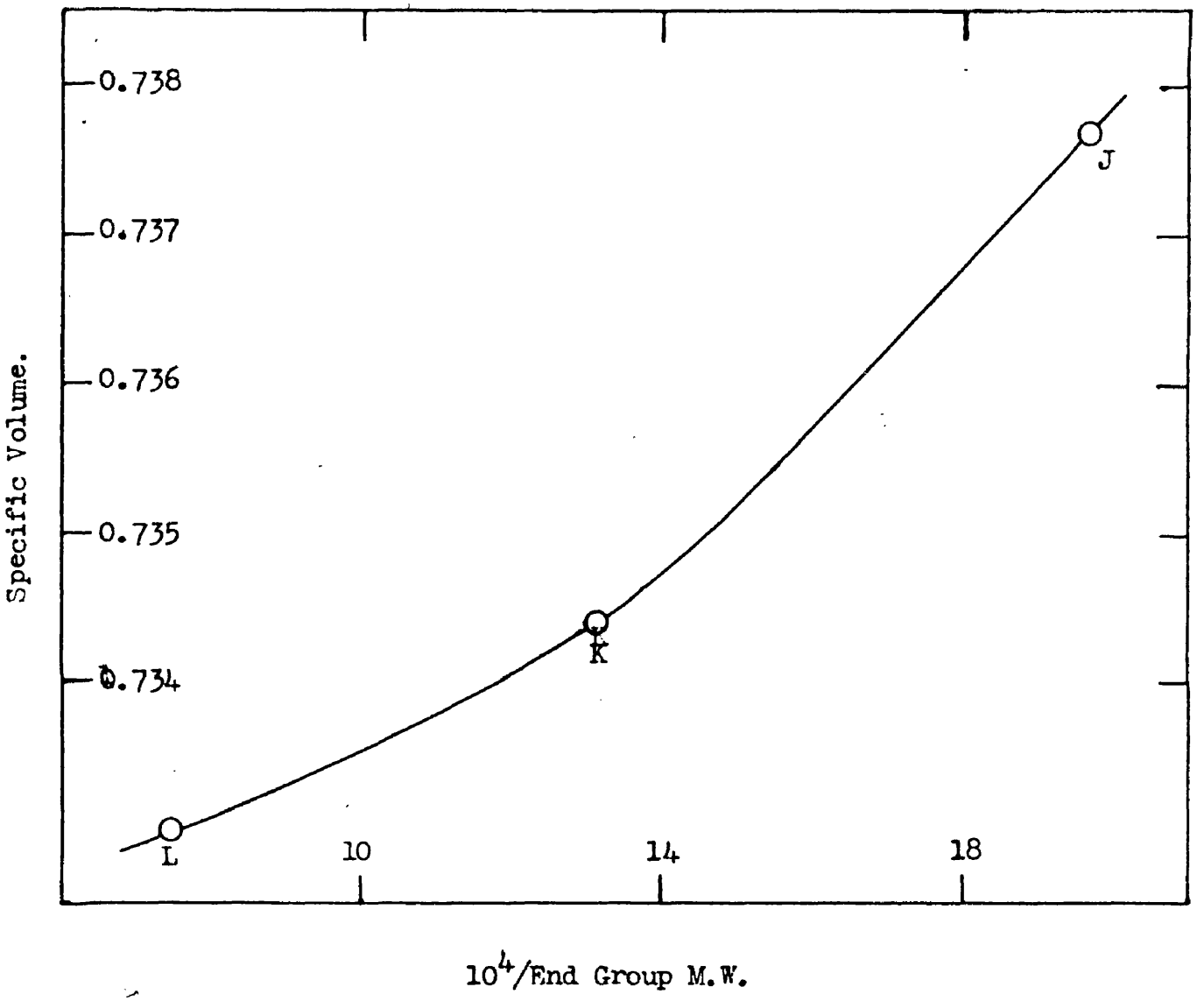

Figure 3. Pyknometric specific volumes (300°K.) vs. reciprocal (end-group) molecular weights of polyethylene fumarate, for condensation run J-L.

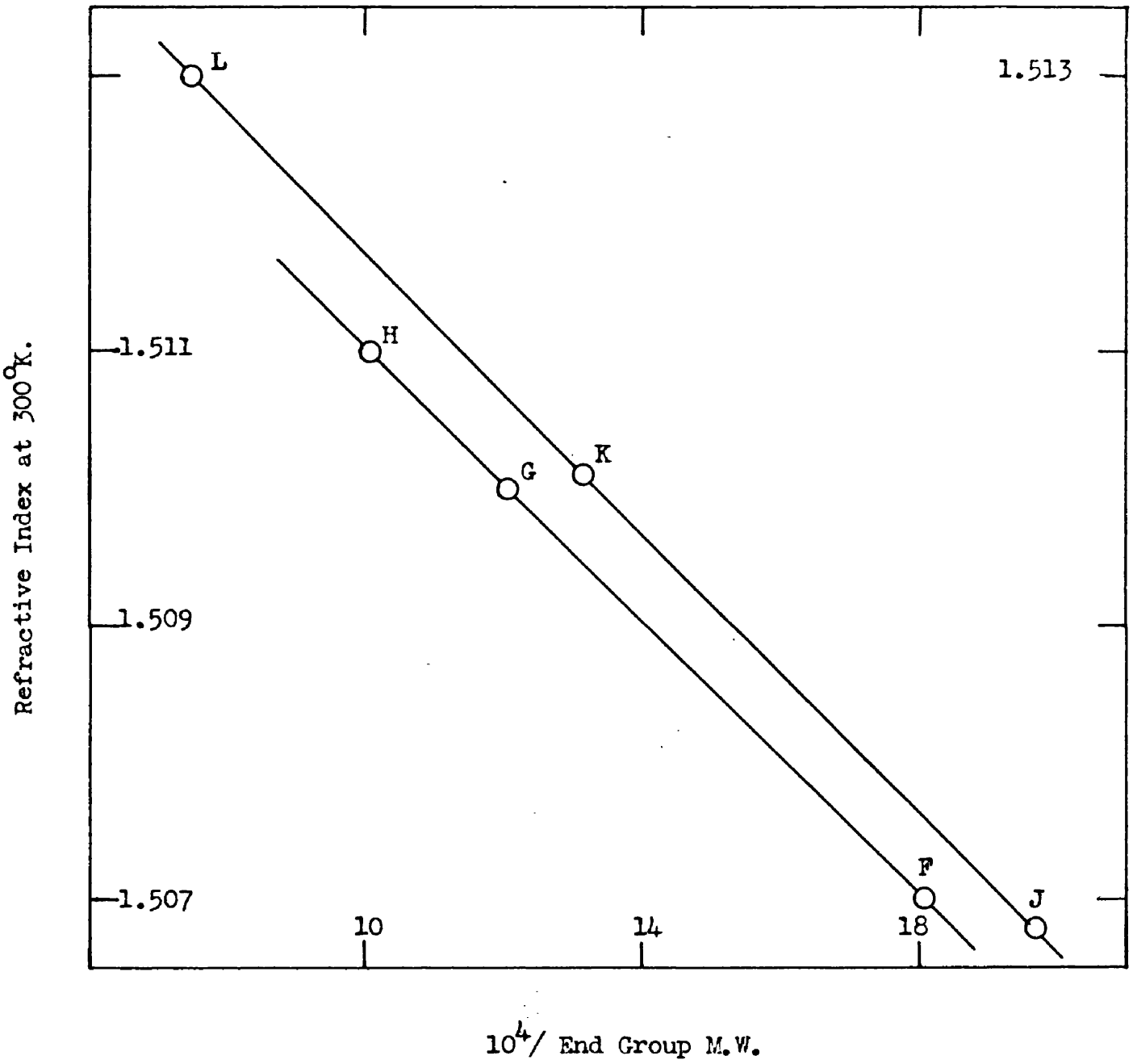

Figure 4. Refractive index for sodium D line (at 300°K.) vs. reciprocal (end-group) molecular weight of polyethylene fumarate, for condensation runs F-H, and J-L.

set at 1.33235. Small samples were smeared on the prism with a hot spatula and five readings were taken for each sample. Results are graphed in fig.4.

All DP_{ne}, DP_n, density and refractive index values found are tabulated in the Appendix (table 20).

1.4. Rate and reproducibility of polycondensation. Without attempting a critical kinetic analysis of the polycondensation reaction it is nevertheless desirable to establish the reproducibility and rough kinetic behaviour of the formation of PEF. The results of four separate condensation runs, namely resins A, B-E, F-H and J-L are plotted in fig.2. showing a sufficiently smooth graph of DP versus reaction time to justify the claim to reasonable reproducibility of the reaction. This reproducibility is probably not critically dependent on the purity of the starting materials since the ethylene glycol and maleic anhydride used in condensation run 4 (J-L) were not purified by the usual procedure of distillation and recrystallisation. From fig 2 it is seen that, after a rapid initial reaction, the DP varies about linearly with time in the range $3 < DP_n < 6$, for both end-group and cryoscopic determinations. This linearity implies that in this range the reaction is kinetically of the second order since the DP varies inversely as the concentration of unreacted functionalities. Flory[8] has shown that in the polycondensation of saturated dicarboxylic acids a third order reaction occurs, in which the DP varies linearly with $(\text{time})^{\frac{1}{2}}$. However, in the absence of more refined kinetic measurements of this system it is not possible to discuss the

condensation mechanism more fully.

The reproducibility of the condensation reactions finds added confirmation from refractive index and density measurements. Fig.3 shows that for condensation run 4 (J-L) the specific volumes vary smoothly with DP_{ne}. The refractive indices vary linearly with DP_{ne} (fig.4) and in addition are seen to be gratifyingly reproducible from run to run, for though there is a real parallel displacement it may be regarded as insignificantly small.

A comparison of measured DP's and those interpolated from figs.2-4 is made in table 1 with respect to condensation run 5(N-P).

Table 1

Comparison of measured and interpolated DP's.

Resin	DP_{ne}			DP_{ne}	DP_n
	Rate curve	Density curve	R.I. curve	End-group	Cryoscopic
N	3.5	3.7	3.98	5.05	3.29
P	5.05	5.0	5.65	8.61	5.02

Table 1 shows that a mean value of $DP_{ne} = 3.73$ is obtained for resin N by interpolation compared with the actual measured value of 5.05. The high DP_{ne} values measured for resins N and P are consistent with a shortage of carboxylic end-groups, perhaps partly caused by the formation of ring compounds (see Section 1.6).

On the whole, the evidence contained in figs. 2-4 suggests that over the range studied the formation of the polyethylene fumarate resins is reasonably reproducible with the resins exhibiting an

intelligible gradation of physical properties.

1.5. Equimolarity of the resin. Under the conditions employed for the preparation of PEF, water of condensation is removed from the system by distillation in a current of inert CO_2 gas. Unfortunately the constituents of the reaction mixture, particularly the lower boiling glycol, are also liable to be lost by distillation. In an effort to compensate for this loss and obtain a final polymer which

Table 2.

Mass balance of resin L.

	Moles.
Maleic anhydride used	3.23
Glycol used	3.39
Distillate (46ml. collected in 320 min.)	
Water calculated	2.33
Water found (uncorrected for evaporation losses, etc.)	2.05
Glycol found	0.0643
Acid (calculated as fumaric acid)	0.0438
Mole ratio r of glycol units in polymer, calculated from mass balance.	$= \frac{3.23 - 0.0438}{3.39 - 0.0643}$
	$= 0.958$

is as nearly as possible equimolar, (i.e. containing exactly one carboxyl and one hydroxyl group per number average molecule as in I), a 5% molar excess of ethylene glycol was used over the maleic anhydride as recommended by Carothers and Arvin[5]. The effect of this on the

molarity of the product can be seen from a rough mass balance from condensation run 4, resin L.

The acid dissolved in the distillate was assumed to be fumaric (or maleic) and was determined by titrating an aliquote portion of the distillate with N/20 caustic soda and phenolphthalein indicator. The glycol was estimated from the density of the distillate (1.038gm/ml) on the assumption that it contained only water, fumaric acid and glycol. This was done by preparing two solutions of 0.0438 moles maleic anhydride in 46ml. of water and in 46ml. of ethylene glycol. By interpolating between the densities of these two solutions (1.030gm/ml and 1.1293gm/ml respectively) it was calculated that the distillate contained 8.4% glycol.

Flory[8] has derived an equation for the error E in calculating DP_{ne}, on the assumption that the mole ratio acid/glycol r = 1, for small deviations of the true r from unity, thus:

$$E = \frac{(1 - r)}{2} \times DP_{ne} \qquad (4)$$

Accepting the result of r = 0.958, the error in the DP_{ne} computed (table 3) would amount to almost 15% for resin L (i.e. the highest DP made). For resin G, the highest molecular weight resin used in this work, the DP_{ne} value would be only 9% high. Finally, for resin J, the lowest molecular weight used, (42ml. distillate collected in 93 min.), the error in DP_{ne} would amount to under 6%.

It seems questionable whether such a small correction can

be reliably based on the analysis described, and throughout this work, true equimolarity (r = 1) of the resin is assumed.

1.6. Sidereactions producing rings and crosslinks. Jacobson and Stockmayer have shown by viscosity measurements that ring formation can occur[9] when decamethylene glycol condenses with a saturated dicarboxylic acid. Again, the monomeric ring caprolactam can be extracted from Perlon polyamide in proportions up to 15%[10] and in attempts to synthesise polyethylene isophthalate the cyclic dimer of ethylene isophthalate has been isolated.[11] Moreover, crosslinking and even gelation are known to present difficulties in condensing glycols with unsaturated dicarboxylic acids in both an industrial and laboratory scale. In a preliminary condensation run, when the temperature of the reaction mixture was allowed to rise to 210-220°C, the mixture became dark yellow in colour and set to a solid mass in 45 minutes.

The possibility of ring formation and crosslinking of the PEF therefore cannot be ignored. To investigate these two points cryoscopic and end-group degrees of polymerisation (DP_n and DP_{ne}) are compared. For the purely linear polycondensation polymer I, prepared from equimolar proportions of maleic anhydride and ethylene glycol, these two degrees should coincide. Crosslinks due to the reaction of double bonds clearly raise the DP_n, while they do not affect the concentration of terminal carboxyl and hence leave DP_{ne} unaffected. Conversely, ignoring minute changes due to the weight

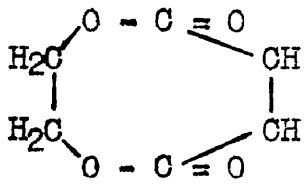

II

of water eliminated, cyclisation leading to species such as II uses up carboxyls and hence raises the DP_{ne} while the cryoscopic average DP_n is not affected.

Table 3.

Comparison of number-averages and the weight fraction c_1 of cycles.

Resin	DP_{ne}	DP_n	c_1
A	3.43	2.66	0.084
B	3.75	2.94	0.073
C	4.88	3.90	0.051
D	6.04	4.42	0.060
E	7.38	6.88	0.010
F	3.78	2.90	0.080
G	5.73	5.58	0.005
H	6.68	5.65	0.027
J	3.46	2.93	0.053
K	5.25	5.09	0.006
L	9.32	9.81	-0.005
N	5.05	3.29	0.106
P	8.61	5.02	0.083

Values from five condensation runs are analysed in table 3. It is seen that the divergences between DP_{ne} and DP_n never seriously exceed

one unit (with the exception of N and P) and are mostly quite small. It is most unlikely that the agreement achieved arises through cancellation of large opposing deviations attributable to simultaneous cyclisation and crosslinking. The DP_{ne} is generally slightly larger than DP_n, which points to the possible occurrence of some cyclisation. Assuming that crosslinking is absent, that the only nonlinear species present is the monomeric ring II, and that the linear species is of the general formula I, the weight fraction c_1 of cyclic monomer may be calculated from the following scheme.

The appropriate equations for computing the number and weight fractions π_1 and c_1 of monomeric rings, the number and weight averages DP_{nch} and DP_{wch} of the chains I present, and finally the DP_w of all species (cycles plus chains), are derived as follows.

The weight and number fractions are related to the cryoscopic DP_n thus,

$$c_1 = \pi_1 / DP_n \tag{5}$$

The end-group average DP_{ne} is related to DP_{nch},

$$DP_{ne} = DP_{nch}/(1 - c_1) \tag{6}$$

The cryoscopic average is compounded from the average DP_{nch} of the chains and that of the cycles (which is merely unity) thus,

$$DP_n = (1 - \pi_1)\, DP_{nch} + \pi_1 \tag{7}$$

From equations (5, 6 and 7) it is then possible to express DP_{nch} and c_1 as functions of the measured averages:

$$DP_{nch} = 1 + (DP_{ne}(DP_n - 1)/DP_n) \tag{8}$$

$$c_1 = \frac{1}{DP_n} - \frac{1}{DP_{ne}} \tag{9}$$

Thus the weight fraction of cyclic monomer is reduced to a simple expression involving the measured cryoscopic and end-group DP's, to give the values tabulated in table 3. It is seen that c_1 never exceeds 10% (excepting N and P) and it is also significant that it tends to decrease with increasing reaction progress. This runs directly counter to the statistical theory of cyclisation[5] which predicts an increase of c_1 with increasing reaction. A very slight rate of crosslinking is possibly responsible for a progressive masking of the effect of rings on the DP. The resin L of highest DP (fig.2.) was not completely miscible with methyl methacrylate, possibly in consequence of some crosslinks.

Jacobson and Stockmayer's statistical theory leads to the conclusion that the weight fraction c_1 of monomeric ring predominates strongly and makes up the bulk of the total weight fraction Σc_x of cyclic material. The treatment above was simplified by considering only monomer ring formation. The assumption of a cyclic dimer, replacing the cyclic monomer II, would lead to a weight fraction $c_2 = 2c_1$.

Because of the assumptions and experimental errors involved, the calculation described above is far from exact, and serves only to show the small part played by cyclic structures in the resin. On the whole, the degree of agreement achieved between the DP_n and DP_{ne} and the analysis embodied in table 3 justify the assumption in this work, that the polyethylene fumarate resin employed may be treated as a purely linear polymer with a weight average derivable

from end-group analysis with the aid of eqn.(2).

1. 7. Cis-trans isomerisation. The isomerisation of maleic to fumaric unsaturation during the polycondensation of maleic anhydride and ethylene glycol was detected only recently by the work of Batzer and Mohr.

Mr. A. Pajaczkowski and Mr. B.M. Grieveson[12] [13] of the Royal Technical College, Glasgow, investigated the isomerisation of these resins and showed by infra-red spectroscopy that the conversion of cis (maleate) to trans (fumarate) bonds is substantially complete before the number average DP has reached three. While this investigation was in progress, the paper by Feuer and coworkers[14] became available, which reaches the same conclusion by polarographic and other means.

Experimental work by Grieveson[13] on the comparison of resins prepared from ethylene glycol and maleic anhydride or fumaric acid further supports the assumption that these resins can be treated as 100% polyethylene fumarate. The subject is discussed further in Section 2. 4. 9.

SECTION 2.

Investigation of the Gelation Mechanism of the Methyl Methacrylate/Polyethylene Fumarate System.

2.1. Introduction. The gel point of the MMA/PEF system may be interpreted in terms of a theoretical equation (eqn.15 Section 2.4.1.) derived from the classical network theory of gelation, assuming a simple copolymerisation reaction between the MMA and PEF. This equation predicts that with crosslinking reagents of high functionality (such as PEF) the gel point is reached at low conversion and the gel time varies inversely with the functionality of the crosslinking reagent. A general kinetic scheme is derived from the classical theory using the copolymerisation equation, so that the gel time is equated directly with the kinetic parameters for the system. The theory suggests that the gel time should be independent of the nature and concentration of the catalyst and should exhibit linearity with reciprocal fumarate concentration at high fumarate concentrations. Also, the energy of activation of gelation is predicted to be independent of both the feed ratio and catalyst concentration.

The gel time and rate of polymerisation were investigated as a function of monomer feed ratio, the molecular weight of the PEF condensation chains, catalyst concentration and reaction temperature. The polymerisation rates and viscosity were followed by means of a combined viscometer-dilatomer or viscodilatometer.

The experimental and theoretical results are all in satisfactory agreement. The gel time varies with monomer feed ratio as predicted (fig.9) the curves becoming asymptotic at low fumarate concentrations and the asymptotic slopes lie in the correct theoretical ratio. This figure is an absolute test for the classical network theory of gelation. The parameters used for the fit of the theoretical curve are comparable with directly measured values and those found in the literature. The theory is further confirmed since both the gel time and activation energy are independent of the catalyst concentration.

The agreement between theory and experiment is found not to differ seriously. Such deviations as exist are not surprising considering the number of assumptions involved in deriving the kinetic scheme. For example, termination by radicalcombination is assumed and if radical disproportionation was used would differ by a factor of 1.33. Also the primary polymerisation chain lengths of MMA/PEF co-polymer are assumed to be identical with that of pure MMA. Generally, the absolute verification of the gel point theory to polyadditions of high functionality cannot be expected to a factor much less than three.

2.2. Experimental.

2.2.1. Materials.

a.) Polyethylene fumarate. The preparation and characterisation of the preformed condensation polymer chains has been fully described in the preceding section.

b.) Monomeric methyl methacrylate. This was the commercial brand of Kallodoc liquid supplied by Imperial Chemical Industries Ltd. The monomer was purified in the following manner.

Approximately one litre of solution was successively washed with caustic soda solution in a separating funnel until the rejected aqueous phase was colourless. It was next washed at least three times with distilled water then dried by the addition of anhydrous calcium chloride. Following this the solution was distilled twice at approximately 20mm.Hg. pressure with CO_2 gas being bubbled through the solution. The middle fraction of distillate was retained and stored in a stoppered brown bottle at $0^{o}C$. This purification is insufficient to free the monomer from traces of catalysts and inhibitors but more rigorous procedures are not justified, because the PEF component admixed with the MMA cannot be highly purified.

c.) Methyl ethyl ketone peroxide was used throughout the work as "catalyst" or initiator. This was supplied by Bakelite Ltd., as a 60% solution in dimethyl phthalate, as marketed for the hardening of commercial unsaturated polyester resins. The peroxide concentration was checked periodically [13] by iodimetric titration, due allowance being made for any small decrease in peroxide content on storage when dispensing the catalyst.

2.2.2. Preparation of the reaction solution. Polyethylene fumarate (PEF) and methyl methacrylate (MMA) were found to be compatible in all proportions. Monomer feed ratios R were based on the ratio (PEF/MMA) of the double bonds of each species; e.g. a solution of feed ratio

R = 1 was one in which the moles of fumarate repeat units and methyl methacrylate was equal, allowing for PEF end-groups.

$$\text{Feed ratio R} = \frac{\text{Wt.(PEF)} \times DP_{ne} \times 100}{\text{Wt.(MMA)} \times \text{M.W.(PEF)}} \qquad (10)$$

A quantity of PEF was weighed in a weighing bottle and the calculated quantity of MMA added dropwise from a weighing burette. It was necessary to warm the mixture slightly and stir with a glass rod to dissolve the PEF completely.

The reaction solution was prepared immediately before use in all the experiments in this section.

The calculated weight of MEK catalyst was added dropwise from a micro-pipette or weighing burette immediately before the start of the experiment.

2.2.3. Viscodilatometer measurements of rates and gel times. A detailed account of the development, manufacture and use of the viscodilatometer is given elsewhere [13] [15] but the use of the instrument will now be summarised. In the instrument, viscosity is measured in terms of the rate of flow of a column of resin through a sintered glass plug acting as a resistance.

The glass viscodilatometer is seen in fig.5., together with the brass stand which allows the angular setting of the instrument to be varied. The instrument consists of a dilatometer bulb, usually of about 2ml. volume, and two capillary tubes, in one of which resides a sintered glass plug. The capillary used here is 1.5mm. precision

bore tubing about 8cm. long for each limb. The plug is made near the end of one limb by sintering crushed Pyrex glass till the required porosity is attained. The plugs used in this work had an average pore size of 90 microns, determined as described by British Standard Specification 1752:1952. The two capillary limbs are attached to the central bulb, care being taken that the two pieces of tubing are collinear. The viscodilatometer is calibrated for volume by measuring the lengths of columns of known weights of distilled water at 20°C and similarly for hydrodynamic resistance by measuring the rate of flow of water. It is filled to the desired degree by sucking up the liquid slowly with a rubber syringe attached to one arm, ensuring that all air bubbles are excluded from the plug. The ends of the two tubes are joined by means of glass tubing and rubber connections as shown. The viscodilatometer is clamped to the brass disc of the stand on top of a calibrated glass scale engraved in 1/3mm. The liquid volume at any time t is deduced from the positions on the scale, read with a magnifying glass, of the menisci in each capillary. If the brass disc is set so that the capillaries make an angle α (e.g. 5 - 20°) with the horizontal, gravity flow causes movement of both menisci and the sintered glass plug acts as a hydrodynamic resistance. A considerable range of viscosities can obviously be covered in one viscodilatometer by adjusting the angular setting.

2.2.4. Use of the viscodilatometer. The use of the viscodilatometer in following the course of the polymerisation of MMA/PEF is seen in fig.6 for the case of resin G, R = 0.5, 2.09% MEK catalyst at 62°C.

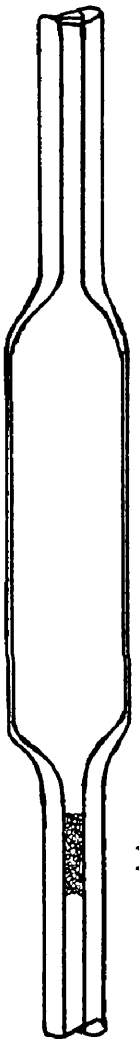

Detail of the
Viscodilatometer

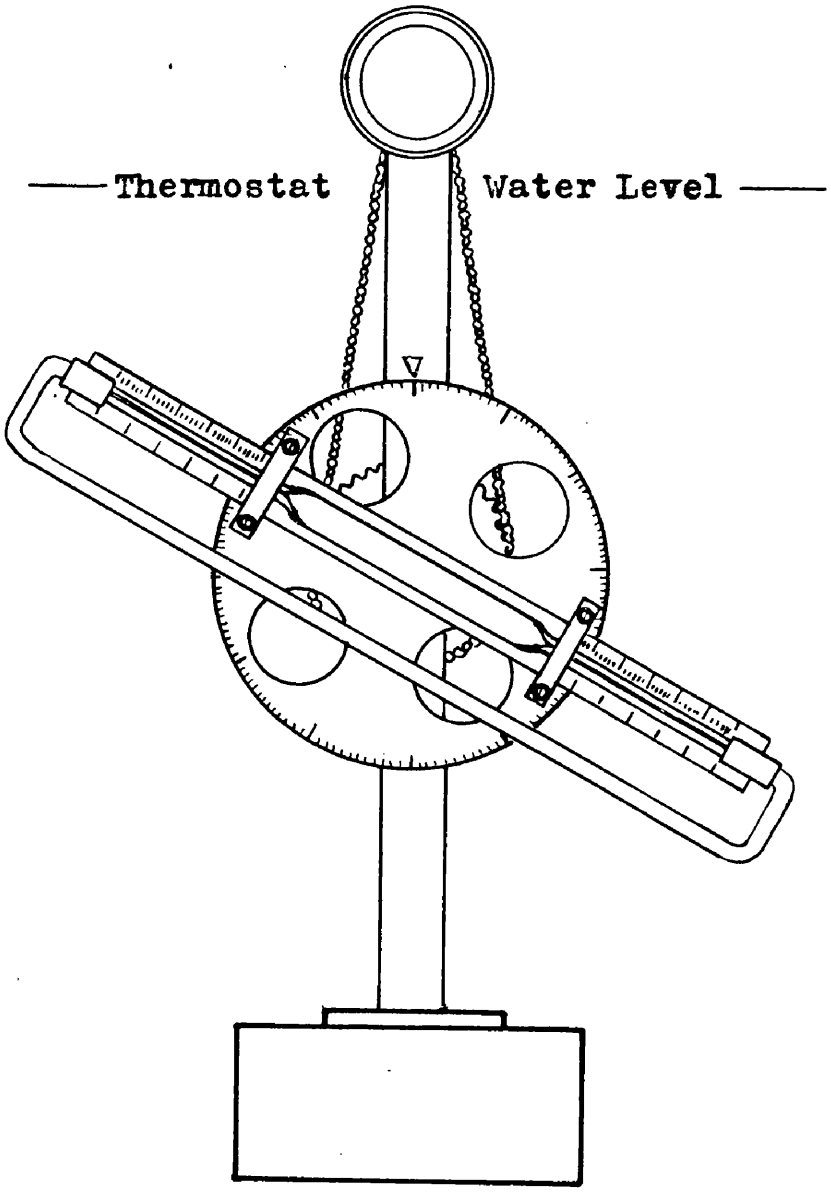

A viscodilatometer
mounted on its stand.

Figure 5 .

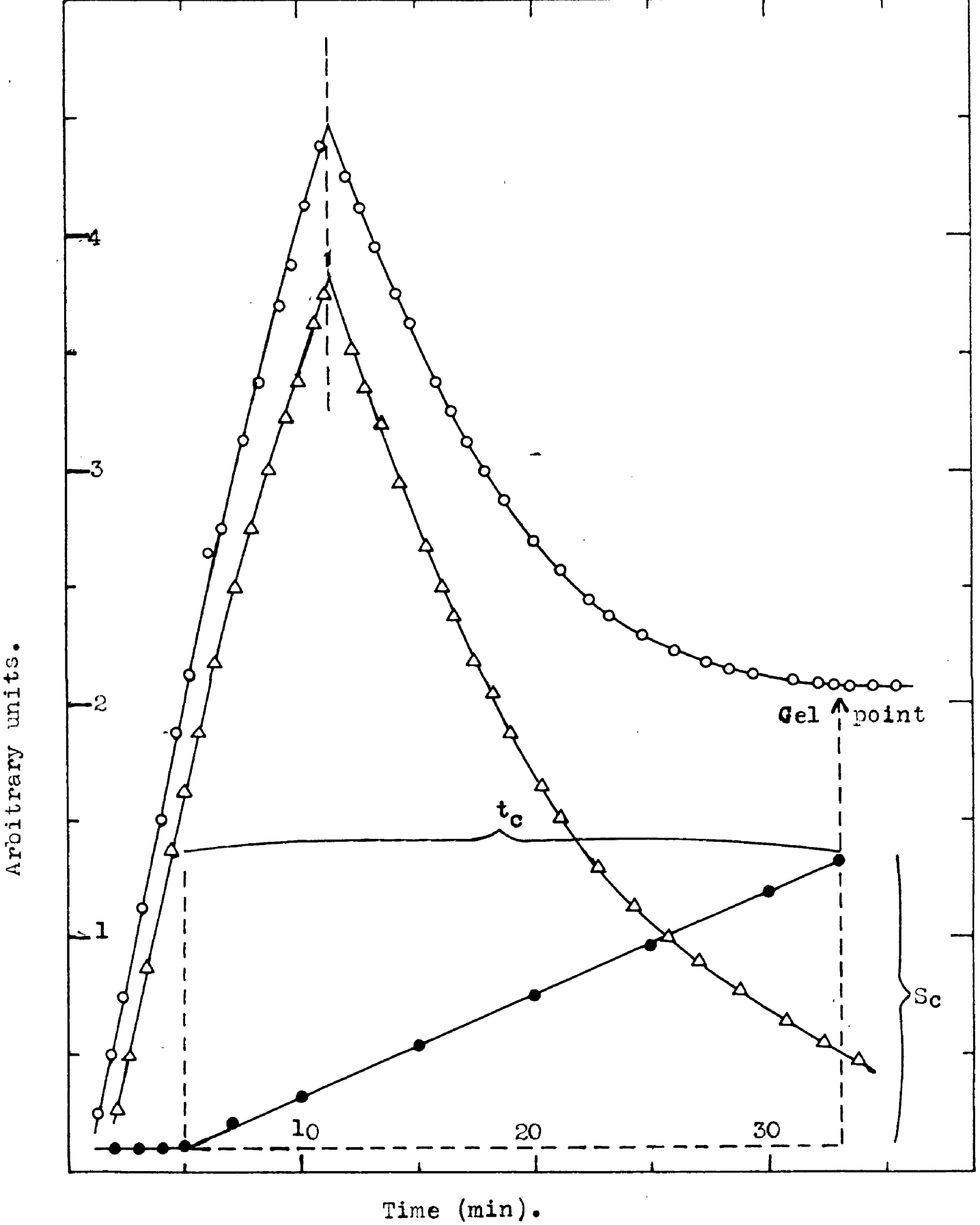

Figure 6 . Viscodilatometer run with resin G; 62°C, 2 % [illegible]; R = 0.5. Top (o): flow curve of meniscus in plug capillary; middle (Δ): flow curve of meniscus in free capillary; bottom (●): difference curve (rate plot).
The gel time t_c (29 min) and the critical shrinkage (S_c) are found as shown. The critical conversion β_c = 0.055 in this run.

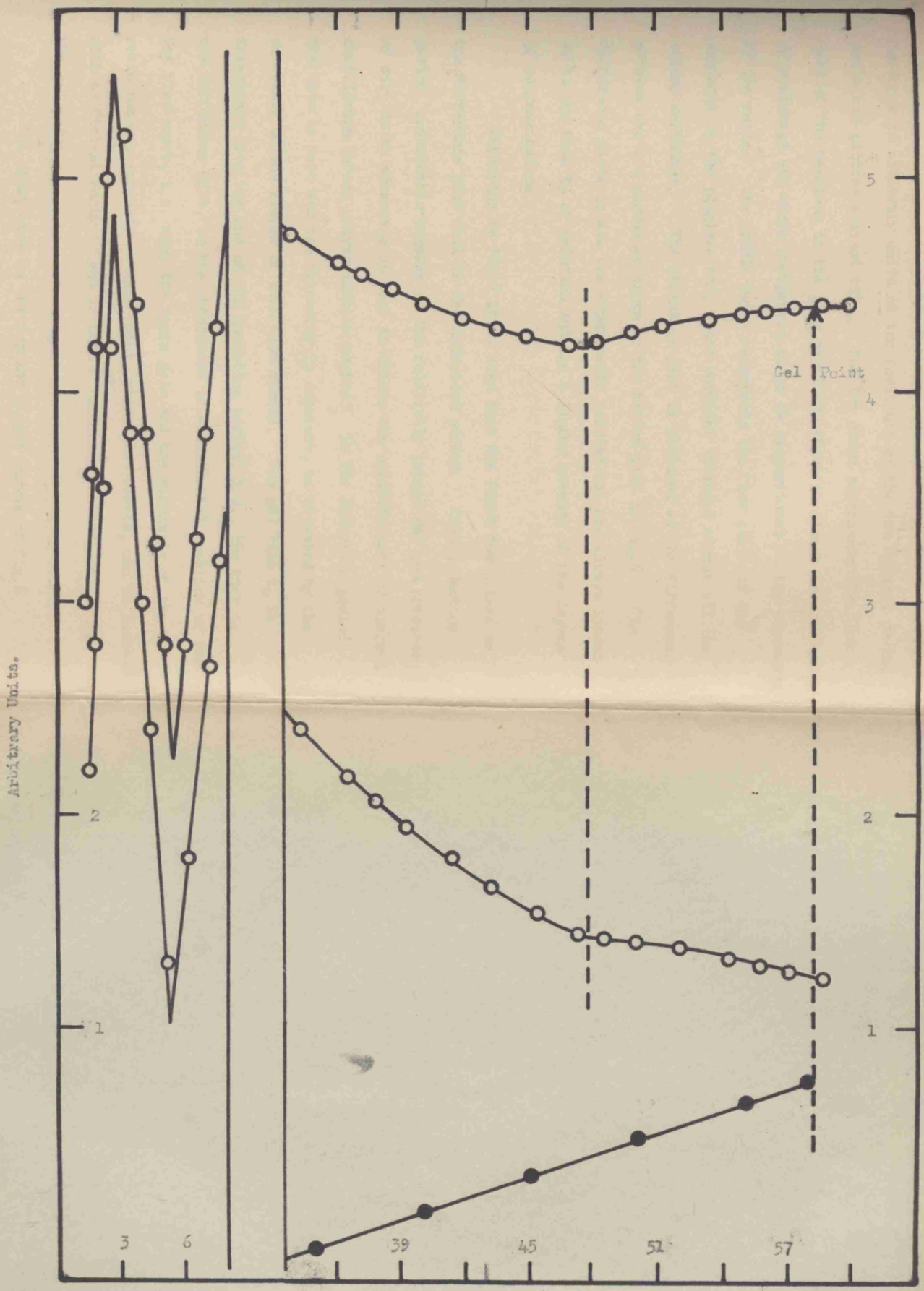

Fig.7. Early and late part of run at low R, (resin G, R = 0.2, Temp = 62.0° C). Even at this high critical conversion, (β_c = 0.108, t_c = 53 min) the gel point is clearly defined.

Readings in arbitrary units of the positions of the two menisci on the scale are plotted against time. The top curve represents the flow rate of the meniscus in the plug capillary which is almost independent of shrinkage and whose reciprocal slope is proportional to the viscosity of the resin. The middle curve represents the flow curve of the meniscus in the plugless end, whose movement includes almost all the volume shrinkage. The shrinkage plot is obtained as the difference between the two curves as shown by the bottom plot in Fig.6. The difference plots in all the experiments carried out are always linear up to the time t_c of gelation and are a linear measure of the degree of polymerisation.

Referring to fig.6 it is seen that the first few points on the difference plot fall in the induction period. This induction period, unavoidable because of the relatively impure PEF and presence of air, is an advantage in that it allows the establishment of thermal equilibrium before polymerisation begins. In the induction period the rate is zero and the viscosity is constant, as attested by the constancy of the slopes of both flow curves. The gel time t_c is determined from the end of the induction period, i.e., the kink in the difference plot, to the attainment of a horizontal position of the top flow curve, i e. when the resin gels and the viscosity of the resin reaches infinity This point, where flow ceases, can be located with sufficient accuracy and is thus a convenient method of finding the gel point.

The sharp kink in the top and middle curves of fig.6

represents the point where the flow is reversed by turning the disc from $+\alpha$ to $-\alpha$, because the plug meniscus approaches the plug. If the resin takes a long time to gel, this reversal can be repeated, running the resin back and forth repeatedly.

The gel point can be determined quite accurately even at high conversion, i.e., when the mixture is slow to gel and the viscosity increases relatively slowly. This can be seen in fig.7 where a solution of R = 0.2 gelled in 53 min. at 0.108 conversion. Here the initial viscosity was so low that the direction of flow had to be reversed several times.

The viscodilatometer can be cleaned with alcoholic potash and fuming nitric acid and used repeatedly, if it is removed from the thermostat immediately after gelation (cf. degradation of gel under flow, Gordon and Grieveson[15]) before the jelly-like resin has a chance to set hard. e.g., Viscodilatometer IX was used for runs D2 - 8 and F16 - 26, and viscodilatometer X for runs G2 - 24 and F2 - 14.

The viscodilatometer was used to investigate the effect of molecular weight, feed ratio, temperature and catalyst concentration on the gel time and rate of MMA/PEF as illustrated in fig.9 - 13.

2.2.5. Molecular weight of Polymethyl Methacrylate. The number average molecular weight of pure polymethyl methacrylate was determined viscometrically. A small sample (2ml.) of methacrylate monomer, purified in the usual way was polymerised in sealed Pyrex tubes with 2% M.E.K. at 62°C, identical conditions to those used in

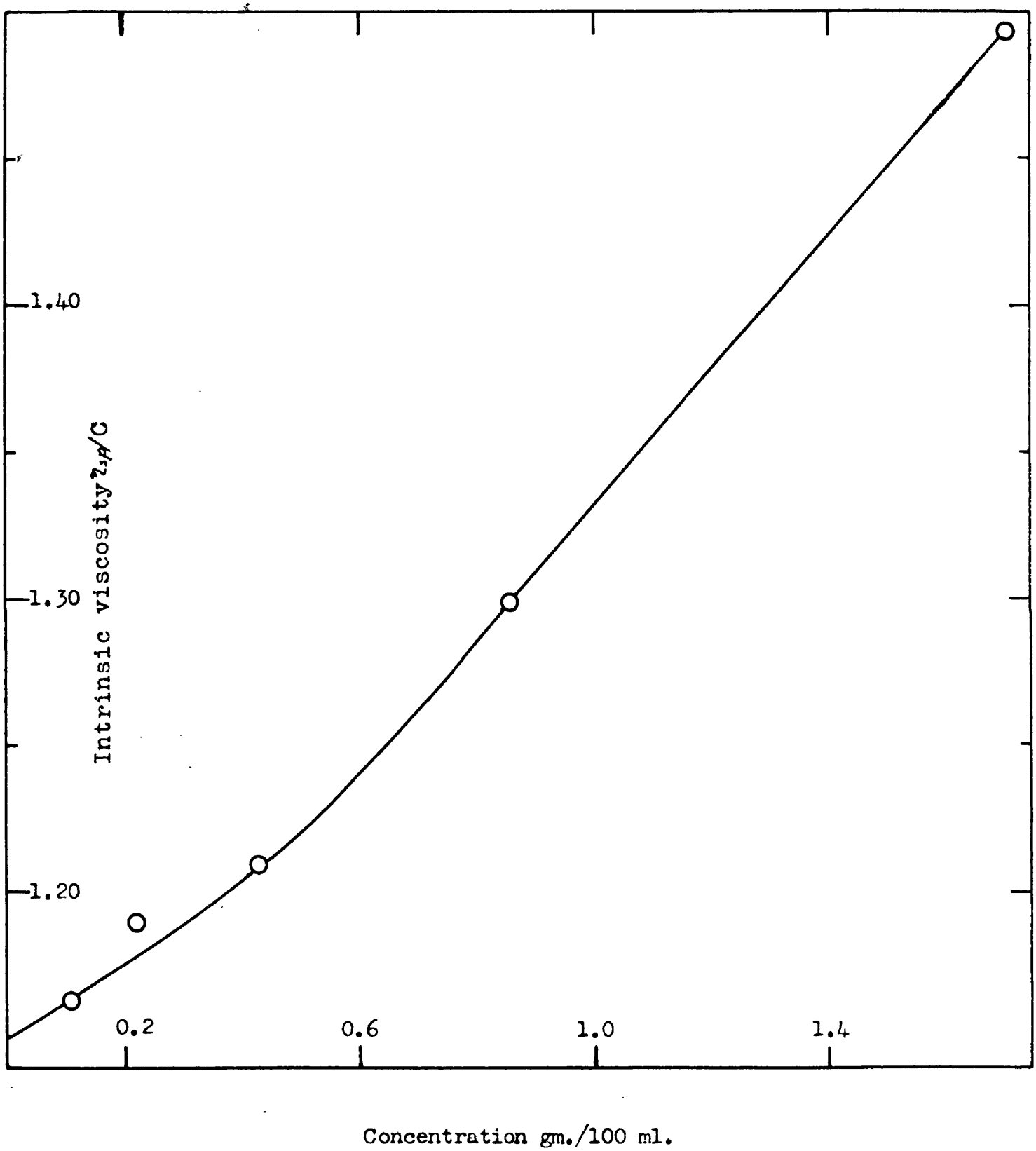

Figure 8. Extrapolation to zero concentration of η_{sp}/C.

the gelation experiments. The samples were polymerised up to about 20% conversion then dissolved in acetone, when the polymethyl methacrylate was precipitated with methanol. The polymer obtained was thoroughly washed before being dried in a vacuum oven at 40°C for 12 hours.

The purified white powdery polymer was dissolved in chloroform to give an approximately 1% solution. This was filtered through a Buchner filter and the strength of the solution determined accurately gravimetrically.

The specific viscosity of the solution was determined in an Ostwald viscometer (No.1) in the usual way, diluting the original chloroform solution by half for successive determinations. A typical extrapolation to infinite dilution is exemplified in fig.8. The intercept gives the intrinsic viscosity equal to 1.15 and, substituting in Baysal and Tobolsky's equation for intrinsic viscosity[16],

$$[\eta] = 2.52 \times 10^{-3} \, DP_n^{0.8} \qquad (11)$$

gives the number average chain length DP_{np} in this case to be 2,110.

2. 3. Results.

The details of all viscodilatometer runs are given in tables (22 & 23) in the Appendix. These results fall into two categories; runs in which both the gel time and polymerisation rate were examined, and runs for which the rate of contraction only was examined specifically for Arrhenius plots. The runs are tabulated in chronological order.

The effect of DP_n and monomer feed ratio is illustrated in figure 9. Arrhenius type plots of gel times (fig.11) give activation energies for resins F and N of 13.8 K cals. and 14.7 K. cals. respectively. The activation energy of the dilatometric rate for pure methacrylate (fig.12) is 15.6 K. cals., compared with that (fig.13) of 16.3 K. cals. for resin F and 16.7 K. cals. for resin N.

The influence of feed ratio on the polymerisation rate is shown in table 4.

Table 4.

Influence of feed ratio on polymerisation rate x 10^4 (mole $l.^{-1} sec^{-1}$) at 62°C, and 2% MEK.

Run	Feed ratio R	Mean rate (resin F)	Mean rate (resin G)
M.4,10	0.0	3.63	3.63
G.20	0.15	-	3.11
F.8,G.16	0.2	3.85	3.05
F.26	0.25	3.94	-
F.6,20,46;G.14	0.33	3.86	3.22
F.12	0.4	3.82	-
F.4,14,16;G.10,12	0.5	3.90	2.84
G.8,24	0.67	-	2.76
F.10,G.6	0.8	3.86	2.48
F.2,18;G.4,22	1.0	3.88	3.06
G.2	1.25	-	4.0
F.22	2.0	6.21	-

2.3.1. Molarity of the reaction solution and conversion at 100% Polymerisation.

In order to present the results in absolute units it is necessary to know the contraction which takes place in the complete conversion of monomer to polymer and also the molarity of the reaction solution at any given time.

a.) For MMA by itself the fractional volume shrinkage for 100% polymerisation has been investigated by several workers. Throughout this work it is assumed that the value for pure MMA is little affected by the presence of PEF. The values of the fractional volume shrinkage are those published by Melville[17] and coworkers.

Temp. °C	% shrinkage at full conversion.
60	24.68
25	23.06
0	21.88

which are in close agreement with values from other sources quoted by Robertson[18]. Drawing a straight line through Melville's values enables, with little error, the fractional volume shrinkage at any temperature in the range (20 - 80)°C to be obtained from the relation:

$$\% \text{ shrinkage} = 21.83 + 0.047T \qquad (12)$$

where T is the temperature °C.

b.) The expression for the density of MMA at T °C has been derived[19].

$$\text{density} = 0.9654 - 0.00109T \qquad (13)$$

Hence the coefficient of expansion of MMA is 0.00124 (experimental value 0.00123, M.22,24), so that the molarity of MMA is 9.36 mole l^{-1} at 27°C and 8.98 mole l^{-1} at 62°C.

Similarly the coefficient of expansion of resin N can be estimated as 0.00055 by linear interpolation since that for a solution of R = 1.75 is 0.0008 (N.72). Thus it follows that the molarity of resin N changes from 9.18 mole l^{-1} at 27°C to 9.0 mole l^{-1} at 62°C. Since the molarity of all the resins lies in range (9.15 - 9.33) mole $litre^{-1}$ and the coefficients of expansion are estimated to be similar (0.0005 - 0.0008) the molarity of the reaction solution will never seriously diverge from 9 mole l^{-1} regardless of the resin used, the feed ratio, temperature or, for the low conversions studied, the extent of polymerisation.

2.3.2. Sample calculation for a viscodilatometer run.

The results for a typical run (G.12, fig.6) for R = 0.5, 2% MEK catalyst and 62°C are obtained as follows:

Total gel time = 33 min.

Induction time = 4 min.

Actual gel time = 29 min.

Initial volume in viscodilatometer (4 mins.) = 1.835ml.

Final " " " (33mins.) = 1.810ml.

Shrinkage = 0.248ml.

% shrinkage = 1.36%

Since (eqn.11), 24.75% contraction is equivalent to 100% conversion at 62.0°C

$$\text{Conversion at gel point (33 mins)} = \frac{1 \times 1.36}{24.75} = 0.055$$

$$\therefore \text{Rate} = 0.055 \times 9/(29 \times 60) = 0.000283 \text{ mole l.}^{-1}\text{sec.}^{-1}$$

2.3.3. Reproducibility of gel times and rates. The reproducibility of the experimental results obtained with the viscodilatometer is illustrated in table 5.

Table 5.

Reproducibility of gel times and rates.
(Resins F and G; 62.0°C, 2% MEK.)

Run	Feed ratio R (= F/M)	Resin F			Resin G		
		Induction period (mins.)	tc (mins)	rate $\times 10^4$ mole $l.^{-1}$ sec^{-1}	Ind. period (mins)	tc (mins)	rate $\times 10^4$ mole $l.^{-1}$ sec^{-1}
F.6	0.33	5	67	3.56	-	-	-
F.20	0.33	5	67	3.92	-	-	-
F.4	0.5	5	43	3.39	-	-	-
F.14,G.10	0.5	5	53	4.0	2	31.5	2.71
F.16,G.12	0.5	5	60	4.30	2	29.0	2.83
G.8	0.67	-	-	-	2	28.25	2.62
G.24	0.67	-	-	-	4	30.5	2.87
F.2,G.4	1.0	2	18.5	3.74	4	16.5	3.21
F.18,G.22	1.0	2	17.5	4.01	2	15.0	2.93

By finding the mean rate and gel time for each resin and expressing the difference from the mean for each run as a percentage, the standard deviations are evaluated as follows;

Resin F, 8.2% and 4.1% for gel time and rate respectively.

Resin G, 4.1% and 4.2% for gel time and rate respectively.

The three runs at R = 0.5 for resin F represent the poorest agreement ever obtained. This is to some extent explained by the fact that these three runs were made with different methacrylate solutions namely; MMA solution distilled directly (24 hrs.) before the run, the same MMA used two weeks later, and MMA purified as described in Section 2.2.1. (the normal MMA solution used). Generally, it may be claimed that the rates and gel times determined by this technique are reproducible to $\pm$ 5%.

2.3.4. Calculation of k_t/k_p^2 from molecular weight. The ratio k_t/k_p^2 for pure methacrylate may be calculated from the familiar equation.

$$\text{Rate} \times DP_n = k_p^2 M^2/k_t \qquad (14)$$

Three determinations of DP_n (described in experimental section) are listed in table 6 together with three rate determinations from different methacrylate runs.

Table 6.

Rate and DP_n values for MMA.

DP_n	Rate moles $l.^{-1}$ sec^{-1}	Run
3085	0.000330	M.4
2110	0.000360	M.10
2440	0.000289	M.13

These three results give a mean DP_n of 2545 and a mean rate of 0.000326 mole $l.^{-1}sec^{-1}$, and M = 9 mole $l.^{-1}$.

Hence, from eqn.(14) the value of kt/k^2_p is found to be 98 mole sec.$l.^{-1}$, in satisfactory agreement with the value of 67 mole sec.l^{-1} calculable at 62°C from data by Matheson and coworkers[19], and other similar values in the literature.

2.4. Discussion.

2.4.1. Application of classical gelation theory. Assuming a simple copolymerisation reaction between methyl methacrylate and polyethylene fumarate, measurements of the gel point of the system may be interpreted in terms of the theoretical equation:

$$\alpha_c = 1/\rho\,(DP_{wp} - 1)(DP_{wc} - 1) \qquad (15)$$

where α_c is the critical fractional conversion of PEF unsaturation at the gel point, DP_{wp} is the weight average length of the radical polymerisation chains, DP_{wc} that of the original PEF polycondensation chains, and ρ is the fraction of the polymerised unsaturation which is fumarate as distinct from methacrylate. This equation follows from the gelation theory of Flory[1] and Stockmayer[2] and it degenerates to known special cases. In particular, if $DP_{wc} = 2$, the equation appropriately reduces to that[2] valid for copolymerising MMA with a doubly unsaturated monomer such as ethylene dimethacrylate; if $\rho = 1$ and $DP_{wp} = 2$, the equation degenerates to that for the vulcanisation of PEF chains.

Of the four variables in equation (15), only the weight

average chain length DP_{wc} of the PEF condensation chains is readily accessible, via the number average DP_{nc} from end group titration (section I) α_c, ρ, and DP_{wp} are difficult to measure, but additional relations can be obtained between the four variables from the kinetics of copolymerisation. At the price of making additional assumptions, it is possible to integrate the gel point theory into a general kinetic framework.

The key to equation (15) which involves dilution of a polyfunctional reagent (PEF) by means of a difunctional one (MMA), lies in the simple role played by the dilution parameter $1/\rho$, to which the critical conversion α_c is seen to be proportional. With crosslinking reagents of high functionality, the gel point is reached at low α_c, even when the value of $1/\rho$ is quite large. Under such conditions of gelling at low conversion the proportionality of α_c to $1/\rho$ can be extended to many related variables. Thus at low conversion all interesting measures of reaction progress, in whatever units may be chosen, will remain proportional to α_c. The critical fraction β_c of all double bonds (fumarate and methacrylate) polymerised, or even the critical gelling time tc, become useful indirect measures of α_c. Again, the fraction ρ of polymerised bonds which are fumarates remains proportional to the concentration F_o of fumarate double bonds in the initial monomer mixture, when both ρ and F_o are small. There is, therefore, a general expectation for any system of the type contemplated, to exhibit linearity between critical conversion parameters and $1/F_o$ at high $1/F_o$ values.

2.4.2. Copolymerisation equation and kinetic scheme. The concentration of fumarate unsaturation remaining unreacted is denoted by F (mole/l.), that of methacrylate unsaturation by M(mole/l.), and their ratio by

$$R = F/M \tag{16}$$

As seen in section 2.3.1. the total concentration of unsaturation in the initial monomer mixture is given to an excellent approximation by

$$F_o + M_o = 9 \tag{17}$$

which will be used to simplify the equations. Moreover, where appropriate, F,M,R, dF/dt, dM/dt, and ρ are treated as constants equal to their initial values F_o, etc., and the steady state free radical concentrations F^* and M^* are also assumed to be constant. This is the usual practice, permissible because the gelling experiments are confined to changes in $M < 20\%$ while those in F are much smaller. The fractional conversion β of the overall unsaturation is given by:

$$\beta = 1 - ((F + M)/(F_o + M_o)) \tag{18}$$

The constancy of $d\beta/dt$ was checked dilatometrically in every run by the constancy of the rate of shrinkage. Thus the typical rate plot in fig.6 is seen to be linear up to the gel point, and

$$\beta_c = (d\beta/dt)\, t_c. \tag{19}$$

From the definitions already given, it follows that

$$\rho = (F_o - F)/(F_o - F + M_o - M) \tag{20}$$

The copolymerisation equation

$$dF/dM = \rho/(1-\rho) = R(Rr_F + 1)/(r_M + R) \qquad (21)$$

introduces the usual monomer reactivity ratios r_F for fumarate and r_M for methacrylate radicals. They are defined in terms of propagation rate constants, thus:

$$r_F = k_{F^*F}/k_{F^*M} \text{ , and } r_M = k_{M^*M}/k_{M^*F} \qquad (22)$$

in an obvious notation. Thus k_{F^*M} denotes the rate constant for attack of an F^* on an M, etc. In particular, use is made of the fact that k_{M^*M} is identical with the propagation constant for pure MMA, denoted simply by kp. Solving eqn.(21) yields:

$$\rho = R(Rr_F + 1)/(r_M + R(Rr_F + 2)) \qquad (23)$$

The fraction β of the total, and the fraction α of fumarate, unsaturation reacted are related thus:

$$\beta = \alpha R/\rho(R + 1) \qquad (24)$$

The critical value of the former is found from equations (15),(16),(17) and (23), by substitution in (24):

$$\beta_c = \frac{M^2(r_M + R(Rr_F + 2))^2}{9(Rr_F + 1)^2(DP_{wp} - 1)(DP_{wc} - 1)F} \qquad (25)$$

This exhibits the linearity of β_c with $1/F$ predicted above for low values of F, where in fact $M \sim 9$ (eqn.17) and $R \sim 0$ (eqn.16). Further transformations of (25) concern the weight average chain length DP_{wp}

of the polymerisation chains. As the number average chain length DP_{np} is more readily expressible in terms of the kinetic scheme, it is convenient to use the substitution,

$$(DP_{wp} - 1) = 1.5\ DP_{np} \tag{26}$$

which is correct for termination by radical combination, and will rarely be far from the truth in reactions of the type under discussion. While it is not possible to obtain directly an expression for DP_{np} which is free from the unknown radical concentrations F* or M*, or from the initiation rate, the product of DP_{np} and the reaction rate can be obtained. This suggests a transformation from β_c to t_c with the aid of eqn.(19)

Thus it is assumed that the four propagation steps with rate constants k_{M*M}, k_{M*F}, k_{F*M}, and k_{F*F} make up the total propagation rate, while three termination steps together exhaust the possibilities of chain termination. These involve the binary radical collisions of the type M* + M*, M* + F*, and F* + F*, with respective rate constants k_t, k_t' and k_t''. The product of rate and DP_{np} can then be written

$$(d\beta/dt)DP_{np} = \frac{(k_{M*M}M*M + k_{M*F}M*F + k_{F*M}F*M + k_{F*F}F*F)^2}{9(k_tM*^2 + k_t'M*F* + k_t''F*^2)} \tag{27}$$

The factor 1/9 is provided by eqn.(17). From (27) the unknown radical concentrations F* and M* can be eliminated together, because they occur homogeneously, by means of the customary stationary state assumption

$$k_{F*M}F* = k_{M*F}M*R \tag{28}$$

Substituting for $(d\beta/dt)$ from (19) and for β_c from (25), the final general form of the gel point condition is obtained as

$$t_c = \frac{\dfrac{k_t}{k_{M:F}^2} + \dfrac{k_t' R}{k_{M:F} k_{F:M}} + \dfrac{k_t'' R^2}{k_{F:M}^2}}{1.5\,(Rr_F + 1)^2 (DP_{wc} - 1)\,F} \qquad (29)$$

This form involves directly the gel time t_c without any conversion factors relating to density, volume shrinkage, etc. Measurements of t_c are also important industrially as a variable in production control for which purpose a special measuring device is available.(20)

Equation (29) degenerates, as did (25), to a linear form at sufficiently high $1/F$. The three important aspects of (29) to be considered are the slope of the asymptotic line of the plot relating t_c to $1/F$ (fig. 9 and 10), its intercept on the t_c axis, and the detailed shape of the curve itself.

2.4.3. Detailed shape of the gel time/composition curve. The experimental points plotted in fig 9 conform closely to a linear law when $R < 0.5$. This implies that the curve should approach closely to its asymptote beyond that limit. In other words, the last two terms in the numerator of (29) and the term $(Rr_F + 1)^2$ in the denominator are negligible beyond $R < 0.5$, and the following inequalities should hold:

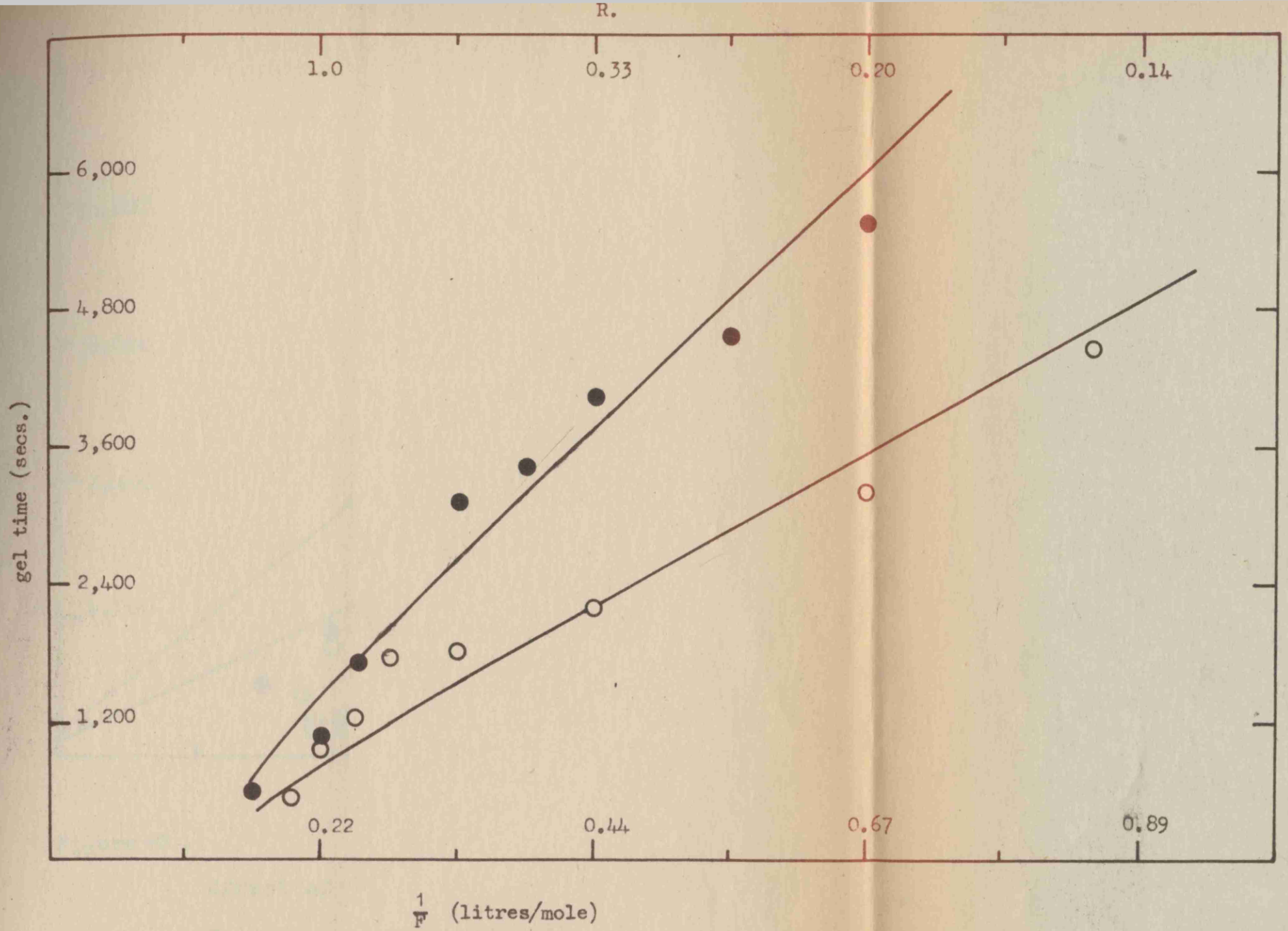

Figure 9 . Absolute verification of the classical gelation theory.
The theoretical curves drawn (eqn.) use the parameters r_m= 29, r_F=0.25.
Independent measurements gave r_m=10-25 and r_F=0.0-0.7.

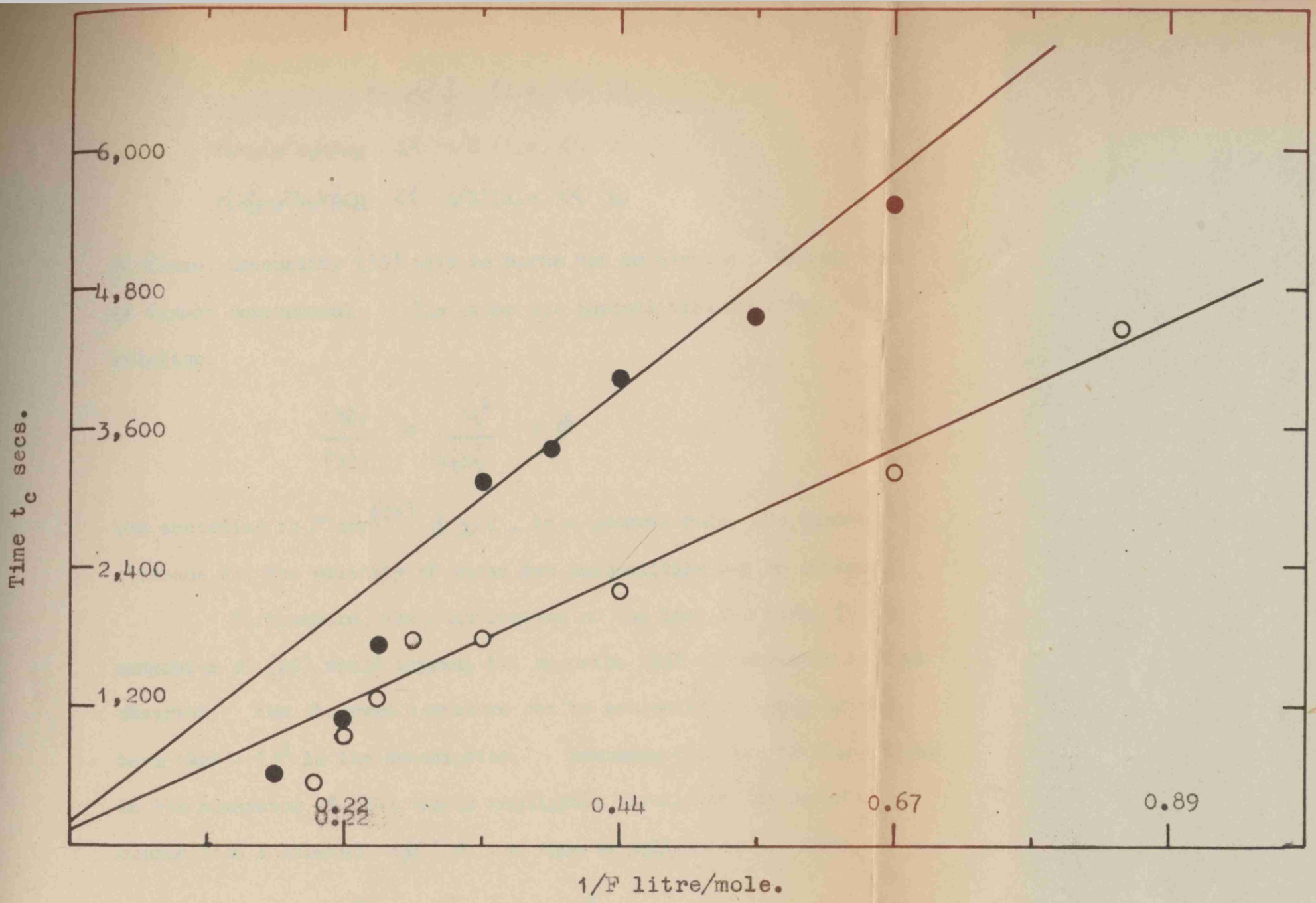

Figure 10 .

Effect of composition and DP_{wc} on gel time.

Comparison of asymptotic slopes.

resin F. resin G.

$$r_F \ll \frac{1}{R} \quad (\text{i.e. } \ll 2) \tag{30}$$

$$k_t' k_{M:F} / k_t k_{F:M} \ll 1/R \ (\text{i.e. } \ll 2) \tag{31}$$

$$k_t'' k_{M:F}^2 / k_t k_{F:M}^2 \ll 1/R^2 (\text{i.e. } \ll 4) \tag{32}$$

Of these, inequality (30) will be borne out in Section 3 of this work by direct measurement. The other two inequalities constitute the relation:

$$\frac{(31)}{(32)} = \frac{k_t^2}{k_t' k_t''} = \phi \tag{33}$$

and according to Flory[21], $\phi \gg 1$, as a general rule. No direct evidence for the validity of these two inequalities can be offered.

Furthermore, the contribution of the last two terms in the numerator of (29) would impress the opposite kind of curvature to that observed. The observed curvature can be accounted for only by the term $(Rr_F + 1)^2$ in the denominator. Assuming that the two last terms in the numerator of (29) remain negligible throughout the range of composition R studied, eqn (29) can then be written in the form.

$$t_c = k_t r_M^2 / (1.5\ k_{M:M}^2 (Rr_F + 1)^2 (DP_{wc} - 1) F) \tag{34}$$

The classical gelation theory embodied in eqn.(34) can be put to a simple absolute test. Experimental points for the gel time with varying R values for resins of two different DP's are compared with the theoretical curves predicted by eqn.(34). These were calculated using values of $r_F = 0.25$ and $r_M = 29$, which lie within or nearly within the range of direct measurements of these two parameters in

in Section 3, namely $0 \leqslant r_F \leqslant 0.7$ and $10 \leqslant r_M \leqslant 25$. The DP_{wo} values used (resin F = 5.56, resin G = 9.46) were deduced from end-group titration. The ratio $k_t/k_{tM}^2 = 98$ mole sec.l.$^{-1}$ was measured as stated earlier and is in satisfactory agreement with the previous literature.

The experimental points are in good agreement with the theoretical curves in fig.9 and constitutes a satisfactory, complete, absolute test for the classical gelation theory.

2.4.4. Slope of the asymptote. As a more restricted test of the classical gelation theory, the constant r_F, which is the most difficult to obtain, can be eliminated by using directly the slopes of the asymptotes of the plots in fig.10 at low R values, obtainable from (34) in the form:

$$\text{slope} = k_t r_M^2 \, 1.5 \, k_{tM}^2 \, (DP_{wo} - 1) \qquad (35)$$

Table 7.

Relative verification of the classical gelation theory from figure 10.

Resin	$(DP_{wo}-1)$	Asympt. slope (mole sec.l.$^{-1}$)	Asympt. intercept (sec)	Ratios of Slopes	Ratios of Intercepts	Ratios of $(DP_{wo}-1)$
F	5.56	8410	204	1.70	1.70	1.70
G	9.46	4970	120			

The fact that the asymptotic slopes in fig.10 are in the ratio of the values of $(DP_{wo} - 1)$ is a verification of the classical gelation theory in

a relative sense, which can be shown to be independent (eqn.15) of the mechanism assumed for the copolymerisation reaction.

According to the diffusion control theory of gelation[3] the slopes and absolute gel times would be practically independent of the condensation chain length DP_{wc}, because of the saturation of the cross-linking capacity assumed to occur under the present conditions. Moreover, such saturation would cause the curves in fig.9 to approach the horizontal at low 1/F, in direct contradiction to fact. A critical re-examination of the diffusion control theory has led Gordon and Roe[22] to reject the theory on general grounds.

2.4.5. Intercept of the asymptote. The intercept of the asymptote on the t_c axis can be obtained from eqn.(29), with the aid of (16),(17) and (35) in the form:

$$\text{Intercept} = \frac{\text{Slope}}{9} \times \frac{k_t'}{k_t} \times \frac{k_{M*F}}{k_{F*M}} \qquad (36)$$

This is less useful here than the slope (35) because the constants k_t' and k_{F*M} are not known. The experimental intercepts are seen to be small absolutely, and small relatively to the slopes, in fig.10. Therefore little support for the theory can be claimed from the achievement of two intercepts which stand, perhaps somewhat fortuitously, in the correct theoretical ratio given by (36),(see table 7). However the smallness of the intercepts compared with the slopes (table 7) does support the validity of inequality (31).

2.4.6. Temperature dependence of the gel point. The theory embodied in eqn.(34) should also account for the influence of temperature on t_c. It does so very plausibly. By ignoring the small contribution from r_F (i.e. putting $r_F = 0$), and substituting for r_M from (22), the following expression is obtained after logarithmic transformation of (34).

$$\log_{10} t_c = \text{const.} + (2E_{M*F} - E_t)/2.3\ RT \qquad (37)$$

The activation energies E_{M*F} and E_t are identified by their subscripts. A linear Arrhenius type of plot is predicted by (37) for $\log_{10} t_c$ against reciprocal temperature. This is verified in fig.11 on two separate resin condensates F and N, polymerised with 2% and 0.5% MEK respectively, the gel points of resin F being determined with a viscodilatometer and those of resin N in a simple dilatometer with a magnetic stirrer (see Section 4.2.1.) Eqn.(37) is also independent of both R and the catalyst concentration. This is verified here for two widely different R values (0.33 and 1.75) and catalyst concentrations (2% and 0.5% MEK), since the overall activation energies obtained from the regression lines drawn in fig.10 are 13.8 and 14.7Kcal. respectively. Further analysis of the mean overall energy of activation of gelation in accordance with (37) gives:

$$E = 2E_{M*F} - E_t = 14.3 \pm 0.5 \text{ K.cal./mole} \qquad (38)$$

Since the activation energy E_t of termination between two methacrylate radicals is [23] about 2 K.cal/mole, this leaves about 8.1 K.cal/mole for E_{M*F} of the cross propagation step. This value is reasonable,

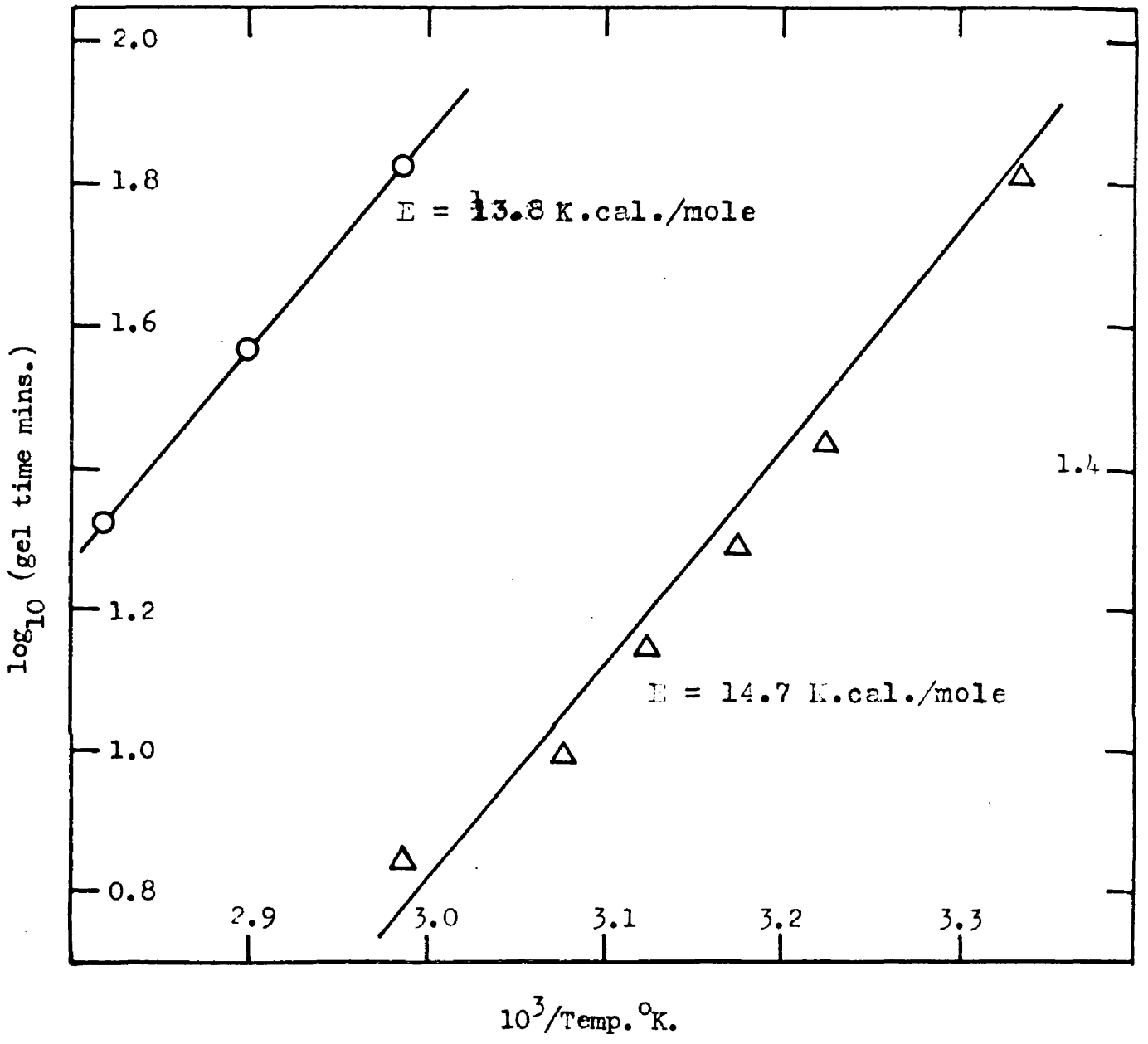

Figure 11. Arrhenius type plot of gel time for resin F; R = 0.33, 2.0% MEK catalyst (O), and resin N; R = 1.25, 0.5% MEK catalyst (Δ).

because it lies about 2 - 3 K. cal. above the activation energy E_{M*M} for pure MMA polymerisation[23] as might well be expected. This analysis pinpoints the term E_{M*F} as predominantly responsible for the effects of temperature on gelation.

2.4.7. Effect of catalyst concentration on the gel time. Eqn.(34) predicts that the gel time t_c should be independent of both the nature and concentration of the catalyst (B). This seems directly counter to the fact that in commercial practice the gelling times of "contact resins" are usually regulated by changing the concentration or nature of the catalyst system[24]. It must be remembered, however, that gelling occurs under conditions approaching adiabacity in commercial practice. The increase of rate is due to the well known heat build up, or lack of temperature constancy due to the poor dissipation of the polymerisation heat through the viscous resin, while eqn.(34) applies only under isothermal conditions.

As already mentioned,[4] the constancy of the gel time with MEK concentration for this system was discovered by the writer in a short exploratory investigation of this topic. This work was somewhat crude, the gel time being measured by injecting bubbles of air into the solution and noting when they stopped rising. A detailed investigation of the effect of the concentration and nature of the catalyst on the system has been carried out by Grieveson[13][15] in this laboratory using the viscodilatometer technique, and his results will be briefly reviewed here. Over a considerable range of two types (methyl ethyl ketone peroxide, MEK, and 1-hydroxy cyclohexyl hydro-

peroxide-1, HCH), of catalyst, t_c was found to remain constant. At the same time, the rate varied in these experiments as the square root of the catalyst concentration, a well known consequence of the pairwise distruction of radical ends in chain polymerisations. Thus a confirmation of the kinetic scheme adopted is provided which is independent of gelation theory.

The constancy of t_c with varying catalyst concentration acts as both a key proof of classical gelation behaviour, and as confirmation of the chain reaction nature of polymerisation of unsaturated compounds. Thus apart from any detailed mechanism, the observed constancy of the gelling time in the face of observed variations of the reaction rate with $(B^{\frac{1}{2}})$ requires some compensating factor which varies with $(B^{-\frac{1}{2}})$. If the reaction were not a chain reaction it seems impossible to see what this factor could be. If it is a chain reaction, then the gel point theory suggests that the compensating factor must be the chain length DP_{wp} and the kinetic scheme leads precisely to the variation of this factor with $(B^{-\frac{1}{2}})$.

2.4.8. Dependence of rate on feed ratio R and on temperature. As seen in table 4 the rate of polymerisation is independent of R in the range $0 \leqslant R \leqslant 1$, but increases somewhat as R rises above unity. The application to the propagation rate of the kinetic scheme adopted above, with the aid of eqn.(16), (22) and (28), leads to the equation:

$$\text{Rate} = k_{M\cdot M} M^{\cdot} M \left(1 + (R(2 + Rr_F)/r_M) \right) \qquad (39)$$

Since the term in square brackets is practically constant up to R = 1 and then increases slowly with R, it must be concluded that variations

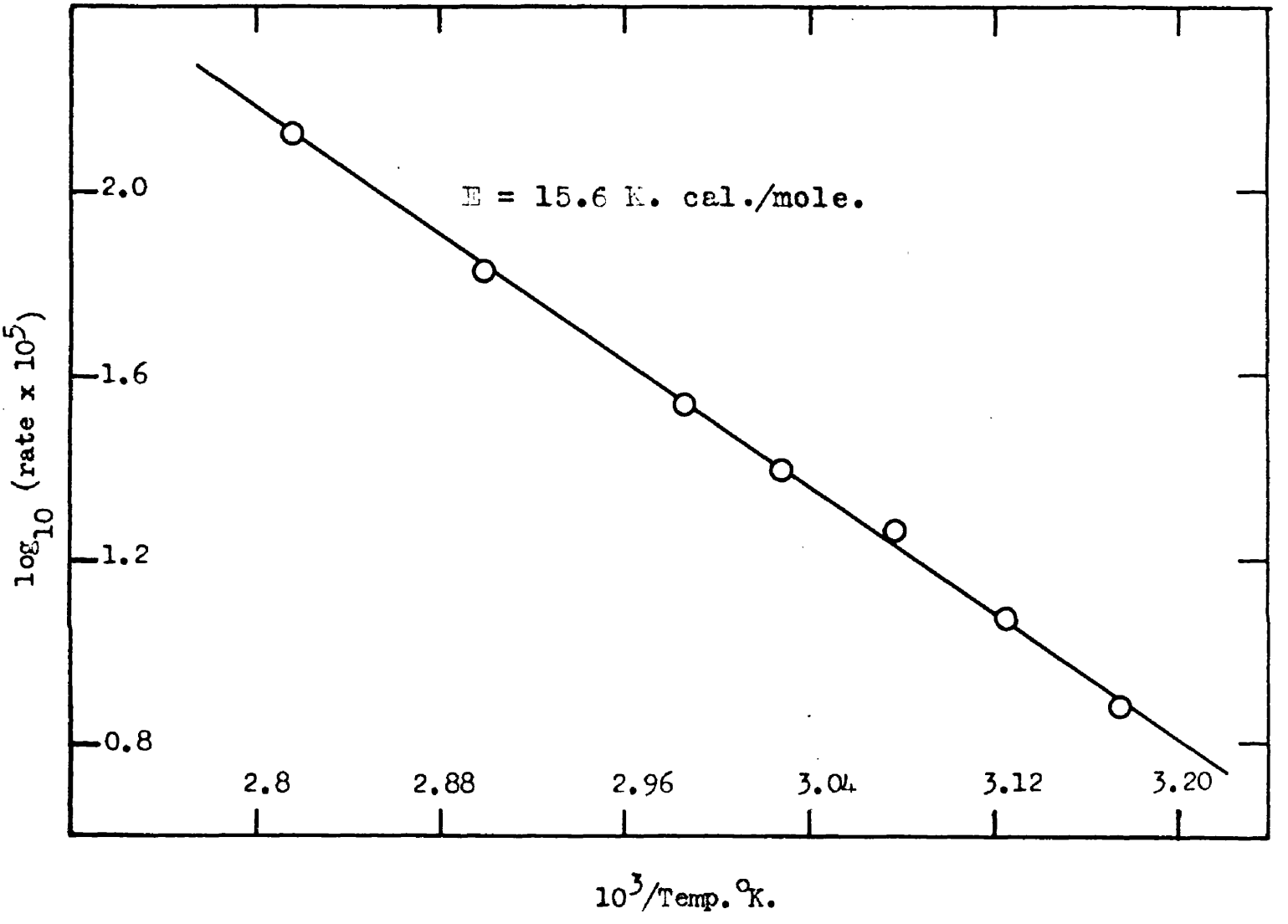

Figure 12. Arrhenius plot of dilatometric rate for pure MMA (R = 0), 2% MEK. catalyst.

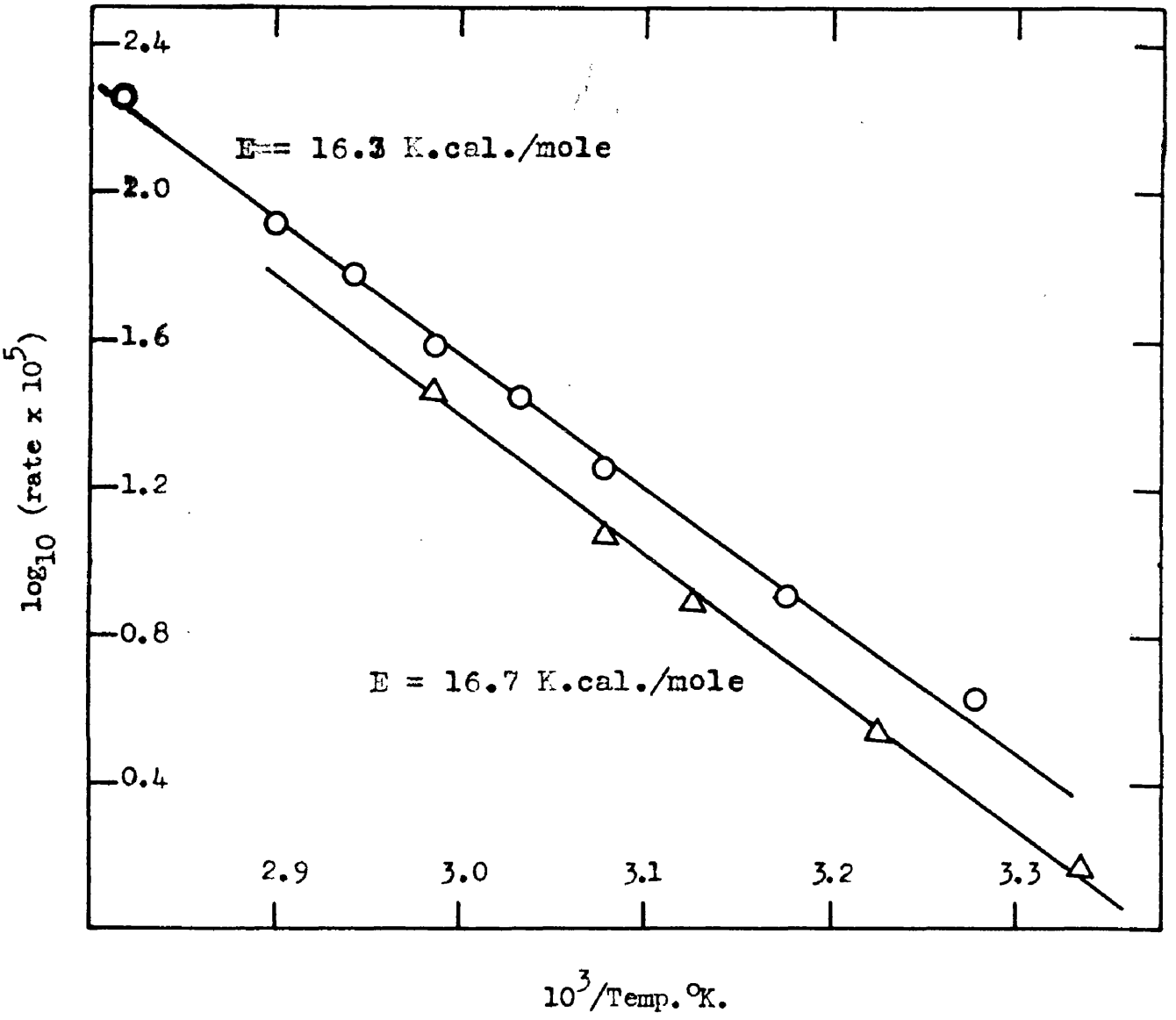

Figure 13. Arrhenius plot of dilatometric rate for resin F; R = 0.33, 2.0% MEK catalyst (O), and resin N; R = 1.25, 0.5% MEK catalyst (Δ).

in M and M* must largely balance so as to keep (M*xM) constant. This behaviour is compatible with the kinetic scheme adopted (cf. Palit[26]), but too many unknown parameters would have to be adjusted to fit the data quantitatively. The rise in the radical concentration M* with falling M must be interpreted in terms of an increase in the rate of radical initiation by the catalyst as the mixture is made richer in PEF and poorer in MMA. If, as, suggested, the termination of radicals occurs largely between couples of M* radicals irrespective of R over the range studied, (i.e. eqn.(34) is independent of k_t' and k_t''), then the DP_{np} varies as M/M*, or as M^2 (since $M^* \times M$ is constant). Thus the primary polymerisation chain length varies about 9-fold over the 3-fold range of M covered by fig.9 and 10. The advantage of plotting t_c directly is again emphasized, since this procedure automatically allows for variations in rate and chain length. Figures 12 and 13 present Arrhenius plots of the overall rate in the absence and presence of PEF. The regression lines drawn have slopes corresponding to overall activation energies of 15.6 K.cals./mole for pure MMA compared with those of 16.3 K.cals./mole and 16.7 K.cals./mole for R = 0.33 and 1.75 respectively. The former value is acceptable for pure MMA and is in accordance with the kinetic scheme here used, as made up of contributions from the activation energy of initiation, propagation, and termination, thus:

$$\text{Overall activation energy} = \tfrac{1}{2}E_i + E_{M^*M} - \tfrac{1}{2}E_t \qquad (40)$$

In the presence of PEF, the three energy terms are liable to change in virtue of the contribution made by this resin to the overall polymerisation.

In particular, the three propagation steps involving PEF might contribute to the term corresponding to E_{M+M} and the two termination steps involving PEF, to the term corresponding to $-\frac{1}{2}E_t$. However, it would be expected that the propagation steps involving PEF make only a small contribution, as is evident for the indicated values of r_M and r_F, and E_t is known to make a very small contribution to (40) in any case. The constancy of the activation energy despite the addition of 55% of PEF in going from fig. 12 to 13 suggests that the activation energy of initiation E_i for PEF is not greatly different from that for pure MMA . The practical constancy of rates and activation energies in presence and absence of PEF obviously support the identity of the mechanism (i.e. radical chain polymerisation) of the hardening reaction of the model "contact resin" and the polymerisation of pure methyl methacrylate.

2.4.9. Analysis of some assumptions. The neglect, inherent in (34), of two side reactions may briefly be discussed.

a.) Firstly, chain transfer reactions have been totally discounted in the kinetic scheme. Chain transfer to MMA monomer is known to be inappreciable. Chain transfer to the PEF resin may occur to a small extent, but the constancy of the gel time under varying catalyst concentration forms a sensitive test for the absence of such transfer.

b.) Secondly, delay of gelation through internal cyclisation reactions[27][28][29] has been entirely discounted. The only detectable effect of such cyclisation in this work would be a rise in the apparent value of r_M calculated from fig.9 with the aid of (34). The fit of the data in fig.9 does require a value of $r_M = 29$ compared to the

range $10 \leqslant r_M \leqslant 25$ obtained by direct measurement in Section 3 and this discrepancy may conceal some internal cyclisation.

c.) A further assumption made in the derivation of (34) is that of radical termination by combination. The extent of radical termination in the polymerisation of MMA is controversial and will be further discussed in Section 4. The assumption of radical termination by disproportionation would require r_M to be increased by a factor of $\sqrt{1.33}$ to fit the data in fig.9.

d.) It is inherent in the use of monomer reactivity constants, particularly r_M, in the gelation theory (34) that all the unsaturation in PEF is equally reactive. The possible effects of variations in reactivity due either to chemical causes, or to the relative position of a fumarate double bond within its condensation chains has now to be discussed.

Chemical causes arise from the interconvertibility of maleic and fumaric double bonds. It has been assumed that the polycondensation chains contain only fumarate unsaturation, i.e. that complete geometric inversion takes place during the condensation of maleic anhydride with ethylene glycol. Infra-red analysis suggests (see Section 1.7.) that such conversion is substantial and that its equilibrium level is attained rapidly before resin samples are collected[12]. It has recently been thought[30] that a noticeable fraction of maleate unsaturation may be present in the equilibrium state. Even if this is so, the present treatment is not seriously affected. Thus if maleate and fumarate unsaturation have equal reactivity ratios in respect of methyl

methacrylate, then the treatment is clearly completely unaffected. On the other hand, the reactivity of maleate to methacrylate radicals might be negligible when compared with fumarate, so that only fumarate units would polymerise. The apparent chain length DP_{wc} in eqn.(29) ought to be reduced corresponding to the fraction f of the total unsaturation in the condensation chains which is fumaric (and therefore polymerisable). The fraction f would be constant from one DP_{wc} value to another. The relative slopes in fig.9 vary as $1/(fDP_{wc} - 1)$ on this assumption and the agreement would be little affected even if f were as low as 0.5. The absolute comparison of r_M from the slope with direct measurements would be unaffected by f, as both estimates are to be made on the same value of f.

e.) The assumption tacitly made, that all fumarate bonds have equal reactivity constants irrespective of their position in a PEF condensation chain, seems plausible on theoretical grounds. The possibility that terminal bonds only differ in reactivity from all others towards the centre of a PEF chain may be considered. If the terminal bonds were completely unreactive to addition polymerisation, all the apparent DP_{wc} values used would have to be reduced by two, i.e. the number of terminals per weight average chain. This would not significantly affect the treatment. If conversely only the terminal double bonds of a condensation chain were reactive, the gel point would be expected to be delayed as the actual length DP_{wc} was increased. This is completely ruled out by the results in fig.9.

2.5. Summary. Both absolute and relative verifications of the classical network theory of gelation are presented for the model system. Theoretical curves for the dependence of the absolute gel time on the feed ratio of PEF to MMA, and on the chain length of PEF, are fitted to experimental results. Variations in the concentration of a peroxide and hydroperoxide catalyst do not affect the gel time, because the effects on reaction rate and primary polyaddition chain length cancel each other. The classical gelation theory also accounts for the (constant) activation energy of gelation. No interference by diffusion control effects with the classical gelling behaviour is encountered. Gel point measurements are thus vindicated as a theoretical tool, as well as being of much technological importance.

The reaction mechanism of the hardening of MMA/PEF, a model "contact resin" system, is found to be a simple copolymerisation, in which both the reaction rate and its activation energy are practically independent of the feed ratio over a wide range extending down to pure MMA. The polymerisation may be simply explained in terms of the classical gelation theory by reference to fig. 14 and 15 and eqn. (15). Thus the critical conversion α_c depends on two factors $\rho(DP_{wp} - 1)$ dealing with the horizontal (polymerisation) chains, and $(DP_{wc} - 1)$ dealing with the vertical (condensation) chains. The first term is equivalent to the weight average number of double bonds on a condensation chain available for crosslinking, and the second gives the number of fumarate units on a polymerisation chain which are available for crosslinking. The fraction ρ depends on the relative ease (or rates)

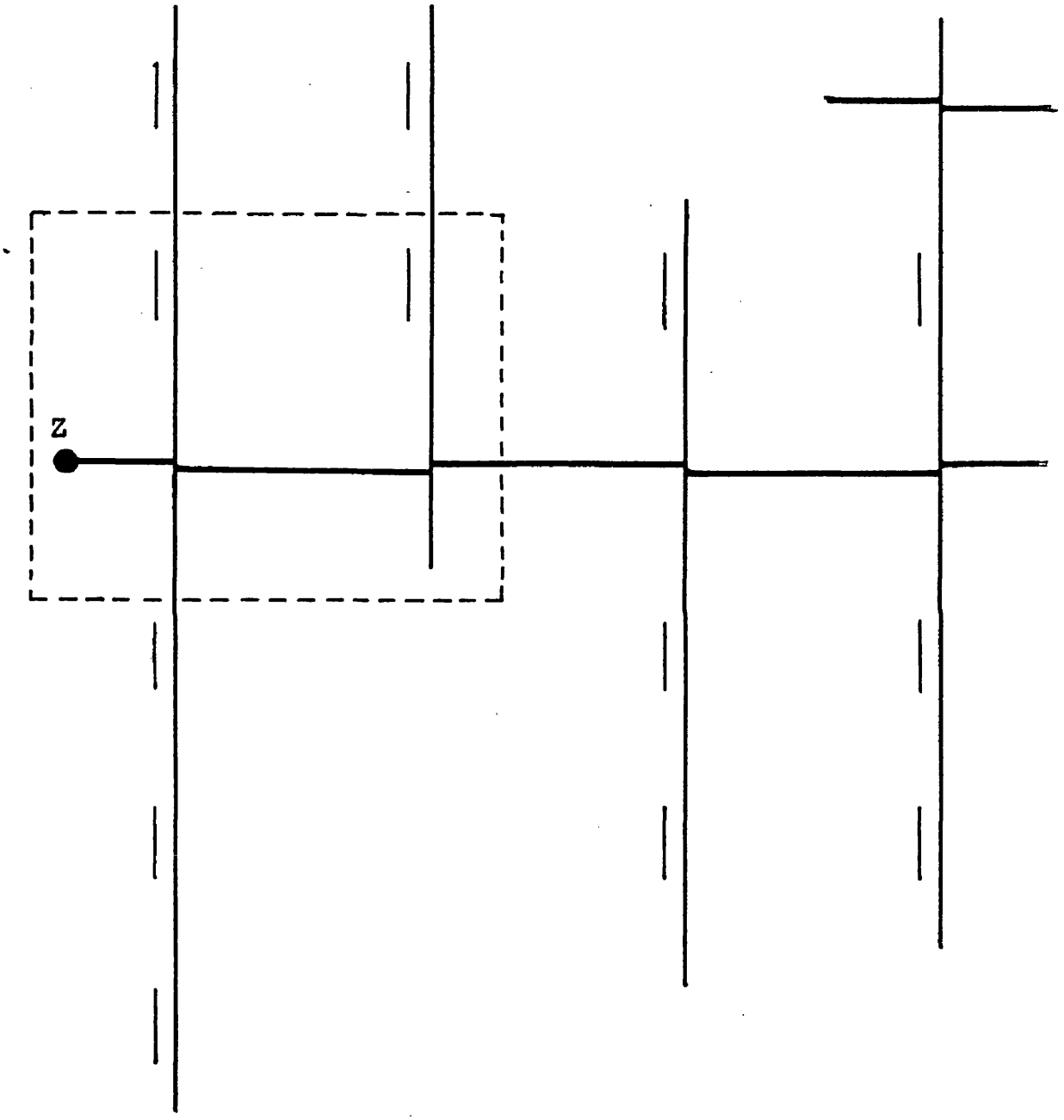

Figure 14 .

Schematic structure of the cross-copolymer. An enlarged detail of the section within the dotted rectangle is shown in fig. 15 .

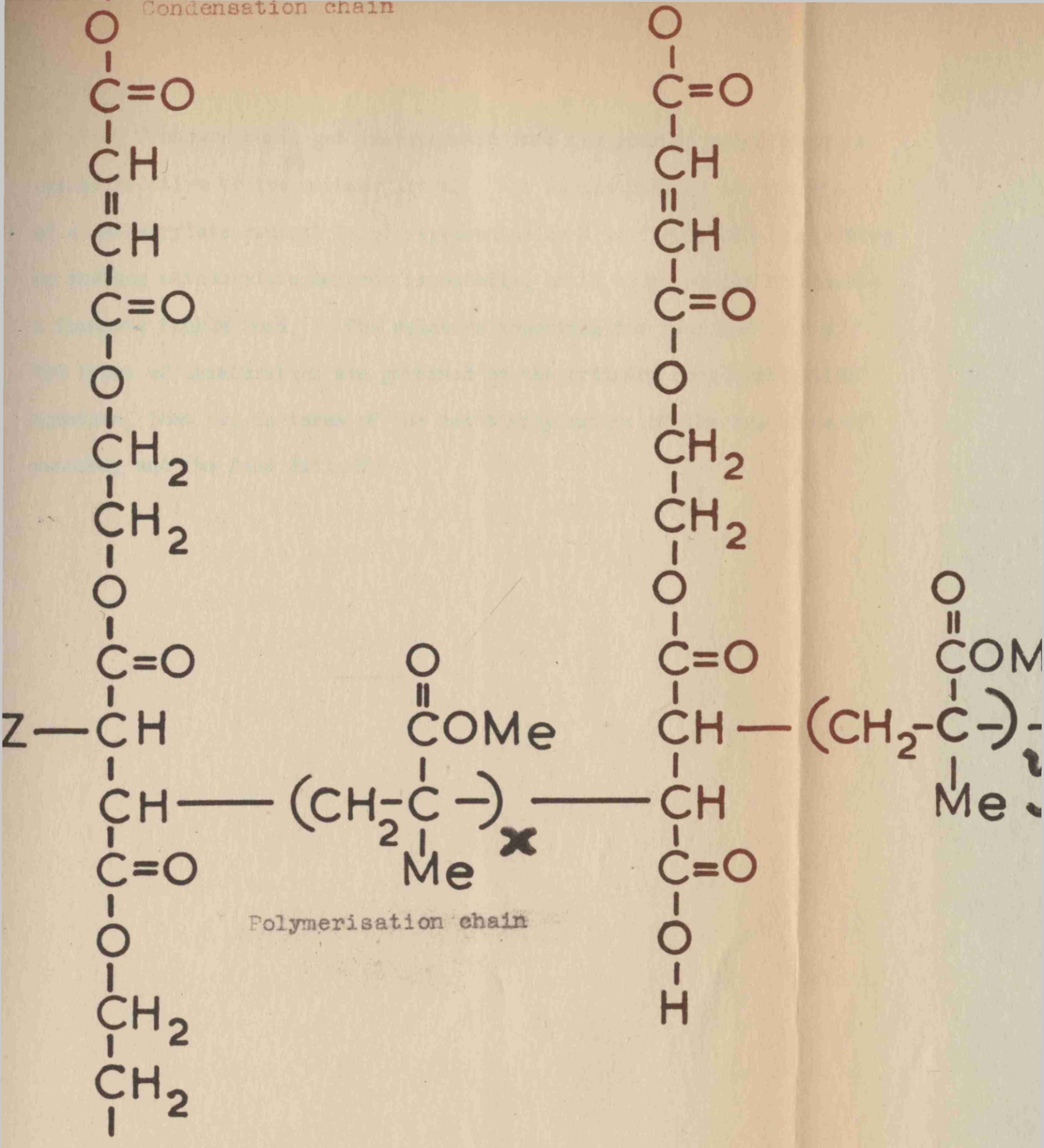

Figure 15. Detail of cross-copolymer. An enlarged detail of the section within the dotted rectangle shown in fig. 14.

at which fumarate bonds get incorporated into the growing polymerisation chains relative to the methacrylates. The simple picture is then one of a methacrylate radical (e.g. represented by Z in fig.14 and 15) picking up another methacrylate monomer repeatedly, until occasionally it attacks a fumarate double bond. The relative appetites for reaction of the two types of unsaturation are governed by the ordinary copolymerisation equation, that is, in terms of the reactivity ratios of the two kinds of monomer, and the feed ratio R.

SECTION 3.

Evaluation of Monomer Reactivity Ratios r_M (Methyl Methacrylate) and r_F (Polyethylene Fumarate).

3.1. Introduction. The copolymerisation kinetic scheme developed from the classical network theory of gelation, in the previous section, uses the values of the reactivity ratios as $r_M = 29$ and $r_F = 0.25$, for methacrylate and fumarate radicals respectively. The evaluation of these two parameters is of paramount importance in order to confirm the gelation theory which uses the aforementioned values of r_M and r_F to fit the experimental data.

The classical method of measuring the reactivity ratios of the cross-copolymer is to isolate it and determine its composition. This is done by a repetitive solvent extraction procedure and the isolated cross-copolymer is analysed by density measurements, carbon and hydrogen microanalysis and by hydrogenation of the double bonds present. The values presented for the reactivity ratios were derived from the density measurements, which were thought to be the most reliable as well as being most easily accomplished. The values from microanalysis and microhydrogenation measurements are in satisfactory agreement, (see fig.19).

The values of the parameters found in this way are bracketed in the ranges $10 < r_M < 25$ and $0 < r_F < 0.7$ which agree reasonably enough to the theoretical values to confirm the validity of the classical network theory of gelation and the copolymerisation kinetic scheme. The nature of the model system makes a direct verification of the ratios

extremely difficult (as reflected in the relatively large ranges assigned to them), for in contrast to a normal difunctional copolymerisation reaction the polyethylene fumarate, which formally takes the place of one of the two usual comonomers is itself a low molecular weight polymer. It is not a pure compound but hetero-disperse and may contain some ring compounds as well as linear molecules. It contains condensation chain molecules with multiple unsaturation functionalities, the reaction of any one of which suffices to attach it to the cross-copolymer (fig. 14 and 15). Thus the freeing of the cross-polymerised copolymer from unattached monomers requires lengthy and repetitive separation procedures, it being particularly difficult to extract completely the free PEF condensation chains none of whose double bonds has become incorporated in an addition polymerisation chain.

3.2. Note on nomenclature. It seems to be customary (especially in Britain) to speak of crosslinking the polyester resin with a monomer such as methyl methacrylate, while occasionally (especially in U.S.A.) the polyester is referred to as the crosslinker for the methacrylate. In as much as the polyester is the polyfunctional component, it seems preferable to associate it nominally with the crosslinking process, so the latter usage is adopted here. It should be obvious from the symmetry of the geometrical structure underlying fig. 14 of the copolymer, in which a rotation through 90° will interchange the horizontal with the vertical lines of atoms, that it is arbitrary which of the two is considered to contain the crosslinks (cf. the decision as to which of two numbers is the multiplier and which the multiplicand in a product).

In the network theory of size distributions, gelling, etc., the arbitrary choice of "crosslinks" from the bonds occurring in the meshes is reflected in alternative routes of deriving precisely the same equations. The words cross-polymer (or cross-copolymer) will be used for the structure typified by fig.14.

3.3. Experimental.

3.3.1. Choice of solvents for cross-copolymer extraction. When the MMA/PEF system gels the gelled solution is a mixture of methacrylate monomer, fumarate monomer and the cross-copolymer. In order to isolate the latter it is necessary to extract the remaining unsaturated monomers by solvent extraction, and a satisfactory scheme was evolved only after an extensive investigation of the effect of a large variety of solvents on the components. Essentially, solvents had to be found for the two monomers which had no effect on the cross-polymer. In the solubility experiments polymethylmethacrylate itself was used to simulate the cross-polymer since the two differ only by the inclusion of PEF branching units. The plan followed was to find a good solvent for each monomer and then examine its effect on Perspex under varying conditions of time and temperature.

The extraction of methacrylate monomer from polymer presented no great difficulty since it is standard practice to extract methacrylate monomer from Perspex with methanol.

Of all the solvents tried for fumarate, it was found that ethylene glycol monoethyl ether (Cellosolve) was the most satisfactory, the resin being soluble in warm Cellosolve, or in the cold after standing.

Cellosolve has no solubilising effect on Perspex unless under drastic conditions. A sample of Perspex was left standing in Cellosolve for nine days at room temperature. Even then the sample remained quite hard and there was no detectable swelling, and the addition of methanol to the Cellosolve did not produce any precipitate or milkiness. Another sample of Perspex was refluxed with Cellosolve under reduced pressure (about 140°C) for two hours then left standing at room temperature for nine days. The addition of methanol gave only a slight milkiness to the solution.

Thus the extraction scheme followed consists of extracting the methacrylate monomer with methanol and the free fumarate condensation chains with Cellosolve, leaving only the cross-copolymer.

3.3.2. Cross-polymerisation and purification procedure. Weighed quantities of MMA and PEF totalling about 3 - 10gm were mixed to a clear solution of the desired mole ratio R in the usual manner. 2% MEK catalyst was added to the solution which was polymerised in sealed Pyrex glass tubes at 62°C until gelled. At the gel point (about 5 - 20% conversion), determined by the probe method described in Section 4.2.1.[22] the polymerisation was stopped by immersing the tube in a freezing mixture of methanol and solid carbon dioxide. The gelled mass was pushed out of the tube and weighed. A tenfold excess of chilled methanol and a trace of hydroquinone, to prevent further polymerisation, were added and the mass was worked by manually rolling and pressing with a glass rod terminating this stage by stirring with a high speed propeller stirrer for about 10 minutes. The methanol

was decanted and the procedure repeated with fresh methanol four times, to complete extraction of unreacted methyl methacrylate. In this process, the originally doughy mass became broken up into small, plastic particles, presumed to contain the cross-polymer and free condensation chains.

To extract these free chains, the second stage consisted in the addition of 100-fold excess of Cellosolve and heating for a few minutes to 60°C with stirring. The particles swelled to clear soft jelly-like globules of much increased volume. The solvent was decanted and the process repeated twice with fresh Cellosolve. The swollen particles were then left in contact with Cellosolve at room temperature for 10 - 20 hours then finally washed with fresh solvent.

In the final stage, the cross-polymer particles were freed from Cellosolve by refluxing with methanol in a Soxhlet extractor, renewing the methanol after three hours and continuing the extraction for a further three hours. The product was washed from the thimble with fresh methanol which was then decanted and the final polymer dried in a vacuum desiccator over calcium chloride for about 15 hours. The polymer was obtained as a white powder suitable both for microanalysis and density determination. The whole extraction procedure (Cellosolve and methanol) was repeated once or twice, i.e. in principle to constant composition and density of the cross-polymer powder. A typical rough yield survey (table 8) may be presented for the runs corresponding to R = 0.5 and R = 0.1.

Table 8.

Yield survey for cross-polymers.

	R = 0.5	R = 0.1
Weight of gelled resins	3.08 g.	6.62 g.
Weight of cross-polymer estimated from shrinkage during polymerisation.	300 mg.	700 mg.
Net yields of cross-polymer powder after		
first extraction	180 mg.	594 mg.
second extraction	94 mg.	304 mg.
third extraction	53 mg.	150 mg.

No allowance has been made for considerable unavoidable losses in handling the polymer during the extraction procedures, or of the minute quantities used for density measurements. Nevertheless, the relatively low net yields reflects real losses by solubility of the cross-polymer in Cellosolve. To reduce this solubility in the two runs of lowest R value in which the effect was most serious, 10% of methanol was added to all the Cellosolve used. This mixture is still a solvent for the free polyethylene fumarate condensation chains.

3.3.3. Density determination of the cross-copolymer. The densities of the cross-polymer samples were determined in a density gradient tube the use of which has been described elsewhere.[31][32] The method makes use of Pyrex glass floats as reference standards which are used to calibrate density as a function of height in the tube by interpolation. The gradient is established in the tube by the vertical interdiffusion of two miscible liquids which have no chemical or physical effect on the

polymer. A particle of polymer film introduced into the tube sinks to a level at which its density equals that of the surrounding liquid.

a.) Manufacture and calibration of glass floats has been described in details by Gordon and McNab.[33] The floats were made practically spherical in shape and about 2 - 3 mm. diameter from thin-walled capillary (1 mm. diam.) drawn originally from 1.5 cm diameter Pyrex tube. Floats in the desired density range were obtained by controlling the glass-to-air ratio. The spheres were stored for two days before being calibrated since incomplete annealing caused an initial small increase in density.

The floats were calibrated for density by the method described by Gordon and McNab involving flotation of the glass sphere in a density bottle containing a solution of the required density. The float densities were found to 0.0001 gm./ml. The density of the cross-polymer samples lies between 1.191 and 1.2876 and five floats were calibrated to cover this range.

b.) Preparation and use of density gradient tubes. The density gradient was formed in a dumb-bell shaped tube[31] of about 25 cm. stem length and 2 cm. diameter. The heavy solution was placed in the tube with the meniscus in the centre of the stem and carefully topped with the lighter solution so as to preserve the interphase. The floats were then introduced and rested on the interphase. A fine wire coil stirrer was then moved up and down through the interphase with strokes of increasing amplitude so that interdiffusion of the solutions caused the formation of the density gradient which was observed in

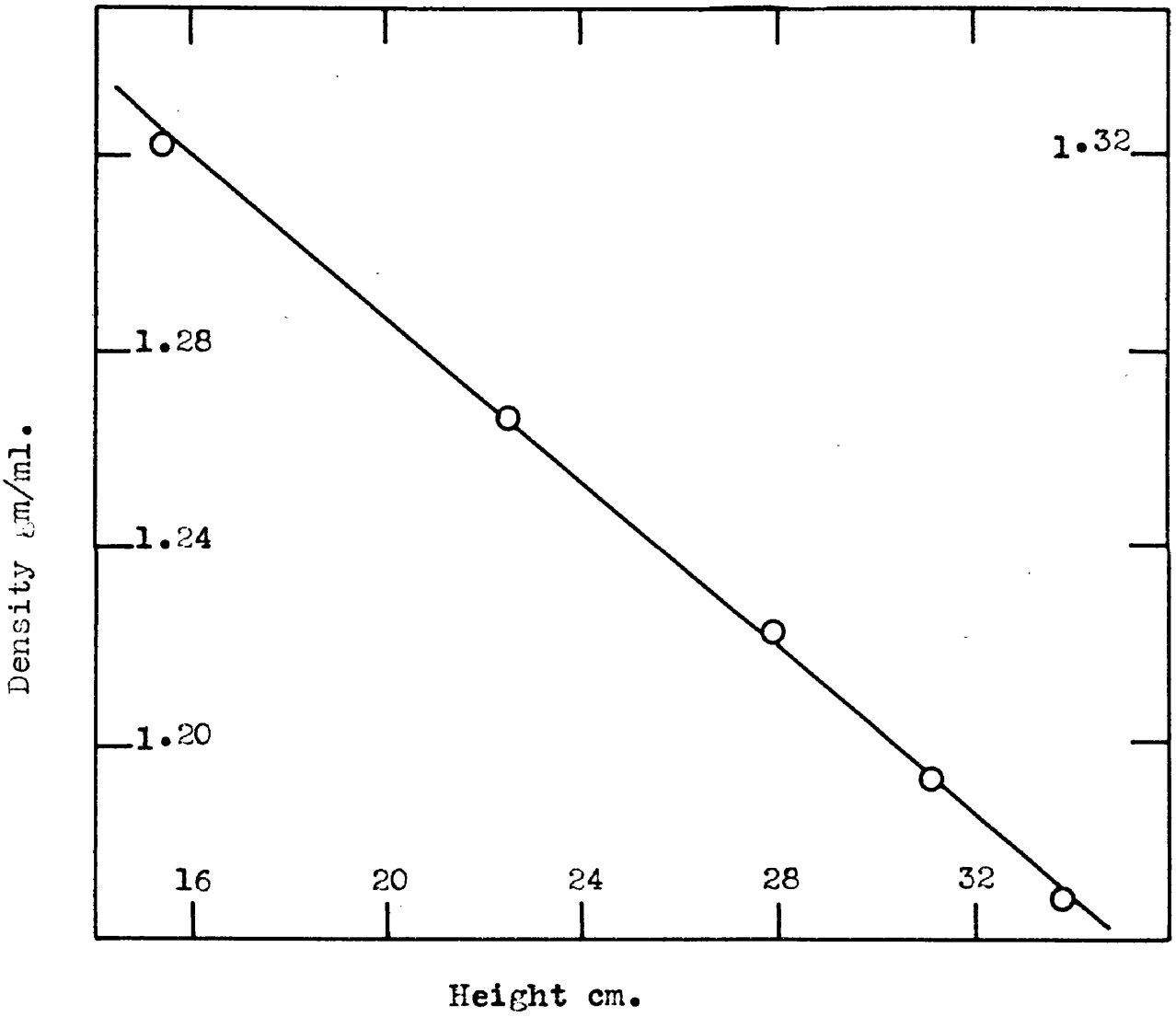

Figure 16. Typical plot of height against density for central portion of tube 1, for cross-polymer samples.

○ represents Pyrex floats.

Plot is expanded for accurate determination of density.

terms of the vertical spreading of the floats. The height against density plot is always sigmoid, approaching the vertical at each end, i.e. at the height of the dumb-bell reservoirs where the density is constant with height.

Individual small particles (a few milligrams) from a polymer powder were pressed to clear films about 1 - 5 mm^2 in area at approximately 150°C for 30 seconds under ca.100 atm. between glass plates. These plates, cut from microscope slides to 5 x 5 mm. in size, were pressed along their edges by two spring-loaded ("bull-dog" type) clips, and a jet of superheated steam directed against each plate. The films were cut into distinctive shapes with a clean razor blade and placed in the gradient tube which was immersed in a 26.7°C water thermostat for 15 mins. The height of the floats and the polymer particles were measured using a cathetometer and plotted as typified in fig.16. The polymer densities determined graphically in this way were accurate to 0.0010 gm./ml. or better.

The solution used in the gradient tube was calcium chloride which was previously degassed in order to prevent the formation of air bubbles on the floats and polymer particles.

3.3.4. Microanalysis and michrohydrogenation of the cross-copolymer.

a.) The cross-copolymer samples were analysed for carbon and hydrogen content by Drs. Weiler and Strauss of Oxford.

b.) The residual unsaturation of the cross-copolymer samples was determined by Dr. A.C. Syme of the Royal Technical College by a microhydrogenation technique. The polymer samples were left standing

in the cold in glacial acetic acid when they became highly swollen and in a suitable state for microhydrogenation. A blank run was carried out on polymethyl methacrylate polymerised, isolated and purified in exactly the same manner as used for the cross-polymer.

3.4. Evaluation of monomer reactivity ratios r_M and r_F. The procedure for calculating monomer reactivity ratios for a binary linear polymerisation consists in analysing the number fraction ρ of monomeric repeat units (fumarate) in the polymerisation chains as a function of the feed ratio R. At low conversions, the following linear equation is obtained by rearranging eqn.(21) and allows the reactivity ratios r_F and r_M to be deduced from slope and intercept by plotting $R\ (1/\rho - 2)$ versus $R^2\ (1/\rho - 1)$:

$$r_F \cdot R^2\ (1/\rho - 1) + R\ (1/\rho - 2) = r_M \qquad (41)$$

As long as not more than one double bond of each poly-fumarate condensation chain has become incorporated into a polymerisation chain, eqn.(41) remains applicable since we are dealing with a linear copolymerisation (free from crosslinks). For this very reason, the same equation applies at the gel point of the MMA/PEF copolymerisation as an almost exact approximation. Of the order of scores of condensation chains enter into each polymerisation chain. At the gel point, however, only one of these chains on average will have a second double bond which has polymerised and thus serves as a crosslink with a second polymerisation chain (fig.15). This average of one crosslink per polymerisation chain follows from the network theory of the gel point

on the assumption that cyclic structures can be neglected in the network.[2] The general applicability of this network theory of gelling to this system was demonstrated in the previous section. Accordingly the experimental polymerisations were carried to the vicinity of the gel point, which occurred at $< 20\%$ conversion of the unsaturation present, and the polymer composition analysed in terms of eqn.(41).

The classical method for determining the number fraction ρ is by elementary microanalysis of the purified polymer. Because in this system, one of the components to be removed (viz. the free polyester condensation chains) is itself polymeric and the gelled polymer is no longer completely soluble, the swelling and extraction technique described had to be adopted. The purified polymer obtained by this method could hardly be expected to be in the state of purity normally obtained in simple systems by repetitive precipitation and redissolution.

The normal method of analysis of the purified polymer depends on the fact that the carbon (or hydrogen etc.) percentage C_F and C_M (or H_F and H_M etc.) of the two homopolymers obtainable from the two monomers F and M separately will generally differ. The weight fractional compositions of copolymers are deducible by linear interpolation of the carbon percentage $C_{copolymer}$ between C_F and C_M, etc. Thus the weight fraction of component F in the copolymer is given by:

$$w_F = \frac{C_M - C_{copolymer}}{C_M - C_F} = \frac{H_M - H_{copolymer}}{H_M - H_F} \qquad (42)$$

These equations are applied to this system for carbon and hydrogen

analysis. Because $C_F - C_M$ and $H_F - H_M$ are small (10.23% and 3.65% respectively) this procedure is not very accurate. Experimentally, it is simpler and more convenient to analyse the copolymer by specific volume measurements, deducing the weight fraction w_F of polyethylene fumarate units by linear interpolation between the specific volumes of pure methyl methacrylate polymer and that of a hypothetical polymer (see fig.17). Thus

$$w_F = \frac{V_{MMA} - V_{resin}}{V_{MMA} - V_{hypothetical\ polymer}} \qquad (43)$$

where V is the specific volume denoted by its prefix. This method, though in principle more accurate than elementary analysis, gave in practice, results in satisfactory agreement but of only the same order of precision.

3.4.1. Range of feed ratios available. Eqn.(41) naturally gives results of the monomer reactivity ratios which are the more accurate the wider the range of R values employed The system here presents yet another difficulty in that the experimentally manageable range is restricted. At high proportions of polyethylene fumarate ($R > 1.5$), the mixtures become too viscous for handling and the conversion at the gel point so low, that efforts in this direction had to be abandoned. Accordingly only the range $0.1 < R < 1.5$ has been covered here in four steps ($R = 0.1, 0.5, 1.0, 1.5$) corresponding to extractions (E, C, B and D respectively).

3.4.2. Conversion of weight fraction w_F to number fraction ρ .

The composition variable w_F, i.e., the weight fraction of (polymerised + unpolymerised) fumarate units in the cross-copolymer, is experimentally accessible from density measurements and microanalysis. According to eqn. (41), however, the number fraction ρ (fraction of polymerised units which are fumarate) is required for evaluating r_M and r_F. To compute ρ from w_F, two statistical assumptions are required. Firstly, as already explained, the number of fumarate units polymerised per condensation chain in the cross-polymer is taken not significantly to exceed unity at the gel point. It is also necessary to know the average number N of fumarate units in those polycondensation chains which are bound in the cross-copolymer. Simple statistical analysis leads to the following results concerning the appropriate average:

a.) Low conversion: The initial copolymer formed incorporates condensation chains whose number average DP is the weight average of the original free polycondensation chain distribution.

b.) Full conversion: The polycondensation chains incorporated in a hypothetical copolymer containing all the initial condensation chains necessarily have the same number average DP as the original distribution.

For an original distribution obeying equations (1) and (2), this implies that the required average N falls in a calculable manner with the copolymerisation progress reaching about half its initial value at full conversion. Because of the low conversion of fumarate bonds when the reaction is stopped at the gel point, case (a.) is assumed to be applicable and the number average of fumarate units per condensation

chain is equated to the weight average DP_{we}, calculated from end group analysis. Then ρ must be calculated from w_F as follows:

$$\rho = \frac{100w_F}{100w_F + 142DP_{we}(1 - w_F)} \qquad (44)$$

3.4.3. Estimated density of polymerised condensation polymer. In order to calculate w_F from specific volume measurements (eqn.43) it is necessary to estimate the specific volume of the hypothetical condensation polymer when one double bond per weight average chain has polymerised. This was done in the following manner from the values of per cent shrinkage P per double bond and reciprocal molar volume $1/M_v$ for ten divalent monomers, quoted in the literature by Nickols and Flowers[34] (see Appendix table 31). The regression line from these values was found to be:

$$P = \frac{2180}{M_v} \qquad (45)$$

Then, for resin F say, substituting for $1/M_v = 1.3475/950$ from the density and DP_{we} values of resin F, P is found to be 3.1%. That is, the polymerisation of one double bond per weight average polymerisation chain (the condition at the gel point) lowers the specific volume of the polyester from 0.743 to 0.720 as shown in fig.17.

3.4.4. Reactivity ratios from density measurements. Despite the excellent reproducibility normally attained with this technique, films prepared from any one cross-polymer sample here gave a considerable

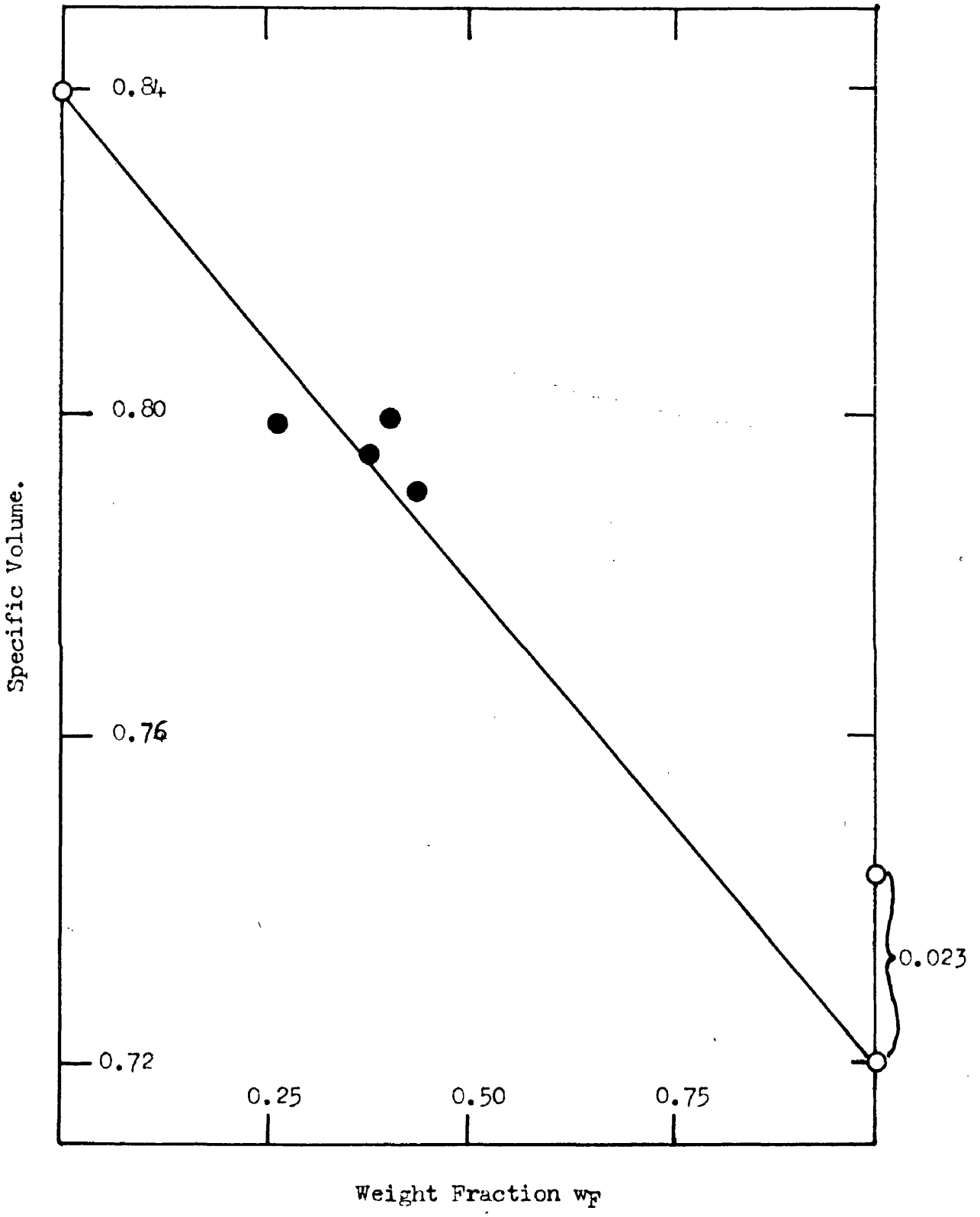

Figure 17. Specific volume of the cross-copolymer at 300°K. vs. fraction w_F of ethylene fumarate units: (●) Experimental points from mean of carbon and hydrogen content. On the ordinate $w_F=\phi$, the upper point shown is for unpolymerized polyethylene fumarate resin F. The point 0.023 unit below this is the estimated specific volume when one double bond per weight-average chain has polymerized.

scatter of density values as exemplified in columns 3 and 5 of table 9. This scatter naturally infects the calculated composition parameter ρ (through eqns. 43 and 44) as also seen in columns 4 and 6 of table 9.

Table 9.

Reproducibility of density measurements of purified (twice extracted) polymers at 300°K.

Film fragment	Pure MMA density	Cross-polymer R = 0.1		Cross-polymer R = 1.5	
		Density	$R(1/\rho - 2) \leqslant r_M$	Density	$R(1/\rho - 2) \leqslant r_M$
1	1.1911	1.2019	13.3	1.2748	15.1
2	1.1910	1.1980	21.2	1.2736	15.6
3	1.1909	1.1973	23.6	1.2718	16.2
4	-	1.1938	55.6	1.2671	18.1
5	-	-	-	1.2606	20.95

The relative reproducibility of the density was found to be unaffected by moderate variations in the time of hot-pressing of the films thus, two fragments from extraction B pressed for 10 and 45 seconds had densities of 1.2535 and 1.2522 gm./ml. respectively, but appeared to be caused by real inhomogeneity of the powder before hot-pressing. This is attributed to the limited efficiency of the purification process, i.e., the extraction of free condensation polymer from gel particles instead of the normal dissolution and reprecipitation of linear polymers. Accordingly, table 9 shows that the higher the R value the worse is the scatter, and excellent reproducibility is seen to attend the determination of the density of polymethyl methacrylate uncontaminated by condensation chains (R = 0), polymerised and purified from monomer by exactly the same

technique as described for the cross-polymer. Superimposed on the difficulty of completely extracting the free condensation chains, there is a marked tendency of the attached condensation chains in the cross-polymer to polymerise further when heated in air. This manifests itself in an increase in density, loss of thermoplasticity and loss of swelling power of the cross-copolymer in Cellosolve after repeated extractions. Both incomplete extraction and after-polymerisation lead to high densities, high ρ and low calculated values of the reactivity ratio r_M. For this reason, it would appear that the most reliable ρ value is obtained after the second extraction, and fig.18 is, accordingly, based on these values of the composition parameters. In the absence of the disturbing after-polymerisation just described, the density and ρ values should decrease somewhat with progressive purification and then remain constant when no free condensation chains are left to be extracted. The reasonable degree of attainment of this ideal is illustrated in table 10 for the runs at R = 0.1 and R = 1; the corresponding points are plotted in fig.19.

Table 10.

Constancy of mean density at 300°K and composition of cross-polymer after repeated purification.

	R = 1.0		R = 0.1	
Purification cycle	Mean density	ρ	Mean density	ρ
1	1.2646	0.0676	1.2005	0.00639
2	1.2510	0.0508	1.1978	0.00454
3	1.2530	0.0532	1.1980	0.00469

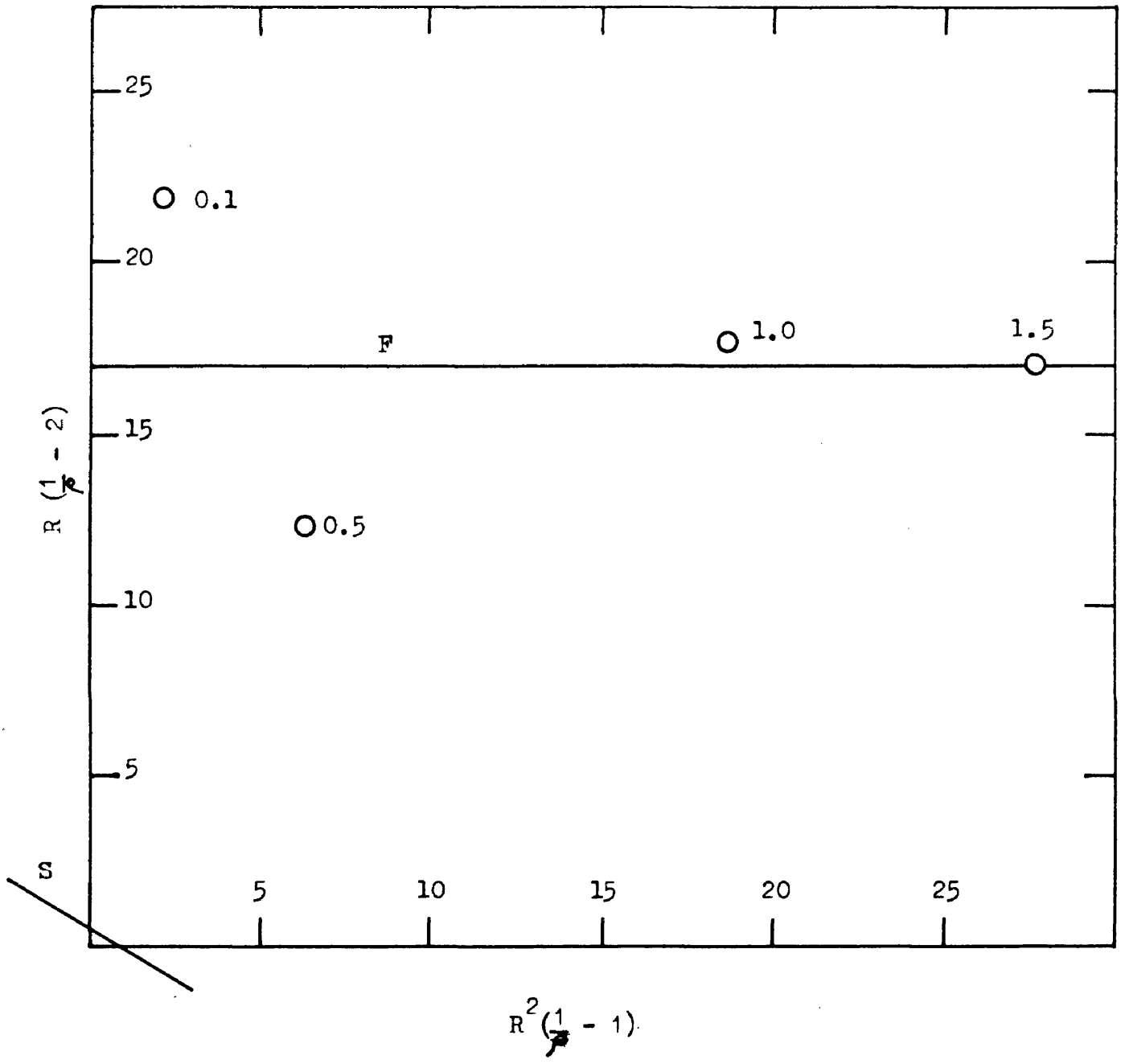

Figure 18. Evaluation of monomer reactivity ratios for methyl methacrylate/polyethylene fumarate. The mean results (from densities) after the second extraction for the R values 0.1, 0.5, 1.0, and 1.5 are plotted. The horizontal line F is intended roughly to represent the data (r_m = intercept = 17, r_F = - slope = 0). The line S for the system methyl methacrylate/styrene (r_m = 0.5, r_S = 0.5) is shown for comparison.

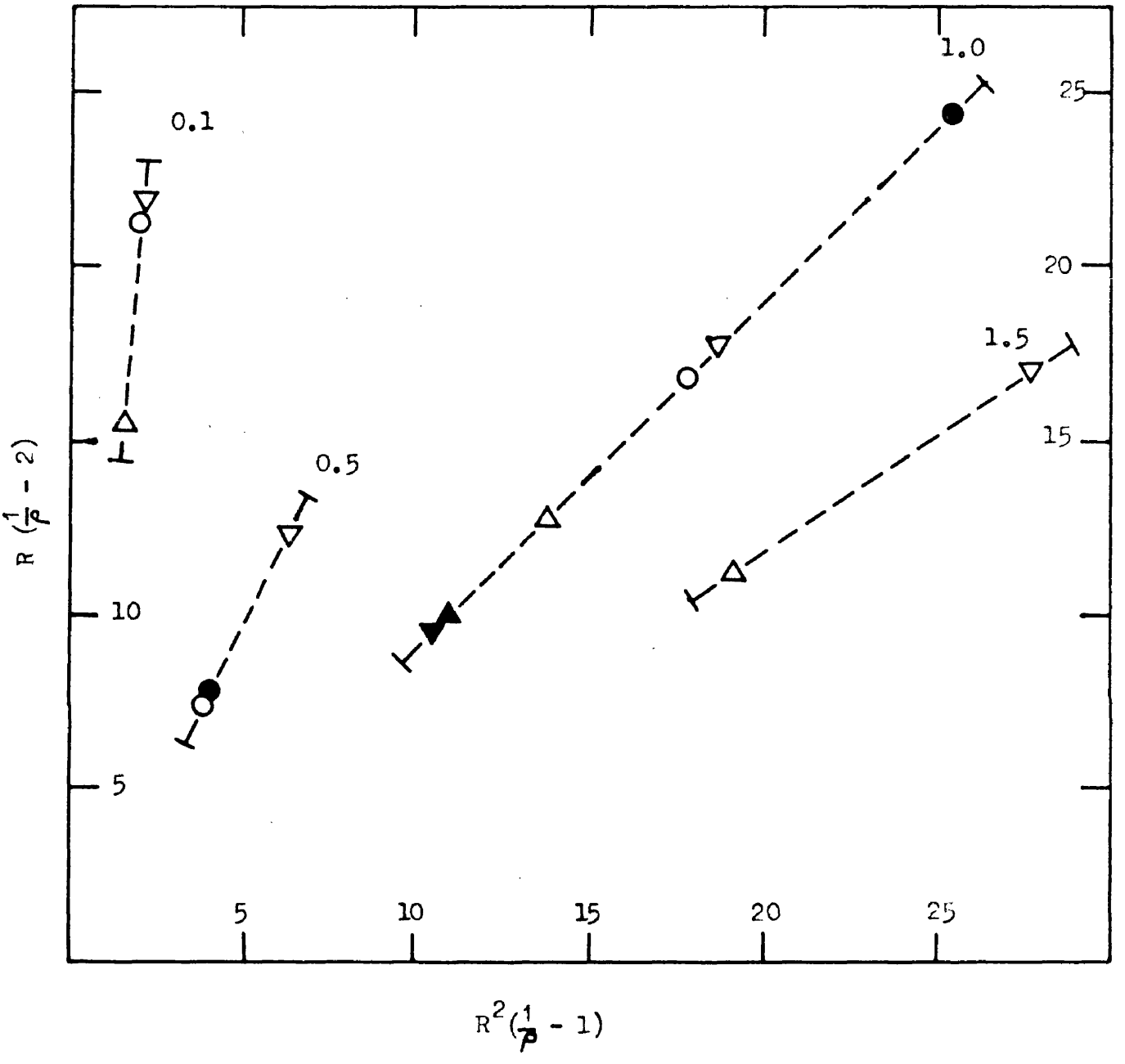

Figure 19. Comparison of microanalysis and density measurements.

The plot reflects the changes in the apparent values for the R values 0.1, 0.5, 1.0, and 1.5. The mean ρ values calculated from C and H microanalysis and from density are compared.

	Mean of C & H microanalyses.	Density.
First extraction.	▲	△
Second extraction.	▼	▽
Third extraction.	●	○

The densities of film fragments for successive purification cycles of individual extractions are tabulated in the Appendix (table 32). Mean densities of successive purification cycles for individual extractions and the parameters calculated therefrom, are tabulated and compared in table 12.

3.4.5. Reactivity ratios from microanalysis: discrepancy between carbon and hydrogen analysis.

The values for the carbon and hydrogen contents of the copolymer when substituted in eqn. (42) gave two different values of w_F (the weight fraction of fumarate component), the carbon analysis invariably giving a value a few per cent higher than the hydrogen value. Since methanol was the last substance in contact with the copolymer (in the final solvent extraction) before drying and analysis, it seemed probable that a small amount of this remaining in the copolymer might be responsible for the discrepancy. From equations based on the carbon and hydrogen contents of methanol and the copolymer (see Appendix P.114), it was calculated that in each sample analysed there was in the region of 3% of methanol impurity present.

Table 11.

Specimen	Analysis Figures		Calculated Methanol Impurity %
	Carbon %	Hydrogen %	
B.1	55.1	6.62	2.5
B.2	55.4	6.67	2.7
B.3	56.75	7.28	3.2
C.3	55.4	6.95	4.3

A similar calculation made on the assumption that Cellosolve was the impurity, showed that about 10% (8.4% in extraction B.2) would need to be present in the copolymer samples in order to account for the difference in analysis. This was thought to be an unlikely explanation since such a relatively large amount of Cellosolve would almost certainly have lowered the temperature required for fusion of the copolymer samples to well below the 150°C found to be necessary in the density measurement technique. As methanol is the most likely impurity, and since only a small and roughly constant amount present in the copolymer would account for the discrepancy in the analysis, it seems probable that it is in fact the cause of the difference.

In order to calculate ρ from eqn. (44) the average of the w_F values from carbon and hydrogen analyses was used. The calculated parameters determining r_F and r_M are tabulated in table 12 and illustrated in fig. 18 and 19 and are seen to give reasonable agreement with those calculated from density measurements.

3.4.6. Reactivity ratios from microhydrogenation - sample calculation.

Microhydrogenation experiments gave the amount of hydrogen absorbed by a given quantity of cross-copolymer. e.g. For extraction B.3 (Resin F, $DP_{we} = 6.56$, $R = 1.0$):

3.357 m.g. of cross-polymer absorbed 0.158 ml.H_2 at N.T.P.
(A blank run on pure polymethyl methacrylate showed no H_2 absorption.)
i.e. 3.357 mg. absorb $0.158/22400$ moles $H_2 = 7.06 \times 10^{-6}$ moles H_2.
Now, for each condensation chain attached to a polymerisation segment of "a" units there are $(DP_{we} - 1)$ points for absorption. i.e. 5.56 moles

(double bonds) saturate a molecular weight of 950 + 100a.

$$\frac{7.06 \times 10^{-6}}{3.357} = \frac{5.56}{950 + 100a}$$

$$a = 16.9 = \frac{R + r_M}{R(Rr_F + 1)} = \frac{1}{\rho} - 1$$

The results of the microhydrogenation experiments carried out are tabulated in table 12. They tend to give rather lower values of r_M, but never admit values below 5.96.

3.4.7. Tabulation and comparison of results from density, microanalysis and microhydrogenation. Results from density, microanalysis and microhydrogenation experiments are tabulated for comparison overleaf.

3.5. Discussion. The plot according to eqn.(41) of the mean results (from density measurement) after the second extraction for the four R values studied is shown in fig.18. A straight line with intercept r_M and slope $-r_F$ is expected, but the first impression of fig.18 reveals the rather poor linearity achieved in practice. This reflects not only the many experimental difficulties already discussed, but also the apparent values of r_M and r_F. However, useful information can be extracted even from the relatively inaccurate results of fig.18. To put matters in a proper perspective the line S has been drawn for comparison, which from the known values of the appropriate reactivity ratios, is applicable when the polyethylene fumarate in this system is replaced by styrene. It is then immediately clear in what sense lie the considerable deviations of the fumarate system from the styrene one, and what is the

Table 12.

Specimen	Density measurements				
	density	w_F	$1/\rho$	$R^2(1/\rho-1)$	$R(1/\rho-2)$
D.1(R=1.5)	1.2876	0.5260	9.55	19.2	11.3
D.2 "	1.2696	0.4350	13.3	27.6	17.0
B.1(R=1.0)	1.2646	0.4080	14.8	13.8	12.8
B.2 "	1.2510	0.3360	19.7	18.7	17.7
B.3 "	1.2530	0.3470	18.8	17.8	16.8
C.1(R=0.5)	1.2562	0.3640	17.52	4.15	7.76
C.2 "	1.2388	0.2710	26.5	6.4	12.3
C.3 "	1.2587	0.3770	16.7	3.93	7.4
E.1(R=0.1)	1.2005	0.0521	156.5	1.56	15.5
E.2 "	1.1978	0.0372	220	2.19	21.8
E.3 "	1.1980	0.0387	213.5	2.13	21.2

Specimen	Microanalysis				Microhydrogenation		
	w_F	$1/\rho$	$R^2(1/\rho-1)$	$R(1/\rho-2)$	$1/\rho$	$R^2(1/\rho-1)$	$R(1/\rho-2)$
B.1(R=1)	0.435	12.0	11.0	10.0	-	-	-
B.2 "	0.402	11.5	10.5	9.5	-	-	-
B.3 "	0.264	26.4	25.4	24.4	17.9	16.9	15.9
E.1(R=0.1)	-	-	-	-	61.6	0.606	5.96
E.2 "	-	-	-	-	64.1	0.631	6.21

order of magnitude of these deviations.

Next it must be borne in mind that a line drawn through these data with a positive slope would be meaningless, as $-r_F$ must be $\leqslant 0$ as defined by eqn.(41). This restricts the range of lines that could be fitted. For the same reason, the ordinate $R(1/\rho - 2)$ of each point gives a minimum estimate of the intercept, r_M. The four mean values of the ordinates in fig.17, as well as the nineteen individual values from which those means were obtained (exemplified in table 9 and table 32), all lie above 7. As the principal experimental errors have been seen to lead to low results of r_M, it would seem reasonable to conclude that $r_M > 7$. It is well known that for values of r_M as large as this, the companion reactivity ratio $r_{(F)}$ is very nearly zero, which corresponds to a nearly horizontal line in a plot such as fig.18. In view of these remarks the line F has been drawn giving $r_M = 17$, $r_F = 0$ as a reasonable fit to the data, and it seems quite justified to assign the limits $10 < r_M < 25$, $0 < r_F < 0.7$. A pair of values ($r_M = 17$, $r_F = 0$) puts a strain on accuracy even with simple systems, and the pair lies outside the useful range of the elegant nomograph published by Whelan for evaluating copolymerisations.(35)

Measurements of monomer reactivity ratios are customarily correlated with the structures of the radical pair concerned. As these measurements are ratios of rate constants, they do not greatly differ for systems in which the substitution pattern around the double bonds of the monomer pair are similar. The application of this test to these measurements on MMA/PEF and the three related systems reported in the

literature is successful. As is evident from table 13, the four systems are characterised by r_M values well in excess of unity, and the companion values $r_{(F)}$ are close to zero.

Table 13.

Comparison of monomer reactivity ratios for related systems.

Methyl methacrylate:	$r_M = 3.5 \pm 0.5$	Fumaronitrile[36]	$r = 0.01$
Methyl methacrylate:	$r_M = 6.7 \pm 0.2$	Maleic anhydride[37]	$r = 0.02$
Methyl methacrylate:	$r_M = 10 - 25$	Polyethylene fumarate: (This work)	$r_F = 0\text{-}0.7$
Methyl methacrylate:	$r_M = 20$	Diethyl maleate.[38]	$r = 0$

The general meaning of these figures is that the methyl methacrylate radical and the maleic or fumaric companion radical both have a marked tendency to react with MMA monomer and little tendency to react with maleic or fumaric companion monomer. The monomer reactivity ratios, together with a given feed ratio R, fix the composition of the cross-copolymer. As an illustration it is convenient to choose a feed ratio of unity, i.e., an equimolar mixture of MMA and PEF unsaturation. Accepting the values $r_M = 17$, $r_F = 0$, which have been approximately suggested by the measurements described above, it follows that the initial cross-copolymer incorporates (eqn.41) in its polymerisation chains one reacted fumarate bond for each $(r_M + R)/R = 18$ reacted methacrylate bonds. More precisely, the numbers x, y.. etc., in fig.15 of methacrylate units intervening between fumarate units follow the usual (approximately exponential) distribution, with a mean of 18. This calculation illustrates the key position of the monomer reactivity ratios

in the quantitative description of a cross-copolymer such as a cross-polymerised unsaturated polyester.

However, it must be remembered that in the later stages of the "curing" of such a resin, the immobilisation of functional groups is expected to lead to variations from the simple copolymerisation scheme underlying eqn.(41), as discussed for related systems by Loshaek and Fox,[39] and in Section 4 of this work.

Though the measurements of r_F and r_M here discussed have been based on density determinations, the validity of the results is borne out by comparison with the values from microanalysis and microhydrogenation experiments in table 12. Indeed the degree of agreement obtained by three totally different methods of measurements is most encouraging.

Two assumptions have been made in the theory given here for the copolymerisation reaction. One, the substantial equality of all the fumarate bonds in a condensation chain, irrespective of their position (e.g., at the end or near the centre of such a chain), has already been justified in the previous section. The other assumption is that no significant fractionation occurs in the purification of the insoluble cross-polymer, i.e., that the fraction remaining insoluble after the final extraction, about 1/5 of the total copolymer, has a ρ value which practically coincides with the remaining 4/5 (table 8). The number N of fumarate chains attached to primary polyaddition chains of fixed length varies about the mean number. The distribution of N is an exponential distribution which is very sharp provided the mean is large (i.e., of the order of scores). The DP of a polyaddition chain is found

to be several thousand, as shown by molecular weight measurement on pure polymethyl methacrylate, so that of the order of scores of fumarate units are incorporated into each polyaddition chain. Therefore, although the exact fraction ρ incorporated may vary slightly from one polyaddition chain to another, statistical theory shows that these variations are negligible.

3.6. Summary and conclusions. The reactivity ratios of the monomers in the system MMA/PEF are found to lie in the ranges $10 < r_M < 25$ and $0 < r_F < 0.7$, these values being based on the density measurements of the extracted cross-copolymer and supported by microanalysis and micro-hydrogenation measurements. These values are in reasonable agreement with the values of $r_M = 29$ and $r_F = 0.25$ used to fit the experimental data to theoretical curves in Section II. The measurements of r_M and r_F presented here thus support the classical network theory of gelation and the copolymerisation kinetic scheme postulated in Section II.

Though it would be desirable to be able to measure these parameters directly with greater accuracy it is not immediately clear how this could be effected. The problem really centres on the extraction of the cross-copolymer in a pure form and not on the method of analysis of the cross-copolymer itself. The difficulties involved in the attainment of this ideal cannot be stressed too strongly. This work does not claim to give accurate measurements of these reactivity ratios but serves rather as a corroboration of the general nature of the copolymerisation involved and it is thought that this has been accomplished satisfactorily.

SECTION 4.

Kinetic Investigation of the Post-Gelation Rate Plot.

4.1. Introduction. The first stage of the bulk polymerisation of the MMA/PEF system occurring at low conversion and viscosity, so that the rate plots could be treated by mass law theories, has been shown to behave as a classical copolymerisation, for which the important kinetic parameters have been approximately deduced. The end of this first stage is marked by the gel point since immediately afterwards the rate plot in this and other similar systems[15][22] has been observed to increase suddenly (Trommsdorf or gel effect).[40][41]

As the result of experiments on the system methyl methacrylate and ethylene dimethacrylate (MMA/EDMA) Gordon and Roe have proposed a model[22] for this second stage in a vinyl bulk polymerisation, that of diffusion control of the termination step, of non-linear polymerisations. This model predicts the shape of the rate curve after the gel point, and the model is applied here to the MMA/PEF system.

The present investigation entails a critical examination of the post-gelation rate plot, to the limit of applicability of the dilatometric technique under a wide range of experimental conditions, namely, feed ratio, catalyst concentration and temperature. The range of experimental conditions is limited, however, since polymerisations of this type can only be followed dilatometrically to about 20% conversion when the shrinking gel developes an internal tension as it becomes less deformable, and eventually breaks. It is therefore

necessary to obtain a set of conditions so that the gel point occurs at as low conversions as possible. This necessarily precludes low feed ratios, high temperature and catalyst concentration.

The reduced rate curves are found to superpose over the wide range of experimental conditions (fig. 23 and 24) as demanded by the theoretical treatment, but theory exaggerates the extent of the Trommsdorf rate acceleration since it does not allow for termination between pairs of crosslinked radicals.

Two additional polymerisation systems, used industrially as laminating resins, are examined as regards their absolute gel points, and the shape of their rate plots is compared and contrasted to that of the MMA/PEF system. The absence of a kink in their rate plots is attributed to their relatively short primary chain lengths.

4.2. Experimental.

4.2.1. Emergent stem dilatometer. A fully immersed dilatometer (or viscodilatometer) cannot be used at high conversions after the gel point, and the experimental technique involving a dilatometer with an emergent stem[4][15] was employed. The instrument is sketched in fig.20. It consists of about 10cm. length of 1.5mm. precision bore capillary tubing joined to a dilatometer bulb of from 1.5 - 7ml. volume depending on the experimental conditions, so that down to 0.0025% contraction per minute could be detected with accuracy. A clamping rod attached to the bottom holds the dilatometer in position. The instrument was clamped so that the level of the thermostatted water bath ($\pm 0.05^{\circ}C$) was about 1cm. above the join of the bulb and stem. The resin in the stem

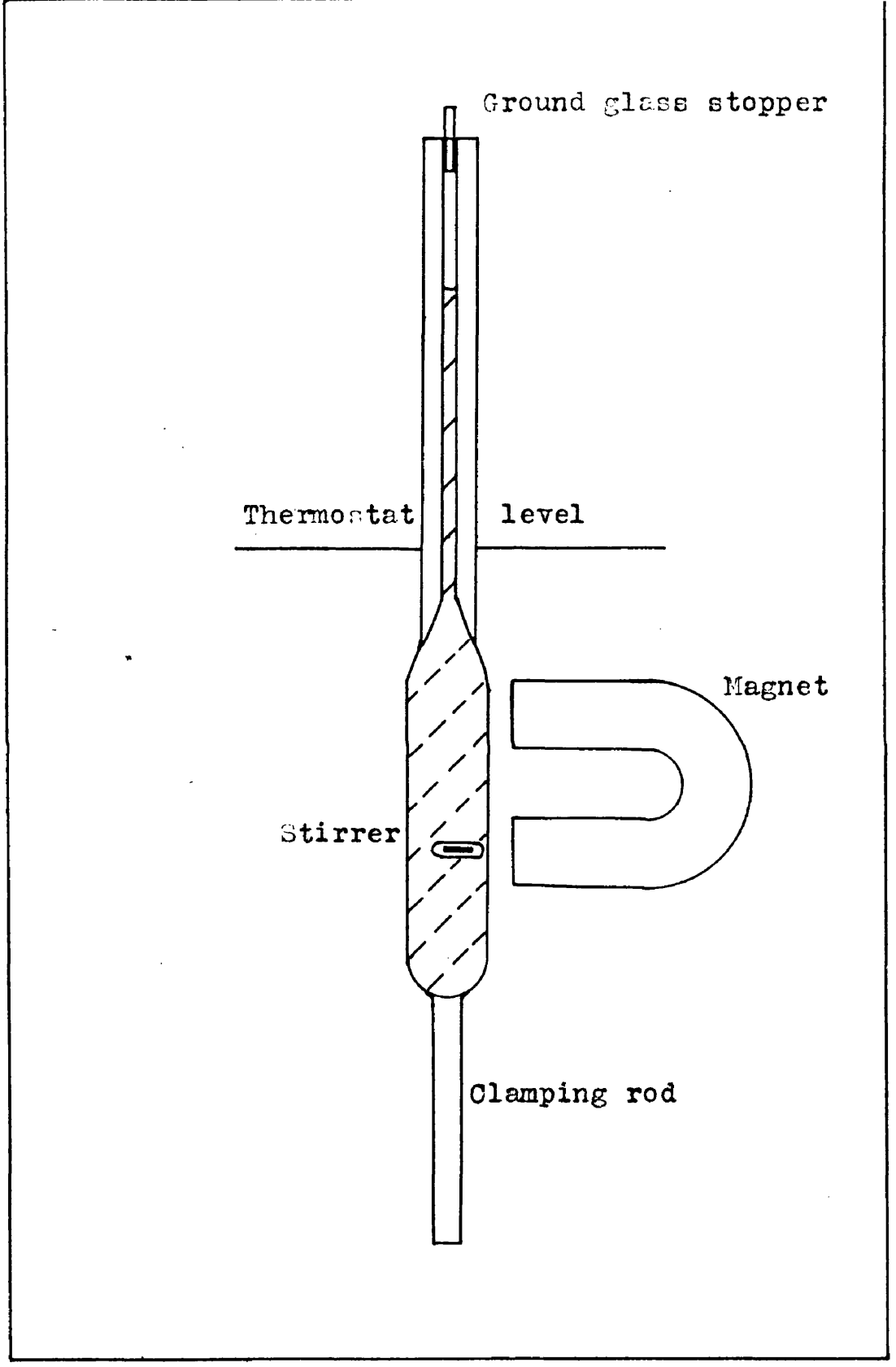

Figure 20.

Emergent stem dilatometer with magnetic probe.

then remained liquid even when the bulk of the resin in the bulb had gelled. As the resin contracted the liquid column was drawn slowly into the bulb, the movement of the capillary meniscus being followed with a cathetometer and its position plotted against time. The intrusion of the colder liquid in the stem into the bulb was not serious since the amount was small compared with the total. The dilatometer was filled through the stem by a finely drawn out capillary funnel. A ground glass stopper was fitted into the stem to prevent monomer evaporation.

The gel point was located by the stirrer probe, consisting of a glass covered steel wire, which could be raised magnetically as illustrated and allowed to drop under gravity. Observations, typifying the sharpness of gelation are given in table 14.

Table 14.

Typical observation on the sharpness of gelation, for resin N,R = 1.25, 0.50% MEK and 42.0°C.

Actual reaction time (min.)	Conversion %	Movement of probe	Remarks.
0	0.0	Falls freely.	End of induction period.
15.5	0.50	Falls freely.	
17.5	0.56	Falls slowly to bottom.	
18.5	0.59	Falls very slowly.	Probe viewed through cathetometer.
19.5	0.62	Does not fall to bottom.	Gel point.
20.5	0.69	Moves in "cell" bounded by gel.	
22.5	0.78	Completely immovable.	
144.5	9.9		Gel breaks implosively.

Gel formation near the bottom of the dilatometer bulb always preceded that in the rest of the bulb by a short time. The first appearance of gel was always taken as the gel point, i.e., the time when the probe stopped falling under gravity as viewed through the cathetometer. As reported by Gordon and Roe, the probe could be moved by the magnet, for some minutes after the gel point, in a liquid "cell" caged in by gel which they attributed to the mechanical degradation induced by the movement of the probe. This mechanical degradation of weak gel was reported and discussed by Gordon and Grieveson in an earlier publication.(15)

The polymerisation was followed as described for as long after the gel point as possible, usually till the internal tension developed by shrinkage caused the gel to break. The break usually took the form of a sudden mild implosion. Sometimes the liquid in the stem gelled before the internal tension reached this critical point and generally it was not possible to follow the polymerisation beyond 20% conversion.

The volumes of dilatometers used in these experiments were calibrated with distilled water. It was impossible to clean out the bulb and a new dilatometer had to be manufactured and calibrated for each run. Typical plots of conversion versus time are shown in fig.21 and an enlarged detail of the rate increase at the gel point is shown for one typical run in fig.22.

A list of the runs carried out in this manner is shown in table 15, the reproducibility of the gel point and rate measurements by this method being clearly demonstrated.

Table 15.

Details of kinetic runs with resin N and commercial resins.

Run	Feed ratio R	Temp. °C	% MEK	Time in mins. of Induction	Time in mins. of gel point	Time in mins. of kink	Ratio of slopes at kink	10^5 rate mole.l^{-1} sec.$^{-1}$	% Conversion at gel point
N72	1.75	62	0.52	4.0	3.0	4.0	1.14	35.9	0.96
N42	1.25	70	0.51	2.0	3.0	4.0	1.30	149.4	1.10
N10	1.25	62	1.00	3.5	9.5	10.0	1.31	35.8	2.27
N12	1.25	62	0.54	5.0	7.0	7.0	1.29	29.4	1.37
N60	1.25	62	0.51	5.0	7.0	7.5	1.21	28.40	1.32
N62	1.25	62	0.62	5.0	7.0	8.0	1.21	29.25	1.56
N46	1.25	52	3.85	11.0	52.0	-	-	21.55	7.46
N50	1.25	52	2.50	9.0	34.0	39.0	1.18	19.53	4.43
N54	1.25	52.7	1.96	7.0	20.5	20.5	1.17	20.50	2.81
N14	1.25	52	0.51	4.0	11.5	11.5	1.40	12.20	0.93
N22	1.25	51.7	0.55	11.5	10.5	10.5	1.42	11.07	0.70
N24	1.25	52	0.54	11.5	8.5	9.5	1.23	12.23	0.69
N58	1.25	52	0.52	11.5	9.5	11.5	1.25	11.02	0.70
N26	1.25	52	0.50	11.5	7.5	8.5	1.20	12.14	0.61
N48	1.25	52	0.11	23.0	9.5	14.0	1.25	7.55	0.48
N56	1.25	52	0.13	23.0	10.0	12.0	1.20	7.20	0.48
N16	1.25	47	0.51	18.5	16.0	17.5	1.39	7.56	0.81
N28	1.25	47	0.50	19.5	12.5	12.5	1.21	7.95	0.66
N18	1.25	42	0.51	34.0	20.0	21.0	1.28	4.46	0.53
N20	1.25	42	0.50	35.5	19.5	19.5	1.24	4.75	0.62
N30	1.25	42	0.53	32.0	19.0	19.0	1.18	5.15	0.68
N32	1.25	37	0.52	58.0	27.5	29.0	1.20	3.50	0.64
N34	1.25	27	0.51	199.0	66.0	72.0	1.16	1.61	0.71
N36	1.25	27	0.50	210.0	65.0	70.0	1.19	1.40	0.60
N8	1.0	62	1.97	3.0	17.0	15.5	1.20	56.40	4.39
N64	1.0	62	0.54	6.5	14.5	14.5	1.20	27.40	2.64
N44	0.8	70	0.51	2.0	13.5	13.5	1.23	99.00	3.80
N6	0.5	62	1.97	3.0	61.0	64.0	1.24	39.40	16.00
N40	0.5	62	0.53	6.5	48.5	47.0	1.19	23.10	7.45
N70	0.5	62	0.54	7.0	56.0	56.0	1.21	20.45	7.64
N66	0.2	62	0.51	4.0	96.0	-	-	24.0	15.33
N68	0.2	62	0.51	5.0	90.0	95.0	1.13	22.70	14.39
28c	0.25	52	0.40	27.0	12.0	No kink		31.4	2.51
28o	0.25	42	0.53	66.0	90.0			4.16	2.50
TAC	-	62	0.51	25	1420.0	No kink		0.47	8.85
TAC	-	62	0.51	20	1360.0			0.46	8.45

4.3.1. Measurement of the rate kink. Typical rate curves for the system are illustrated in fig.21. The rate increases linearly with time in all runs up to the close vicinity of the measured gel point then accelerates linearly for a short time as shown in greater detail by fig.22. In each of the thirty runs where the polymerisation proceeded far enough, this increase of the rate at the gel point, marked by a sharp kink in the rate plot, was observed. The values for the ratios of the slopes in column 8 of table 16 were measured as typified in fig.22, drawing the portion of the rate plot on each side of the gel point in a large scale and calculating the gradient of each line graphically. The comparison of the graphical with the ratios of the slopes of the regression lines (after and before the kink) are given in table 16.

Table 16.

Graphical tangent ratios compared with calculated regression line ratios.

Run	Ratio of tangents.	
	Graphical method	Calculated regression line
N.26	1.20	1.200
N.32	1.20	1.206
N.34	1.16	1.148
N.36	1.19	1.183

The excellent agreement between the tangent ratios found by the graphical method and those from the calculated regression lines for the four runs selected at random provides a satisfactory test for the accuracy of the tangent ratios found graphically and tabulated in table 15.

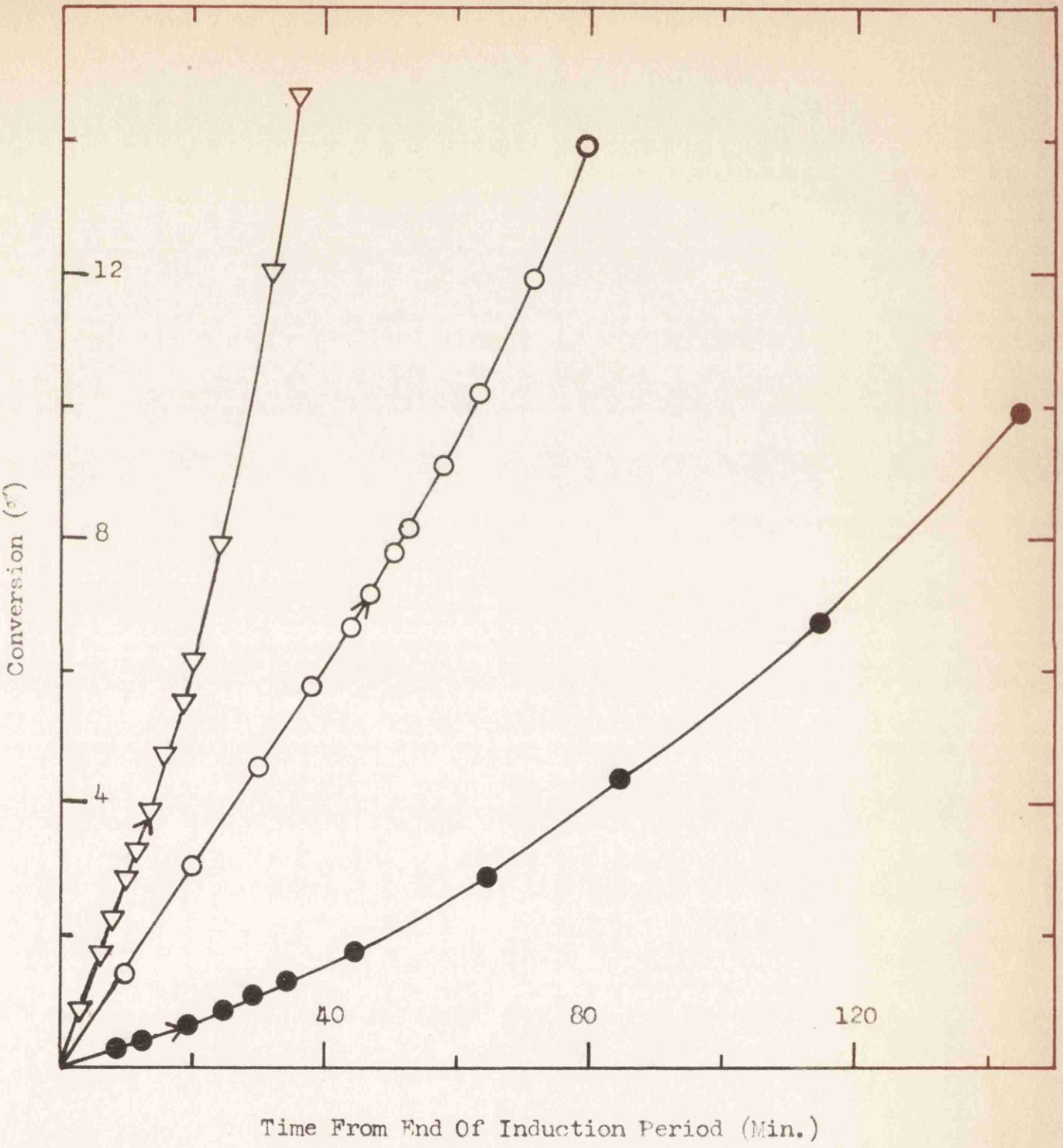

Figure 21. Rate curves for M.M.A./P.E.F. (Resin N.) showing Trommsdorf rate acceleration. Arrows mark the observed gel points. The same curves are reduced to coincidence in figure 22 where the gel points correspond to $t' = 1, \nu = 1$.

	R	% M.E.K. catalyst	Temp. °C.
●	1.25	0.5	42
○	0.5	0.53	62
▽	0.8	0.51	70

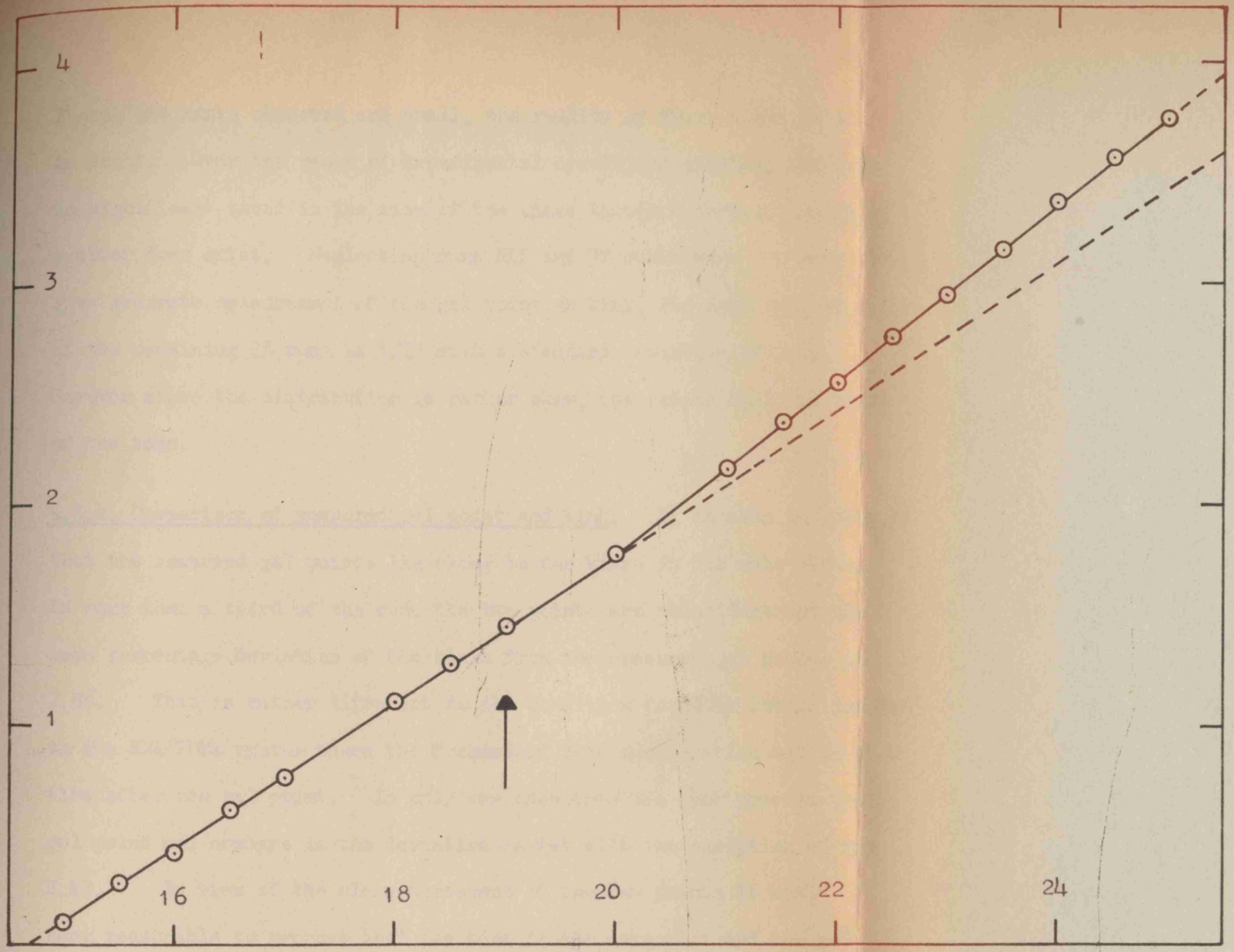

Figure 22 . Enlarged view of portion of rate curve in the vicinity of the gel point.

Though the kinks observed are small, the reality of these kinks is not in doubt. Over the range of experimental conditions studied, there is no significant trend in the size of the kinks though a certain amount of scatter does exist. Neglecting runs N42 and 72 which were too rapid to give accurate measurement of the gel point or kink, the mean tangent ratio of the remaining 28 runs is 1.23 with a standard deviation of 0.07. However since the distribution is rather skew, few ratios fall far short of the mean.

4.3.2. Comparison of measured gel point and kink. It is seen in table 15 that the measured gel points lie close to the kinks in the rate plots. In more than a third of the runs the two points are coincident and the mean percentage deviation of the kinks from the measured gel points is 7.5%. This is rather different to the condition found by Gordon and Roe in the MMA/EDMA system where the Trommsdorf rate acceleration set in some time after the gel point. In only one case does the kink precede the gel point and nowhere is the deviation marked with the exception of run N.48. In view of the close agreement of the two points it would seem reasonable to propose that the kink in the rate plot and the gel point occur at the same time.

4.4.1. The Reduced Rate Curve. Typical rate curves for the system are shown in fig.21 showing the rate acceleration which occurs at the gel point, marked by the arrows. This is the well known Trommsdorf effect,[40][41] the accepted interpretation of which is an increase in the rate of monomer consumption attributed to the diffusion controlled

reduction in the rate of radical termination.

Gordon and Roe have extensively investigated the Trommsdorf effect in the MMA/EDMA system and have put forward a theoretical model[22] for interpreting the shape of the rate curve after the onset of diffusion control of the termination step. Their treatment, which will be briefly summarised in this work, leads them to suggest that the crosslinking index ν', defined as the number of crosslinks per weight average primary polymerisation chain, is the key variable in the diffusion controlled termination in bulk polymerisation. Gordon and Roe derived a simple test for this conclusion. The test depends critically on the assumption that for each experiment the crosslinking index ν is unity at the gel point in accordance with the classical network theory of gelation (Stockmayer[2]). This assumption allows ν to be determined at all stages of a copolymerisation run provided the fractional conversion β of the total unsaturation is known, since β is proportional to ν and the gel point fixes the proportionality constant. To apply the test, all the β scales (fig.21) are merely transformed to ν scales by a linear scale transformation. Since only rates relative to the initial rate are required in studying the Trommsdorf acceleration, the initial rate lines are brought to coincidence by a linear transformation of the time scale from t to t'. This means that:

$$\nu = \beta/\beta_c \qquad (46)$$

$$\text{and} \quad t' = t/t_c \qquad (47)$$

The two transformations together amount to a process of bringing the

gel points of all the runs to coincidence by a single linear co-ordinate transformation. The curves so obtained are called reduced rate curves in which the relative acceleration of the polymerisation rate of all the runs is compared at equal $\sqrt{}$ values. This test is carried out in figs. 23 and 24 and is highly successful in the MMA/PEF system, since very diverse curves including the three shown in fig.21 are brought to coincidence within experimental error.

4.4.2. Gordon and Roe quantitative theory of the Trommsdorf effect.[22]

Gordon and Roe assume that, in the steady state of a nonlinear polymerisation where the radicals are widely distributed in size, of the two colliding radicals, the diffusion coefficient of the smaller one is the rate-controlling factor in diffusion-controlled termination. The Gordon/Roe model oversimplifies, however, by assuming a size barrier below which a radical diffuses freely, but above which it becomes completely immobilised, whereas the barrier is more gradual in practice. Their model assumes that each terminating collision involves at least one of the small (freely diffusing) radicals, whose concentration is denoted by c. The total concentration of radicals (small and large) is denoted by C. The termination rate is then:

$$\text{termination rate} = k_t cC \qquad (48)$$

Here k_t is defined as a true constant equal to the initial termination constant. The apparent variations in k_t during the Trommsdorf acceleration are absorbed in variations in the concentration c. Gerrens[42] and Bartholomé[42] have independently pleaded that k_t should be defined

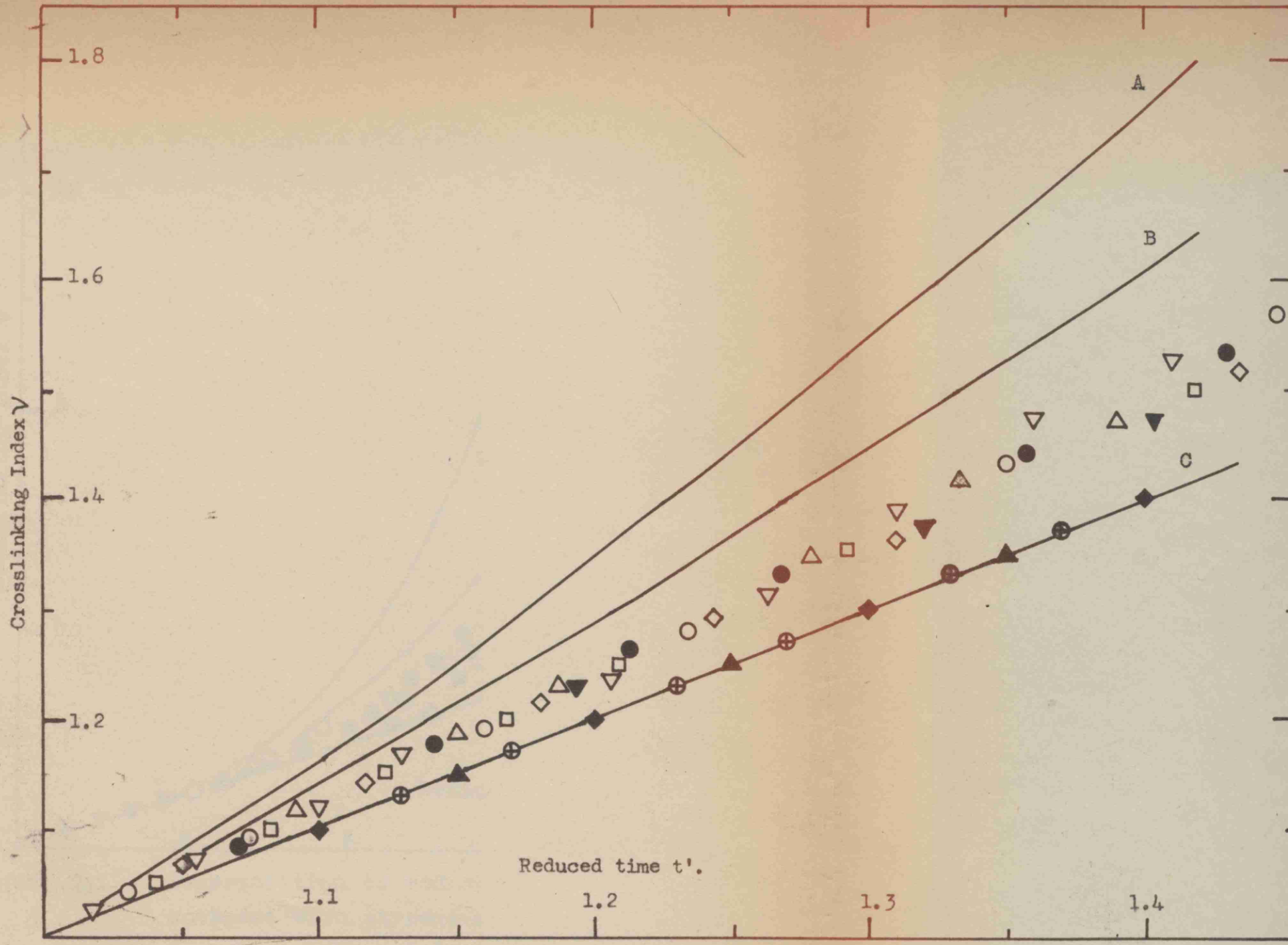

Figure 23. Superposition of reduced rate curves for M.M.A./P.E.F. in contrast with styrene-based polyester, and T.A.C. polyester.

Resin. R. % MEK catalyst. Temp. °C.

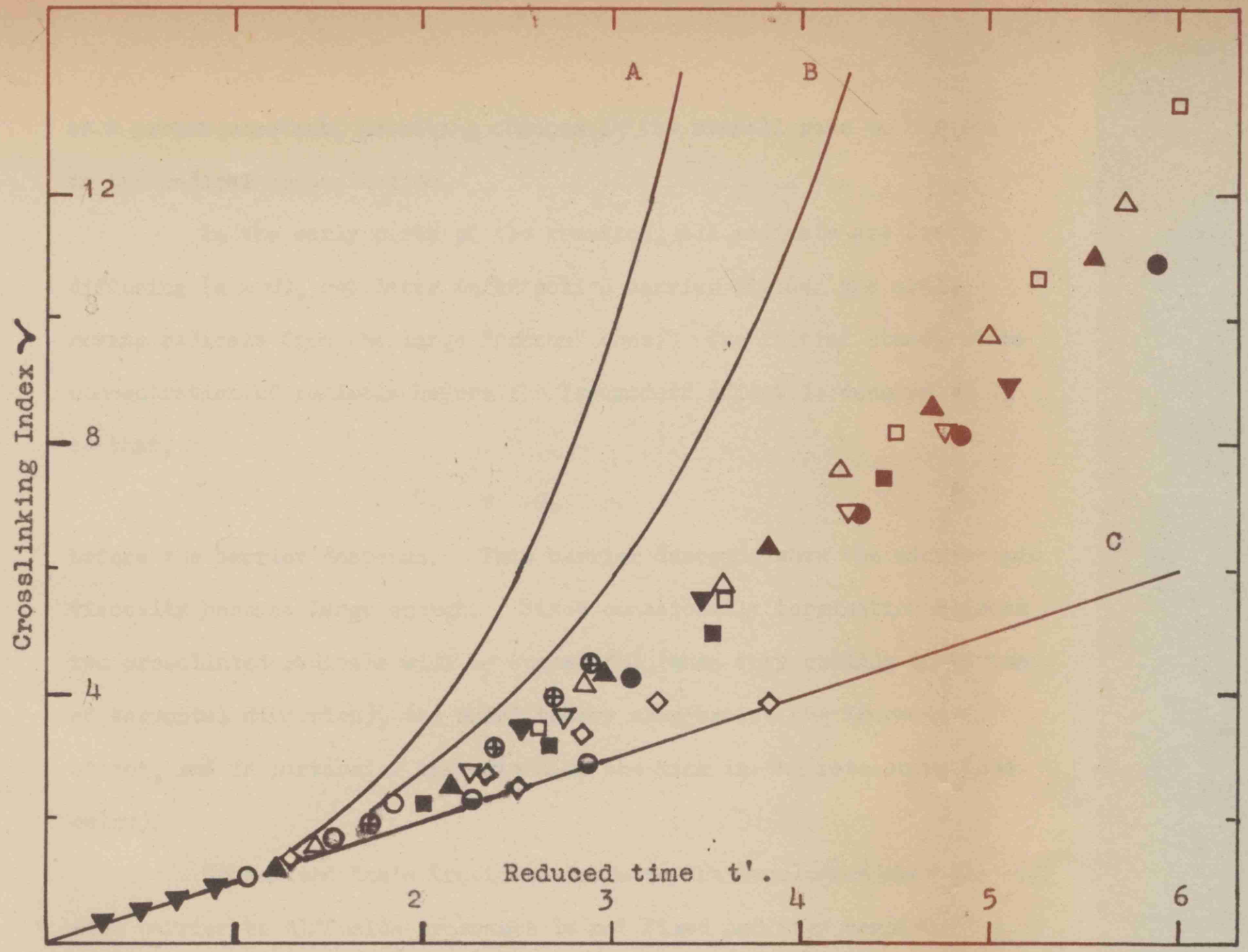

Figure 24. Superposition of reduced rate curves for MMA/PEF and MMA/EDMA in contrast with styrene-based polyester.

Resin.	R.	%MEK catalyst.	T°C.	Resin.	R.	%MEK catalyst.	T°C.
△ PEF resin N.	1.25	0.54	62	▼ PEF	4.28	1.00	62

as a proper constant, ascribing changes in the overall rate to changes in the radical concentration.

In the early parts of the reaction, all radicals are freely diffusing (c = C), but later an effective barrier divides the small moving radicals from the large "frozen" ones. The initial steady state concentration of radicals before the Trommsdorf effect is denoted by C_o so that,

$$C_o = c_o \qquad (49)$$

before the barrier descends. This barrier descends when the microscopic viscosity becomes large enough. Since occasionally termination between two crosslinked radicals will be successful (when they collide in virtue of segmental diffusion), the model theory exaggerates the Trommsdorf effect, and in particular the extent of the kink in the rate curve (see below).

Gordon and Roe's treatment leads to the conclusion that the size barrier to diffusion processes is not fixed and they consider the barrier theoretically, by studying first two limiting cases, A and B, followed by a satisfactory intermediate case C.

Case A. Here c = C, all the radicals are mobile so that there is no diffusion control of termination and the rate curve corresponds to the linear plot (C) in figs. 23 and 24, i.e., complete absence of the Trommsdorf effect.

Case B. In the opposite extreme case, c = 0, all the radicals present at the gel point or generated thereafter are immobilised. They are therefore prevented from engaging in any kind of termination reaction,

and the size barrier is zero (i.e., down to the monomer). The initiation and propagation rates are unaffected since both involve freely mobile monomer molecules. In this case the polymerisation would be almost explosive and the rate curve would become practically vertical almost immediately.

Since neither the extreme cases where none or all the radicals are immobilised conformed to the experimental data Gordon and Roe postulated that the true size barrier lay between these two extreme cases.

Case C. Here all uncrosslinked radicals diffuse freely. A small freely diffusing, growing, radical is pictured. Its most frequent propagation step is the addition of a methyl methacrylate monomer or, less frequently, a free PEF monomer. However, occasionally it may become crosslinked by reacting with a fumarate bond already attached to a fully grown polymer chain which may or may not be crosslinked to further chains. Random statistics leads to the qualitative result that just after gelation, where Gordon and Roe postulate that the size barrier is becoming effective because of the rapid divergence of the viscosity to infinity, a radical will grow on average to the order of magnitude of a dead primary polymer chain before acquiring a crosslink. The radical then becomes attached to a dead polymer chain, which thereafter it must attempt to drag with it when diffusing. The average size of the dead polymer chain acquired by crosslinking is the weight average size of a primary polymerisation chain. This means, qualitatively, that almost every time a radical acquires a first crosslink, its size will increase more than twofold by virtue of such attachment. This led Gordon and Roe to associate the

crosslinking process with the size barrier, by identifying c with the concentration of crosslink-free radicals. Their treatment, in which the concentration c is evaluated as a function of ν, leads to the two equations for the rate curve, for radical termination by disproportionation and combination respectively:

$$t' = 1/4 \left[4 \ln \left(\nu + (\nu^2 + 4)^{\frac{1}{2}} \right) + (\nu^2 + 4)^{\frac{1}{2}} - \nu^2 - 1.934 \right] \quad \text{(disproportionation)} \qquad (50)$$

$$t' = 1/6 \left[9 \ln \left(\nu + (\nu^2 + 9)^{\frac{1}{2}} \right) + (\nu^2 + 9)^{\frac{1}{2}} - \nu^2 - 8.997 \right] \quad \text{(combination)} \qquad (51)$$

The theoretical curves (A and B) predicted by eqns.(50) and (51) respectively are plotted in figs.23 and 24 along with the experimental results for the MMA/PEF system and two commercial resin systems.

4.5. Discussion of results. The superposition of the MMA/PEF runs is shown in figs. 23 and 24. The straight portion of the rate plot immediately after the gel point is shown in fig.23, the regression line of which has a gradient of 1.243 compared to the mean of all the runs listed in table 16 of 1.23 ± 0.07. The ratio of the tangents on each side of the kink is given by the model as 1.62 for radical disproportionation (eqn.50, curve A. fig.23 and 24) and as 1.39 for radical combination (eqn.51, curve B, fig.23 and 24), i.e., the model exaggerates the extent of the kink as noted earlier. The rate curves summarised in table 15 and figs. 23 and 24 cover a molar feed ratio R of fumarate to methacrylate unsaturation between 0.2 and 1.75, and a range from 0.11 to 2.15 weight per cent of methyl ethyl ketone peroxide catalyst. A 45°C range of

temperature has been included as a variable not previously considered by Gordon and Roe. The absolute initial rates varied over a 100-fold range. In conformity with the model theory, none of these variations affect the superposability of the reduced rate curves in figs. 23 or 24. It can be seen from fig 23 that at high catalyst concentration the rate curve does not increase so steeply. It is possible that at high catalyst concentration there is some chain transfer involving catalyst itself and clearly further work in this direction is desirable. Fig. 24 includes some representative points from Gordon and Roe's paper on MMA/EDMA,[22] a system which itself gives rate curves which superimpose well after reduction. It is seen that the reduced rate curves of the two systems agree within experimental error, though the common component (MMA) sometimes makes up less than half the weight of the mixtures. The catalysts employed were also different for the two systems, viz. MEK and benzoyl peroxide respectively. The constancy of the reduced rate curve in the face of chemical changes forms the severest possible test of the model theory.

It may be mentioned that a central point in the theoretical treatment has found incidental verification in the work of Schulz[42] on the homopolymerisation of MMA(R = 0). He showed that the chain length during the second stage remains proportional (cf. reference 22, eqns. 3 and 4) to the rate over an 80-fold range. (Over this large range he had to make corrections for transfer to monomer, and for changes in monomer concentration, both of which are negligible in the present applications).

The agreement between the quantitive theory and the combined experimental runs in fig.23 and 24 depends on the nature of the termination mechanism assumed. Equation (51) which assumes radical combination is seen to give a much closer approach to the experimental curves. The degree to which disproportionation and combination participate in MMA polymerisation is controversial. Baysal and Tobolsky[43] have argued that combination alone is operative, while Bamford and Jenkins[44] from coupling work with block copolymers have reported strong evidence for termination by radical disproportionation. Figures 23 and 24 clearly incline to the former view but the agreement is seen not to be quantitative. The deviation, however, is not serious, and is in the sense of an observed termination rate faster than predicted from eqn.(51) on the assumption that c denotes crosslink-free radicals only. Gordon and Roe showed that the agreement cannot be substantially improved by raising the assumed size barrier, i.e., by including radicals bearing exactly one crosslink, (as well as those bearing none), in the concentration c.

4.5.1. Styrene-based polyester and triallyl cyanurate. Dilatometric polymerisation rate curves of a commercial styrene-based polyester (Scott-Bader resin 28o) showed no trace of a kink at the gel point (fig.23) nor did those of triallyl cyanurate. It is shown below that the observed gel points are in substantial agreement with the network theory of gelation, so that the model theory would be expected to apply on this score. The absence of a kink at the gel point means that this is not the point at which termination becomes affected by diffusion control,

i.e., in terms of the model theory, crosslinked radicals do not become frozen at this point. The explanation offered attributes the failure of the model theory to the much shorter primary chain lengths attained by styrene and triallyl cyanurate radical chains when compared to MMA radical chains. More specifically, a styrene radical embodying several crosslinks and a triallyl cyanurate radical embodying hundreds of crosslinks are likely to be smaller in size, and hence diffuse more readily, than an uncrosslinked MMA radical.

The shorter chain length of styrene radicals is similarly evidenced by the much later onset of the Trommsdorf effect in the homopolymerisation of styrene[18] compared to MMA. It is calculable from values of k_p^2/k_t by Bamford and Dewar[45] that at the same temperature (0°C) styrene radicals attain to about 1/25 of the length of methacrylate radicals at equal rates of homopolymerisation of the two monomers. In the case of allyl polymerisations, the primary chains are normally cut to a length of a mere 20 repeat units by degradative chain transfer.[46]

4.5.2. Network theory of the gel point applied to styrene-based polyester and triallyl cyanurate. The following equation for the critical fractional conversion β_c of all the original unsaturation (fumarate and methacrylate) at the gel point is easily derived from equations (15) and (24) in Section 2:

$$\beta_c = R/(R + 1)\rho^2 (DP_{wp} - 1)(DP_{wo} - 1) \qquad (52)$$

where the fraction ρ of the polymerised double bonds which are fumarate rather than methacrylate is given by,

$$\rho = R\,(Rr_F + 1)/(r_M + R(Rr_F + 2)) \qquad (53)$$

DP_{wp} is the weight average polyaddition chain length, and DP_{wc} is the number of fumarate double bonds in the initial weight average polycondensation chain. The reactivity ratios for methacrylate and fumarate radicals are denoted by r_M and r_F.

The dilatometer measurements in table 17 (transforming run N44 with the aid of fig.10 and 12) compare the gel points under comparable conditions of the model system MMA/PEF and a commercial styrene based (S/PPFP) polyester designated as 28c. This commercial polyester contains a condensation resin (1 mole maleic anhydride converted to fumarate ester, 1 mole of phthalic anhydride, and 2.5 moles propylene glycol) of acid number 50. This resin is marketed with styrene monomer in the weight proportions of 35 to 65. It will be seen that at equal polymerisation rates and temperatures, the critical conversions of the two systems are roughly equal.

The only material factors in evaluating β_c for the two systems from eqn.(52) are ρ^2 and $(DP_{wp} - 1)$, and to produce equal gel points in the two systems there must be compensation between these factors. The rough measurements of $r_M = 17$, $r_F = 0.25$ lead (eqn.(53)) to $\rho^2 = 0.0026$ for MMA/PEF. For S/PPFP, ρ^2 will lie close to 0.25, since the reactivity ratios are estimated to be both nearly zero. The polyaddition chains in the styrene system must then be about one hundredth the length of those in the MMA system if the observed gel point is to accord with the classical theory of gelation. Since this ratio of chain lengths is quite plausible in the light of the

polymerisation chain lengths of the pure monomers styrene and MMA (mentioned previously), there is no reason to doubt that the styrene system, like the MMA model system, gels essentially according to the classical theory embodied in eqn.(52).

Table 17.

Comparison of MMA/PEF (resin N) with commercial styrene-based polyester (28c).

Resin	Feed Ratio R	Temp. °C	% MEK	Gel Time min.	Crit.conversion	10^5 x rate mole.l^{-1} $sec.^{-1}$	$(DP_{wc} - 1)$
MMA/PEF (resin N)	0.8	42	0.51	65	0.0184	4.23	5.5
S/PPFP (28c)	0.25	42	0.53	90	0.025	4.16	2.5

For the bulk polymerisation of allyl esters, eqn.(53) may be re-written:

$$\beta_c = 1/(DP_{wp} - 1)(A - 1) \qquad (54)$$

since $R/(R + 1)\rho^2$ is then unity, and the place of DP_{wc} is taken by A, the number of allyl groups per monomer morecule. (Internal cyclisation[28] is ignored in eqn.(54)). Thus the critical conversion β_c should vary as $1/(A - 1)$, i.e., for triallyl cyanurate ($A = 3$), β_c should be one half the value of $\beta_c = 0.16 \pm 0.028$ calculated from Simpson and Holt's data[46] for the diallyl esters ($A = 2$) of phthalic, isophthalic, terephthalic, and oxalic acids. In excellent agreement, it is found that $\beta_c = 0.085$ by dilatometric measurements on triallyl cyanurate. Although differences in the tendencies of these various monomers to cyclise

internally or "incestually"[28] on polymerisation has been ignored, the comparison shows that triallyl cyanurate gelation is in substantial agreement with the network theory.

4.6. Summary. The data in fig.23 and 24 furnish additional evidence that the theoretical picture of diffusion control in bulk polymerisation is sound. The success of the test contained in these two figures confirms that the Trommsdorf rate acceleration is correctly attributed to diffusion control, and that gelation is correctly founded on the effects of random crosslinking. Though this work demonstrates the substantial correctness of the theory underlying the Gordon/Roe model, the generality of the treatment is however restricted to polymerisations in which the primary radical chains are sufficiently long.

Thus the second stage in the MMA/PEF polymerisation can now be understood, on the assumption that every collision between two radicals leading to termination after the gel point involves at least one radical carried on a primary chain free from crosslinks. The rate constants of all elementary steps are taken to remain constant in the second stage, the change in the overall polymerisation rate being caused by changes in the effective radical concentration only. This then leads to a linear pre-gelation rate curve, while the post-gelation rate curve becomes of exponential type.

SECTION 5.

The Final State in the Polymerisation of MMA/PEF.

5.1. Introduction. In the third stage of the MMA/PEF copolymerisation the initiation and propagation steps become diffusion controlled and the reaction stops before complete conversion is attained. It is necessary to find when the reaction stops and what is the state of cure in terms of the composition when it does stop.

The final conversions obtainable by polymerisation at 62°C of the model polyester are measured as a function of the feed ratio R of fumarate to methacrylate unsaturation. As a first approximation, it is confirmed that the reaction becomes arrested when the second order transition reaches the polymerisation temperature. This generally happens when about 90% of the methacrylate and 10% of the fumarate unsaturation have been destroyed by polymerisation. This confirms the earlier conclusion, according to which the polymerisation is largely carried by the methacrylate unsaturation, and shows incidentally that a polyfumarate is not an efficient crosslinker for methacrylate. As a second approximation, the final state of cure, as deduced from the second order transitions, is somewhat variable with R. To account for these variations, the theory of the state of cure is developed in terms of three parameters: the concentration of crosslinks, the concentration of residual methyl methacrylate, and the concentration of residual free polyethylene fumarate chains. A statistical theory leads to symmetrical formulae for the first and third of these parameters.

The results suggest that in the present model system the final state of cure is dominated by the concentration of residual methyl methacrylate acting as plasticiser.

5.2.1. Method of following the final polymerisation. It is an experimental fact, illustrated in the previous section, that polymerisation reactions cannot be followed to completion in a normal dilatometer bulb due to the tension built up in the polymer as it contracts. Thus polymers usually break around 20% conversion when confined in an ordinary dilatometer bulb rendering further readings useless. Schulz and Harborth[48] and Burnett[49] have shown how this can be overcome by the fact that discs of resin of about 30 mm. diam. by 5 mm. thickness can be polymerised to over 90% conversion without any internal distortion occurring. Since a dilatometer of these dimensions would present great practical difficulties in handling, filling and accuracy of reading, the ideal is to confine the resin in the desired shape in a dilatometer bulb with a heavier, inert, solvent. Mercury was the only confining fluid readily available but experiments with various designs of dilatometers failed because the MEK catalyst appeared to oxidise the mercury which then no longer confined the resin satisfactorily. As other techniques of polymerising the resin alone in small ampules presented unsurmountable difficulties, all efforts to follow the MMA/PEF polymerisation continuously in the one reacting system had to be abandoned.

The technique finally adopted to obtain a complete rate curve of the MMA/PEF polymerisation consisted of following the reaction in

two parts. The reaction solution was made up in the normal manner; a dilatometer was filled with one part and the reaction followed as far as possible as described in the previous section. The remainder of the resin was poured into round aluminium moulds of about 25 mm. x 7 mm. and placed in a metal box immersed in the same thermostatted bath as the dilatometer. The aluminium moulds, which did not contaminate the resin, were sealed on the top and bottom with micro-coverglasses and a film of ethyl cellulose. Once the reaction could no longer be followed dilatometrically, moulds were removed from the box as required, the polymerised discs pushed out and their densities determined. The contraction that had occurred in the discs after a specified time was calculated from the initial density of the liquid, thus making the drawing of a rate curve possible. Sometimes a portion of the rate curve remained uncovered, viz. between the implosion in the dilatometer and the attainment of sufficient firmness by the disc for successful handling.

5.2.2. Determination of disc densities. The densities of the polymerised discs were determined by the density tube technique described in Section 3.3.3. The method had to be modified in this case since some of the discs were quite hard and it was difficult to cut off small samples representative of the disc as a whole, without spoiling the whole disc. This was undesirable since the discs were required for relaxation experiments (see below) and it was found that if the whole disc was dropped into a density tube it soon upset the gradient. To overcome this a large density tube about 3ft. high

and 3" diam. was constructed, the gradient being formed by interdiffusing a calcium chloride solution (density about 1.40 gm./ml.) and water. Over a three month period when numerous discs were put in and withdrawn, the gradient was not seriously disturbed. The range of gradient covered is illustrated in fig.25 and 26. The discs, in the majority of cases lay quite flat (a check on uniformity), and a typical section of the tube with three discs is shown in sketch 1.

5.3. Results. Six complete rate curves covering the feed ratios R = 0, 0.2, 0.5, 1.0, 1.25 and 1.75 are shown in fig.27-30, the joining of the two sets of points being indicated in each case by a dotted line. It can be seen that the smoothness of the rate curves at the point of switching from dilatometry to density tube measurement was satisfactory and completely vindicates the validity of the technique.

The total polymerisation attainable from these runs (taken from the horizontal portion of the rate curves) and for the case R = 0.1 (not sufficient points to show a complete rate curve) are tabulated in table 18.

Table 18.

Final composition from shrinkage measurements.

Initial feed ratio R	Mole % MMA $= \frac{100M_o}{M_o + F_o}$	Final % conversion β	Residual unsat. M+F, mole./l.	Final F mole/l.	Final M mole/l.
1.75	36.4	29.5	6.35	5.25	1.10
1.25	44.4	36.5	5.72	4.55	1.17
1.0	50.0	45.0	4.95	4.00	0.95
0.5	66.7	62.2	3.40	2.60	0.80
0.2	83.3	76.5	2.12	1.30	0.82
0.1	91.1	87.2	1.15	0.68	0.47
0.0	100.0	87.0	1.17	0.00	1.17

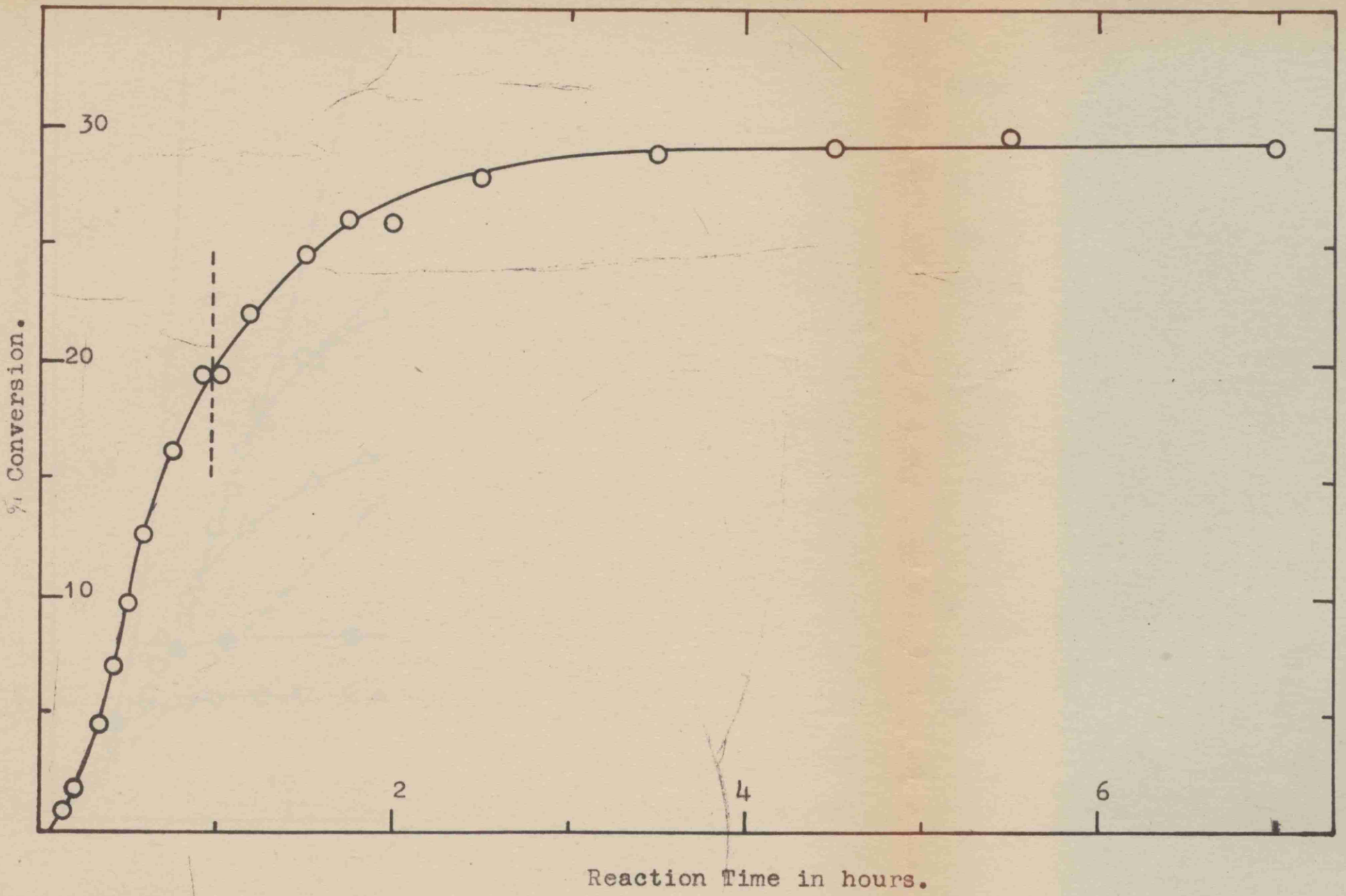

Figure 30. Complete rate curve for MMA/PEF at 62°C, 0.5% MEK and R = 1.75. The dotted line denotes the switch from dilatometry to the density gradient technique.

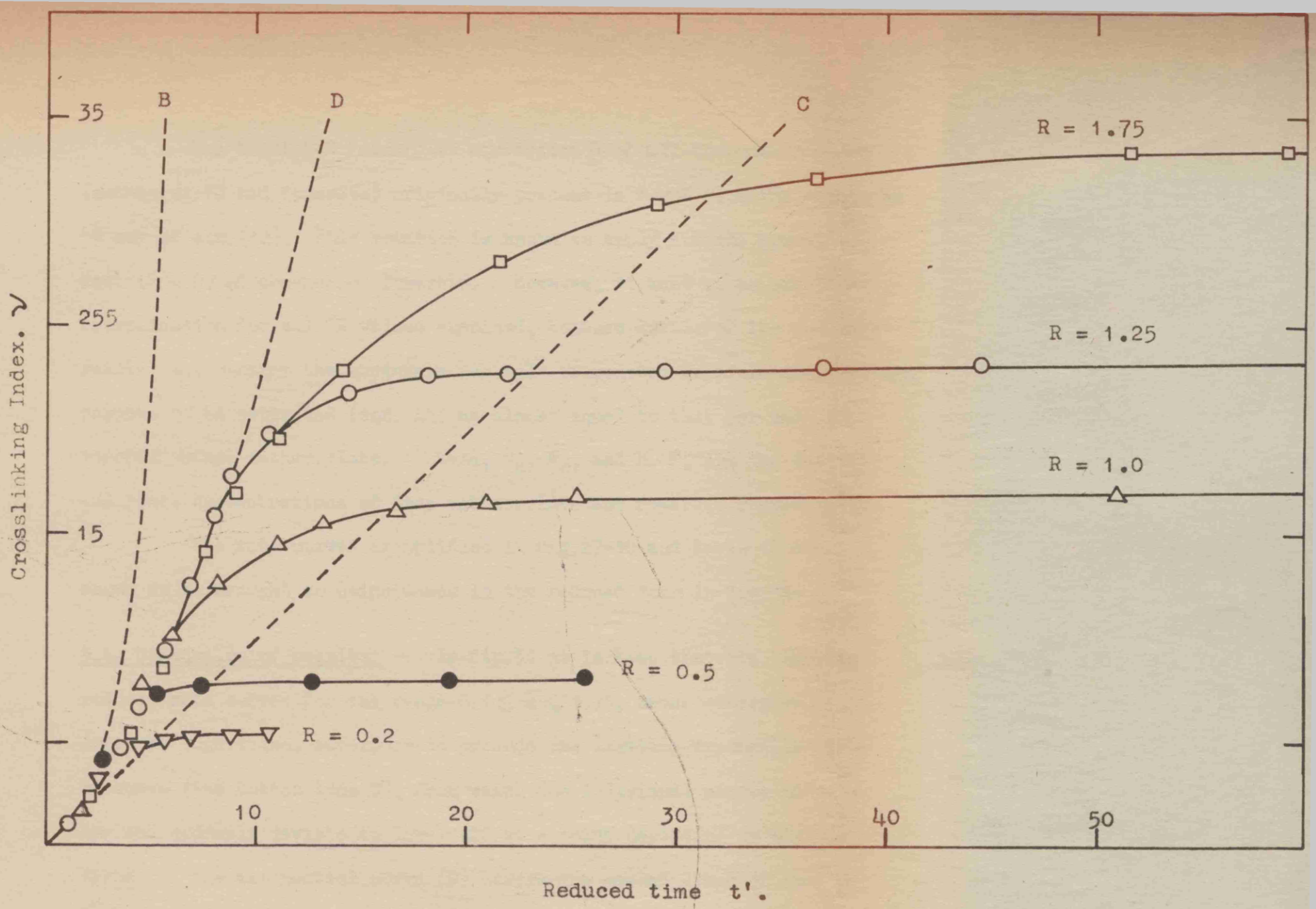

Figure 31 . Complete reduced rate curves for the five different feed ratios R as shown.
(0.5% MEK catalyst, 62°C, PEF resin N.)

B - Theoretical from Gordon-Roe model[22] (Radical combination).

C - Theoretical for absence of Trommsdorf effect.

D - Apparent limiting curve, experimental

The tabulated fractional conversion β of all the unsaturation (methacrylate and fumarate) originally present is found from the shrinkage by way of eqn.(12). This equation is known to apply for the special case (R = 0) of absence of fumarate. However, it must be an excellent approximation for all R values examined, because little of the fumarate reacts, and because the shrinkage per mole of reacted fumarate unsaturation happens to be estimated (eqn. 45) at almost equal to that per mole of reacted methyl methacrylate. Here, M_o, F_o, and M, F, are the initial and final concentrations of free methacrylate and fumarate respectively.

The rate curves exemplified in fig.27-30 and table 18 are shown to be brought to coincidence in the reduced form in fig.31.

5.4. Discussion of results. In fig.31 it is seen that the complete reduced rate curves for the range $0.1 \leqslant R \leqslant 1.75$, under otherwise constant conditions, superpose to produce one limiting exponential type of curve (the dotted line D), from which the individual curves more or less suddenly deviate to level off at a point depending on their R value. The exponential curve (D) covers the second stage of the polymerisation, the levelling off corresponds to the final, third stage. The exponential limiting curve is compared in fig.31 with the theoretical curve ((B) for combination) over a greater range still than in fig.24. It is again apparent that the model theory does not exaggerate the gel effect too seriously, as the comparison of (D) with (B) and (C) shows. On the scale of fig.31, the theoretical curve for disproportionation (not shown) appears to differ but little from that for combination.

The levelling off process of the curves is quite sharp at low

R values. Evidently, the theory of the second stage of vinyl polymerisation there applies till near the end of the realisable polymerisation, with little contribution to the total polymerisation from the slow third stage. Generally, the levelling off process is seen to occupy about 10% of the polymerisable unsaturation, and the detailed kinetics of this slow third stage have been investigated by an elastic relaxation technique by another worker.(13)

5.5.1. Final "equilibrium" cure as a function of feed ratio R. The final states of internal mobility or cure have been studied by a ball relaxation technique similar to that described by Jenckel and Klein,(50) which is appropriate for examining the approach to equilibrium or pseudo-equilibrium. The method employed consisted essentially of dropping a metal ball on the polymer sample and measuring the height of bounce. Thus at the dynamic second order transition temperature the bounce is a minimum, and the energy absorption by the sample is a maximum. While details of the experimental technique and kinetic theory of the relaxation process are treated elsewhere,(13) the final degree of cure at "equilibrium" as a function of R is discussed here. Thus fig.32 shows the typical ball rebound energy absorption peak curves for the final states of polymerisation for different R values at 62°C. The rising branch of the peak constituting the dynamic second order transition (i.e. the branch corresponding to the glassy state) was determined sufficiently quickly (about 2-3 minutes) to eliminate the danger of after-cure during the measurement. Also, the discs used for ball rebound measurement were the same specimens used for determining

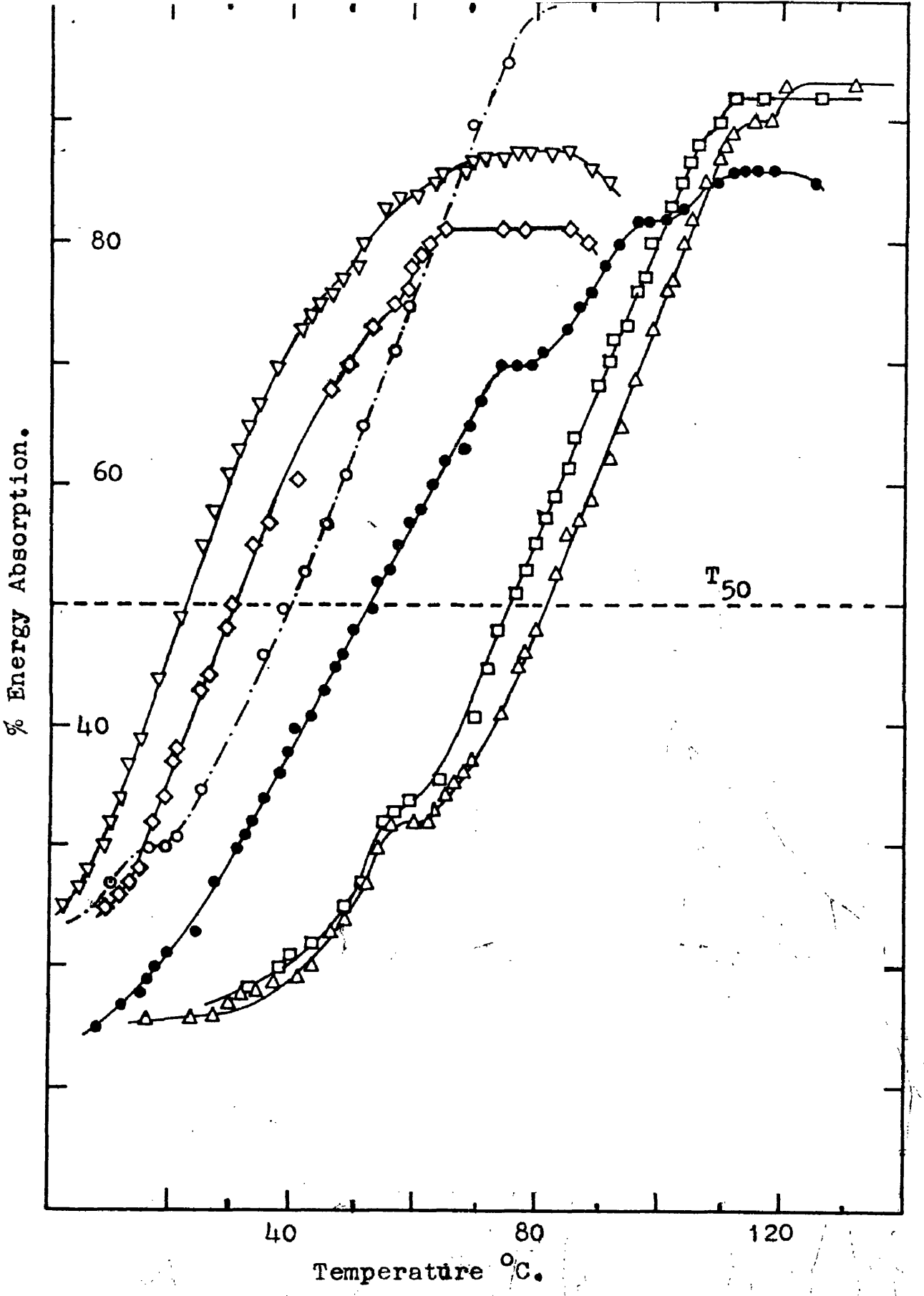

Figure 32.

Ball rebound absorption curves for the final states of cure of polyester resins (PEF resin N/MMA).

○ R = 0: □ R = 0.1: △ R = 0.2: ● R = 0.5: ◇ R = 1.25
▽ R = 1.75.

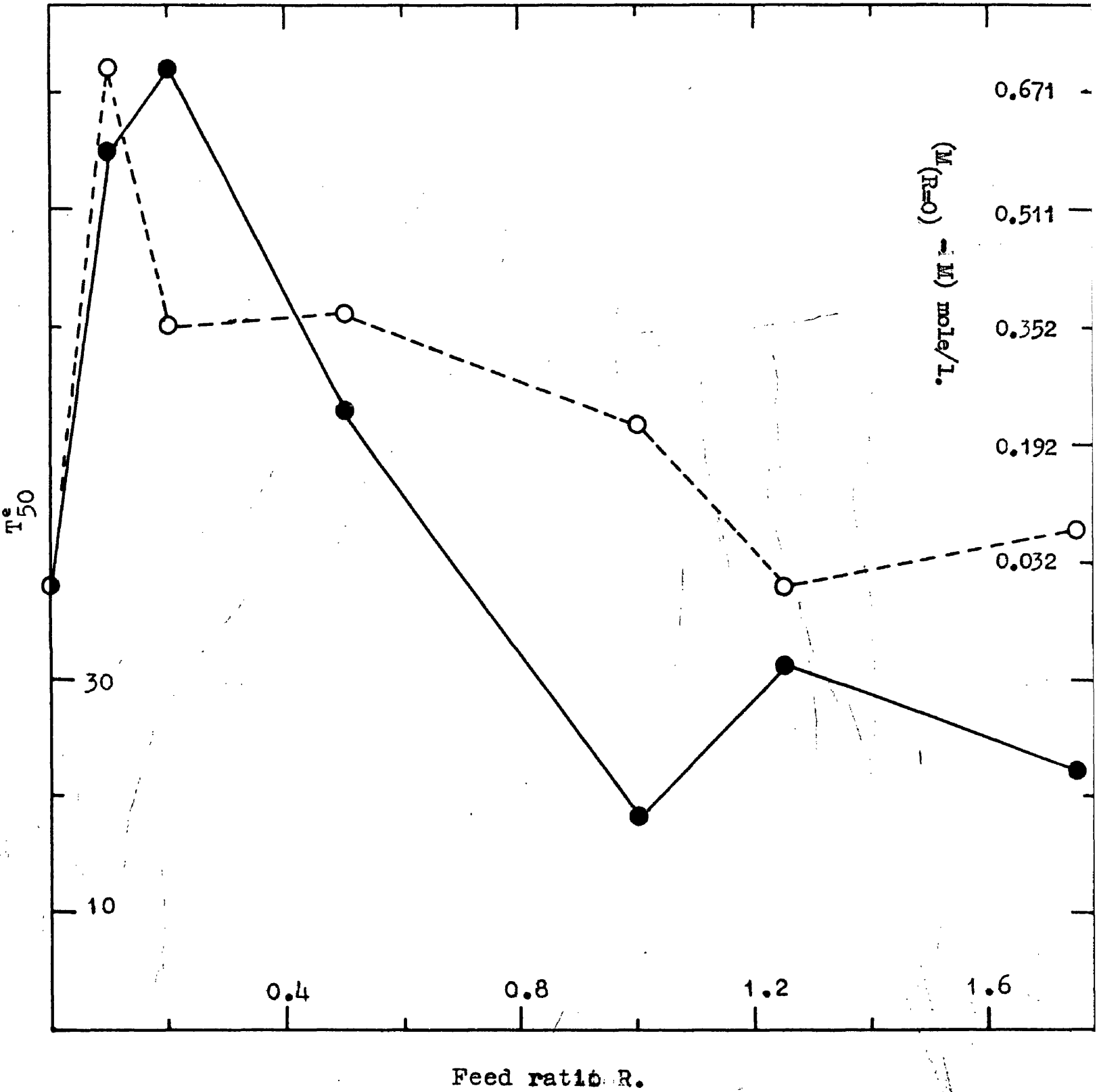

Figure 33 .

Final cures (T^e_{50}) from figure 32. against feed ratio R, in comparison with calculated conversion of methacrylate unsaturation O .

the final points of the rate curves (fig.27-30) by the density gradient technique described in the experimental section, so that the equilibrium (or pseudo-equilibrium) state of the samples is attested by the horizontality of the rate curves.

The T_{50} value, i.e. the temperature at which the rising branch cuts the 50% absorption line (fig.32) will be taken as a measure of the degree of cure. The peak temperature itself corresponds to a segmental relaxation time of 10^{-3} sec., i.e. the impact time of the ball, and T_{50} lies close to the static second order transition at very slow deformation rate. Of course T_{50} rises with the degree of conversion in any one run, and in fig.32 we are concerned with the final T_{50} at equilibrium (T^e_{50}).

Theory suggests that the polymerisation should become arrested at the same mobility or state of cure irrespective of the feed ratio R, viz. when T^e_{50} reaches the polymerisation temperature of 62°C or thereabouts. At first sight, this prediction seems in poor agreement with the results in fig.32, where T^e_{50} is scattered over about 50°C. However, the mean of the results is close to the prediction $T^e_{50} = 62°C$. Moreover, T^e_{50} in any one run is extremely sensitive to the degree of conversion, and the final degrees of conversion differ widely over the range of R values studied, viz. from about 30 to 90% of the total unsaturation originally present. The theory is therefore considered borne out to a first approximation. A better second approximation is obtained below which accounts for the general shape of the curve (fig.33) of T^e_{50} against R in terms of the <u>measured</u> final conversions, though no

theory is offered to account for the small differences between these measured conversions and those which would be required to arrest the reaction at $T^e_{50} = 62^oC$ exactly.

5.5.2. Second approximation theory of cure in polyesters. Linear theories of the effects of structural variables on the second order transition have been successful, e g. for the plasticisation of linear polymers (Jenckel and Illers[51]), for cross-linking and molecular weights (Loshaek[52]) and for copolymer composition (Gordon and Taylor[53]). We therefore expect to be able to approximate to the effect of resin structure on the T^e_{50} value in terms of three structural parameters in a linear fashion. One resinification parameter V should account for the rise in T^e_{50} with increasing branching and crosslinking, and two plasticisation parameters W_F and W_M should account for the fall in T^e_{50} respectively with rising molar concentrations of residual free fumarate condensation chains (not attached to the network), and of residual free methacrylate. The linear approximation, which should be valid for low concentrations of crosslinks and residual monomers, runs:

$$T^e_{50}(R) = T^e_{50}(0) + a\,V - b\,W_F - c\,W_M \qquad (55)$$

where $T^e_{50}(R)$ is the equilibrium value of T_{50} for the composition of feed ratio R at the polymerisation temperature of 62^oC under consideration, and a, b, and c are constants. For large values of V, W_F and W_M, higher power terms would have to be added on the right of eqn.(55). There can be no point in attempting to fit the results in detail to an equation with as many as three constants which are not yet known. For the

present the interdependence of V, W_F and W_M in terms of the kinetic scheme and the choice of the parameters V, W_F and W_M in comparison with possible alternative parameters are discussed. On the basis of a model calculation, a plausible reason is given why the terms in V and W_F occurring in eqn.(55) may have little effect, so that the behaviour of $T^e_{50}(R)$ is dominated by the term in W_M, as is actually found.

1) The plasticisation parameter W_M due to methacrylate will be equated to the residual methacrylate concentration in mole/l., which is calculated from the observed shrinkage (see table 18). Since this shrinkage is due to the polymerisation of both fumarate (F) and methacrylate (M) unsaturation, an assumption is required for apportioning the share of methacrylate and fumarate polymerisation. In the first stage of polymerisation this share is calculable in accordance with the co-polymerisation equation from the rough reactivity ratios measured ($r_M = 17$, $r_F = 0.25$). This calculation is amply accurate enough, because the final results are not sensitive to even considerable changes in the reactivity ratios. In the second stage of polymerisation the same equation based on random copolymerisation is still valid, while in the third stage the copolymerisation equation will overestimate the amount of fumarate reacted. This is because free, and a fortiori attached, fumarate chains will become much more strongly diffusion-retarded in the propagation step with a radical than free methacrylate monomer. However, the third stage usually makes only a rather small contribution to the total polymerisation and always less than 50% (fig.27-30). The composition of the final equilibrium polymer is

therefore calculated from the integrated form of the copolymerisation equation[55] (see Appendix) with $r_M = 27$, $r_F = 0.25$; in other words minor deviations of the equilibrium polymer from the state of random statistics due to differential diffusion control of the propagation step of methacrylate and fumarate unsaturation in the final stage are ignored. The same approximation is used in computing the parameters V and W_F.

The final free methacrylate and fumarate concentrations are calculated from β as shown in the Appendix and tabulated in table 18. This shows that the total polymerisation attainable at any feed ratio R falls just short of the total methacrylate unsaturation originally present. This is true also of the homopolymerisation of MMA (R = 0), as was known from previous workers.[18] The theory that the polymerisation is predominantly carried by the methacrylate unsaturation, based on the various ways of estimating the monomer reactivity ratios, is thus again confirmed.

2) The crosslinking parameter V. The following parameters suggest themselves as suitable measures of the degree of network formation: (a) the molar concentration K of junction points in the network, i.e. of polymerised fumarate double bonds;

$$K = F_{oc} - F_c \qquad (56)$$

where F_{oc} is the number of moles F_c of original fumarate double bonds per litre corrected for volume shrinkage, thus

$$\frac{F_{oc}}{F_o} = \frac{F_c}{F} = \text{(original volume/final volume)} \qquad (57)$$

(b) the molar concentration N of fumarate units which are attached to the network polymer (i.e. which belong to condensation chains of which at least one fumarate double bond has polymerised,

$$N = F_o - W_F DP_n' \text{ (see eqn.61)} \qquad (58)$$

and (c) the molar cencentration V of crosslinks.

It will be shown that the three parameters are equally suitable for theory of cure (eqn.55) since they remain substantially proportional to one another and V will be chosen for detailed discussion.

A crosslink will be defined as a segment of a condensation chain lying between two network junction points. As was discussed in Section 3.2. one can equally use a segment of a polymerisation chain lying between two network junction points. Provided both condensation and polymerisation chains are infinitely long (no loose ends), the two kinds of crosslinks have, by symmetry, the same concentration V. Here the number of loose ends in the short condensation chains is very high, while that of the long polymerisation chains is negligible. Accordingly, the above definition is more accurate for the purpose of counting true crosslinks but not loose ends. As an example of the calculation of a crosslinking parameter, the following expression for V is quoted, which is derived (see Appendix) from the assumption of random copolymerisation by simple statistical theory.

$$V = p\,(1 - q)^2\, F_{oc} / (1 - pq) \qquad (59)$$

Here p is the fraction of fumarate carboxyls esterified (= 0.732 for the resin N used), and $q(= F/F_o)$ is the fraction of fumarate double bonds

originally present which have not polymerised.

3) The plasticisation parameter V_F. The molar concentration of free fumarate chains acting as plasticiser is shown in the Appendix to be given by

$$V_F = q\,(1 - p)^2\, F_{oc} / (1 - pq) \qquad (60)$$

on the same assumption as eqn.(59) - in fact it turns out that V is transformed into V_F by the interchange of p and q.

The number average chain length DP'_n of the unattached chains is always less than that of the original condensation resin (here: 3.73) and is given by

$$DP'_n = 1/\,(1-pq) \qquad (61)$$

5.5.3. A model calculation. To illustrate the behaviour in practice of the parameters defined, the results of a model calculation are listed in Table 19. Random copolymerisation ($r_M = 17$, $r_F = 0.25$) is assumed, and q has been fixed by the assumption that at all R values the final equilibrium concentration M of methacrylate unsaturation (uncorrected for shrinkage) is unity, which is near the truth (cf. table 18).

The salient features of the table are as follows. Both the crosslinking parameter V and the plasticisation parameter V_F increase with the amount of fumarate in the original mixture in a similar fashion. The rate of increase of both parameters decreases with increasing R, and the parameter V reaches a flat maximum near the highest R value used. This is shown graphically in fig.34.

Table 19.

Model calculation of final states (M = 1).

R	F_o	F_{oc}	F	F_c	$q = F/F_o$	V	K	N	K/V	N/V	W_F	DP'_n
1.75	5.73	6.18	5.16	5.57	0.90	0.13	0.61	2.46	4.75	19.1	1.18	2.94
1.25	5.00	5.50	4.47	4.92	0.89	0.13	0.59	2.35	4.43	17.8	1.02	2.89
1.00	4.50	5.02	4.00	4.96	0.89	0.13	0.57	2.13	4.37	16.4	0.92	2.87
0.70	3.71	4.22	3.27	3.72	0.88	0.12	0.51	1.60	4.09	13.0	0.75	2.82
0.50	3.00	3.48	2.65	3.07	0.88	0.10	0.41	1.52	4.13	15.4	0.62	2.81
0.40	2.57	3.02	2.27	2.66	0.88	0.09	0.36	1.14	4.08	13.0	0.54	2.82
0.30	2.08	2.47	1.82	2.16	0.87	0.08	0.31	1.11	3.90	14.0	0.43	2.78
0.20	1.50	1.81	1.32	1.59	0.88	0.06	0.22	0.81	3.97	14.4	0.32	2.79
0.10	0.82	1.01	0.72	0.89	0.88	0.03	0.12	0.44	4.15	15.1	0.18	1.82

Note: This table contains minor rounding-off errors.

The three typical crosslinking parameters defined remain practically proportional to each other, as indicated by the approximate constancy of the two columns of ratios (K/V and N/V). The length DP'_n of the unattached chains is seen to be remarkably constant at 2.86 ± 0.08. (Hence the DP of the attached chains in the network cannot vary appreciably either). It follows that other possible parameters for expressing the plasticisation instead of W_F, such as the weight concentration of unattached chains, would merely run proportional to W_F. Since $q \sim 0.9$ at all R values, only 10% of the fumarate unsaturation present is ever utilised.

The conclusions drawn from the model calculation in this section are generally valid for a lightly crosslinked system, such as a cross-

polymerisation in which little of the crosslinker (here fumarate) is actually utilised.

5.5.4. Interpretation of the observed states of cure. Fig.34 shows that the two parameters V and V_F remain very approximately proportional to one another. From the manner in which they enter eqn.(55) it may thus happen that their effects on T^e_{50} approximately cancel each other. This will happen when the constants a and b have suitable values with a ratio of $a/b \sim 1/6$. This would imply that the rise in cure due to one mole of crosslinks equals the depression caused by 6 moles of free fumarate condensation chains acting as plasticiser. If this condition is only very approximately satisfied, the trends in T^e_{50} will be dominated by the free methacrylate M. The plots of experimental $T^e_{50}(R)$ and $M_{(R = 0)} - M_{(R = x)}$ against R confirm the dominance of the free methacrylate, since there is a marked correlation. On this interpretation, of the three constants a, b, and c, only c makes a substantial contribution to the variations in T^e_{50} with R, and it is readily seen that c must be of the order 100°C depression per mole of free methacrylate per litre of resin. In satisfactory agreement, a depression of $c = 60^\circ C$ is predicted from the known values[54] of the depressions in the second order transition of polymethyl methacrylate by esters similar to MMA monomer, and the same constant is calculated at $c = 120^\circ C$ from direct ball rebound measurement.

It is concluded that the slightly different internal states of mobility (or cure) attained at equilibrium for different R values reflect primarily the survival of slightly different concentrations of free

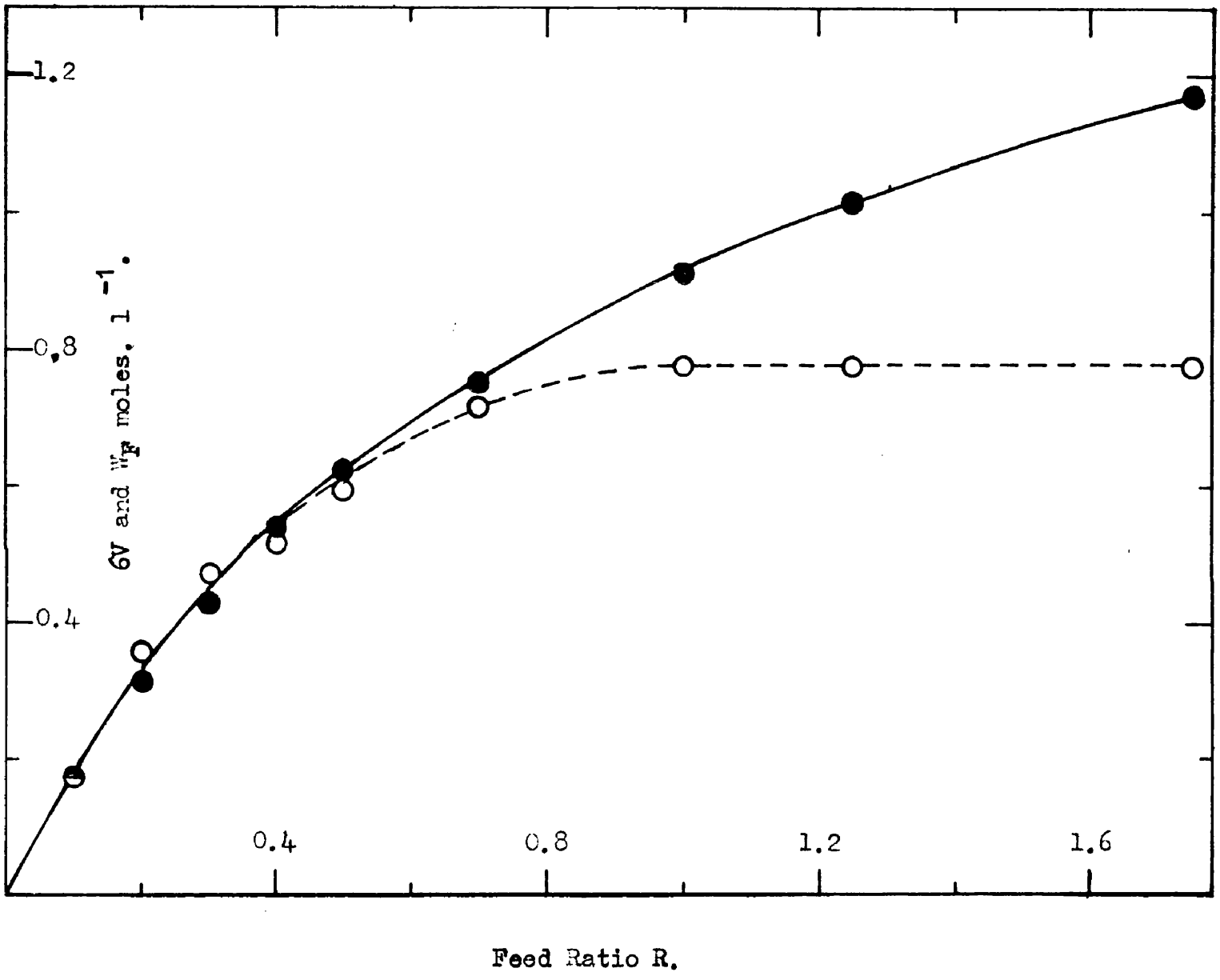

Figure 34 . Calculated final values of crosslink density V (O) and molar concentration W_F of free condensation chains (●).

methyl methacrylate (table 18). We are little nearer to the solution of the technically important problem as to why slightly different degrees of conversion of methacrylate, and hence slightly different degrees of internal mobility are actually achieved.

5.6. Summary. The MMA/PEF polymerisation is seen to accelerate exponentially with time till near the end of the realisable polymerisation when the third stage of the reaction is marked by the onset of diffusion control of the initiation and propagation rates with a subsequent levelling off of the rate curve. This slow third stage contributes little to the total polymerisation. The reaction is finally arrested at approximately the same degree of mobility of the system irrespective of R.

The addition of the polyester to methyl methacrylate, for the purpose of introducing crosslinks is inefficient, as in practice only about 10% of the added fumarate unsaturation is utilised for polymerisation. Much of the polyester survives as completely unpolymerised micro-molecules acting as plasticiser. As regards the stiffness or cure attainable, it has been shown that it is not efficient, therefore, to add more than a small amount of polyester.

An approximate theory has been developed for computing the final cure in terms of the crosslink density and plasticisation by residual monomers. The detailed application of this theory will have to await more exact data.

CONCLUSIONS.

This work shows that a complicated polyfunctional industrial system falls within the scope of a simple mechanism when properly controlled, by reference to a model system. Thus the hardening reaction of methyl methacrylate/polyethylene fumarate, a typical polyester "contact" resin, is a simple copolymerisation reaction. The rôle of the gel point as a tool is emphasised, it being shown that the kinetics of the hardening reaction can be explained in terms of the classical gelation theory. The gel point is defined in terms of a number of fundamental parameters which wholly determine the polymerisation.

A polymerisation of this kind is shown to proceed in three more or less clearly defined stages. In the initial stage the system behaves as a classical copolymerisation controlled by the usual appropriate kinetic parameters until the system gels. In the second stage diffusion control of the termination step causes an increase in the rate of reaction. In the third stage the system becomes so immobile that propagation and ultimately initiation become diffusion controlled and the reaction (or curing) rate decays to zero and an equilibrium state is approached.

The Gordon/Roe model for the diffusion control of the termination step is further verified by this work but it is shown only to hold when the primary polymerisation chain length is sufficiently large.

The preliminary theory of the state of cure attainable shows that PEF is relatively inefficient as a crosslinking agent in the

MMA/PEF system. The general principle then emerges that the ideal system would be one in which the monomer reactivity ratio is > 1, and the primary chain length is relatively short, so that sufficient crosslinker may be incorporated without the system gelling excessively early.

The theoretical prediction of the gel points of polyester resins, in an absolute or even in a relative sense, is technologically important. For instance, the fraction of the total crosslinking reaction which takes place at finite viscosity, i.e. before the liquid sets solid at the gel point, is reflected in the "pot life" of the resin. It is inversely reflected in the amount of undesirable, more or less isotropic, shrinkage of the solid article. Once the resin does gel, its final cure cannot be altered.

REFERENCES.

(1) Flory, J. Amer. Chem. Soc., 63, 3083, (1941).

(2) Stockmayer, J. Chem. Phys., 12, 125, (1944).

(3) Walling, J. Amer. Chem. Soc., 67, 441, (1945).

(4) McMillan, B.Sc. Thesis, University of Glasgow, (1953).

(5) Carothers and Arvin, J. Amer. Chem. Soc., 51, 2570, (1929).

(6) Batzer and Mohr, Makromol. Chem., 8, 217, (1953).

(7) Flory, J. Amer. Chem. Soc., 58, 1877, (1936).

(8) Flory, J. Amer. Chem. Soc., 61, 3334, (1939).

(9) Jacobson and Stockmayer, J. Chem. Phys., 18,1600, (1950).

(10) Hill, Chem. and Ind., 1083, (1954).

(11) Berr, J. Polymer Sci., 15, 591, (1955).

(12) Gordon, Grieveson and McMillan, J. Polymer Sci., 18, 497, (1955).

(13) Grieveson, Ph.D. Thesis, University of Glasgow (in preparation).

(14) Feuer, Bockstahler, Brown and Rosenthal, Ind.Eng.Chem., 46, 1643,(1954).

(15) Gordon and Grieveson, J. Polymer Sci., 17, 107, (1955).

(16) Baysal and Tobolsky, J. Polymer Sci., 9, 171, (1952).

(17) Melville, Bevington & Taylor, J. Polymer Sci., 14, 463, (1954).

(18) Robertson, Trans. Faraday Soc., 52, 427, (1956).

(19) Matheson, Auer, Bevilicqua and Hart, J. Amer. Chem. Soc., 71, 497,(1949).

(20) Cass and Burnett, Ind. Eng. Chem., 46, 1619, (1954).

(21) Flory, "Principles of Polymer Chemistry", Cornell Univ.Press, New York, (1953), 202.

(22) Gordon and Roe, J. Polymer Sci., 21, 27, 39, 57, 75, (1956).

(23) Burnett, Quart. Rev., 4, 292, (1950).

(24) Parkyn, "Glass Reinforced Plastics", Editor Morgan, Iliffe and Son, London, (1954), 59.

(25) Gordon, Grieveson and McMillan, Trans. Faraday Soc., 52, 1012, (1956).

(26) Palit, Trans. Faraday Soc., 51, 1129, (1955).

(27) Simpson, Holt and Zetie, J. Polymer Sci., 10, 489, (1953).

(28) Gordon, J.Chem. Phys., 22, 610, (1954).

(29) Haward, J. Polymer Sci., 14, 535, (1954).

(30) Parkyn, Chem. and Ind., 913, (1955).

(31) Boyer, Spencer and Wiley, J. Polymer Sci., 1, 249, (1946).

(32) Gordon, Ind. Eng. Chem., 43, 386, (1951).

(33) Gordon and McNab, Trans. Faraday Soc., 49, 31, (1953).

(34) Nickels and Flowers, Ind. Eng. Chem., 42, 292, (1950).

(35) Whelan, J. Polymer Sci., 14, 409, (1954).

(36) Price and Gilbert, J. Polymer Sci., 6, 557, (1952).

(37) de Wilde and Smets, J. Polymer Sci., 5, 253, (1950).

(38) Mayo, Lewis and Walling, J. Amer. Chem. Soc., 70, 1529, (1948).

(39) Loshaek and Fox, Ind. Eng. Chem., 75, 3544, (1953).

(40) Trommsdorf, Kohle and Lagally, Makromol. Chem, 1, 169, (1948).

(41) Schulz and Harborth, Makromol. Chem., 1, 106, (1947).

(42) see Z. f. Elektrochem., 60, 282, (1956).

(43) Baysal and Tobolsky, J. Polymer Sci., 11, 471, (1953).

(44) Bamford and Jenkins, Nature, 176, 78, (1955).

(45) Bamford and Dewar, Faraday Soc. Disc., 2, 310, (1947).

(46) Simpson and Holt, J. Polymer Sci., 18, 335, (1955)

(47) Bartlett and Altschul, J. Amer. Chem. Soc., 67, 816, (1945).

(48) Schulz and Harborth, Angew. Chem., 59, 90, (1947).

(49) Burnett, Trans. Faraday Soc., 46, 772, (1950).

(50) Jenckel and Klein, Z. f. Naturf., 7a, 619, (1952).

(51) Jenckel and Illers, Z. f. Naturf., 9a, 440, (1954).

(52) Loshaek, J. Polymer Sci., 15, 391, (1955).

(53) Gordon and Taylor, J. Appl. Chem., 2, 493, (1952).

(54) Jenckel, "Physik der Hochpolymeren", Editor Stuart, Springer, Berlin, (1956), 577.

(55) Lewis and Mayo, J. Amer. Chem. Soc., 66, 1594, (1944).

APPENDIX.

LIST OF SYMBOLS.

A — Number of allyl groups per monomer molecule.

DP'_n — Number average chain length (fumarate double bonds) of free condensation chains (i e. none of whose double bonds have polymerised).

DP_{nc}, DP_{wc} — Number and weight average chain length (fumarate double bonds) of all condensation chains.

DP_{ne} — Number average chain length (fumarate double bonds) of all condensation chains by end-group determination (as distinct from cryoscopy DP_n).

$DP_{nc} = DP_{ne}$ in this work.

DP_{nch}, DP_{wch} — Number and weight average chain lengths of the chains I. present.

Π_1, ω_1 — Number and weight fractions of monomeric rings II. present.

DP_{np}, DP_{wp} — Number and weight average chain length of the polyaddition chains.

EDMA — Ethylene dimethacrylate.

F — Concentration (final)(moles/l.) of fumarate unsaturation.

F_c — F corrected via eqn.(57) for volume shrinkage during polyaddition.

F_{oc} — Initial F corrected for volume shrinkage.

F^* — Concentration (moles/l.) of fumarate radicals.

K — Concentration of junction points in cross-polymer network = concentration (moles/l.) of polymerised fumarate double bonds.

M — Concentration (final)(moles/l.) of methacrylate unsaturation (free MMA monomer).

M^* — Concentration (moles/l.) of methacrylate radicals.

MMA — Methyl methacrylate.

MEK — Methyl ethyl ketone peroxide.

N — Concentration (moles/l.) of fumarate units which are attached to the cross-polymer network, i e belonging to chains of which at least one fumarate double bond has polymerised.

p — Fraction of fumarate carboxyls esterified during polycondensation.

PEF Polyethylene fumarate.

PPFP Polypropylene fumarate/phthalate.

q Fraction of fumarate double bonds not polymerised during polyaddition.

R Feed ratio of unsaturation, i.e. concentration ratio of fumarate to methacrylate unsaturations (F/M) or fumarate to styrene (F/S).

r_F, r_M Monomer reactivity ratios for fumarate and methacrylate radicals.

S Styrene.

t' Time, in multiples of the gelling time (t_c) as unity.

T_{50} Temperature (on the ascending or "glass" branch of the absorption peak) for 50% energy absorption on ball impact.

T^e_{50} Equilibrium value of T_{50} after completion of the attainable polymerisation.

V Concentration (moles/l.) of crosslinks. A crosslink is a portion of a polycondensation chain lying between two polymerised fumarate double bonds (see K).

w_F Weight fraction of (polymerised + unpolymerised) fumarate double bonds in the cross-polymer.

W_F Concentration (moles/l.) of free condensation chains, not attached to the cross-polymer.

W_M Concentration (moles/l.) of free MMA monomer = M.

Z Fraction of original fumarate double bonds which give rise to a crosslink (see under V) during polyaddition.

TAC Tri allyl cyanurate.

28c Commercial S/PPFP resin.

α Fractional conversion by polyaddition of all the fumarate unsaturation initially present.

β Fractional conversion by polyaddition of all the unsaturation initially present.

ν Crosslinking index, number of crosslinks (see under V) per weight average polyaddition chain.

ρ Fraction of the polymerised unsaturation which is fumarate as distinct from methacrylate (or styrene).

Calculation of solvent in extracted cross-copolymer.

If F, M and S are the moles of fumarate, methacrylate and solvent respectively, the following identity can be written.

$$F + M + S = 1 \qquad \text{(i)}$$

a.) For the system, fumarate + methacrylate + methanol, by taking a carbon, hydrogen and oxygen balance for each constituent the following three equations are obtained:

$$49.75\,F + 59.98\,M + 37.48\,S = C \qquad \text{(ii)}$$

$$4.49\,F + 8.05\,M + 12.58\,S = H \qquad \text{(iii)}$$

$$45.85\,F + 31.97\,M + 49.93\,S = O \qquad \text{(iv)}$$

where C, H and O are the weight percent of carbon, hydrogen and oxygen present in such a system..

Solving these equations yields the equation:

$$S = 0.0103\,O + 0.0915\,H - 0.0177\,C \qquad (62)$$

Therefore assuming any residual solvent to be methanol only, the percent impurity shown in table 11 is obtained by substituting the appropriate C, H and O microanalysis figures in eqn.(62).

b.) Similarly, if Cellosolve is the impurity the same equations may be written with the substitution of 53.71 S, 10.52 S and 25.77 S in the third column, and solved for S in the same manner.

Calculation of final F and M.

In order to calculate F and M separately from the residual unsaturation (M + F) of table 18 it is necessary to make use of the integrated form

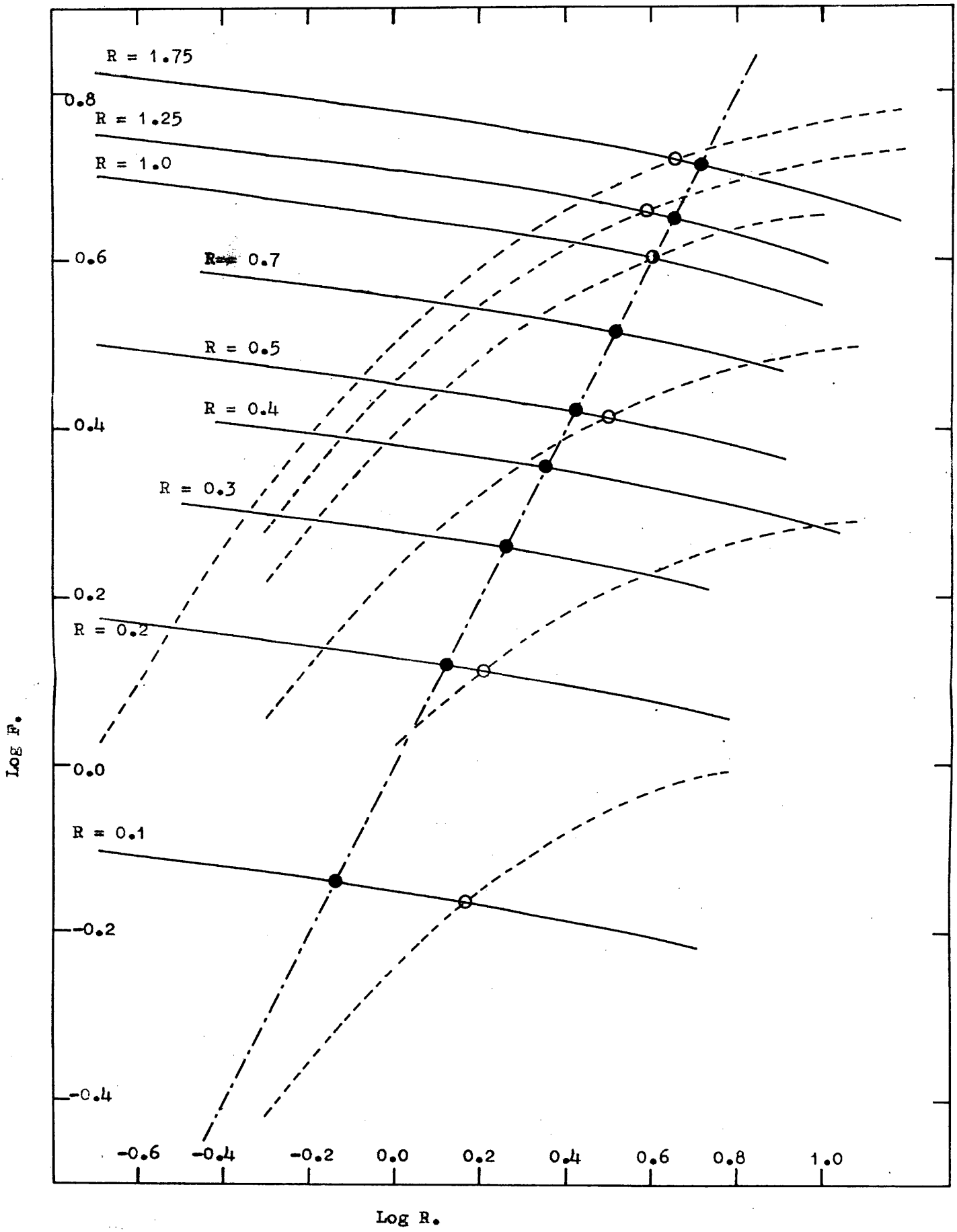

Figure 35. Calculation of fumarate unsaturation. Intersection (O) gives final experimental fumarate unsaturation. Intersection (●) gives final fumarate concentration for model system (M = R).

of the copolymerisation equation[55] which can be written:

$$\log \frac{F}{F_o} = \left\{ \frac{r_F}{1-r_F} \log \frac{F_o M}{M_o F} \right\} - \left\{ \frac{1-r_F r_M}{(1-r_F)(1-r_M)} \log \frac{(r_M - 1)\frac{M}{F} - (r_F - 1)}{(r_M - 1)\frac{M_o}{F_o} - (r_F - 1)} \right\} \quad (63)$$

Substituting the values $r_M = 17$, $r_F = 0.25$, and rearranging:

$$\log F = -\left\{ (0.334 \log R) + 0.271 \log \left(\frac{16}{R} + 0.75\right) \right\} \quad (64)$$
$$+ \left\{ (0.334 \log R_o) + 0.271 \log \left(\frac{16}{R_o} + 0.75\right) + \log F_o \right\}$$

From the definition of $R = F/M$, the identity is deduced:

$$\log F = \log R - \log (R + 1) + \log (F + M) \quad (65)$$

Plotting these two equations over an arbitrary range of R values in fig.35 gives the two curves shown, full line (eqn.64), dashed curve (eqn. 65). The intersection, denoted by (O), gives log F and hence the final F(and M) values. The model calculation in table 19 is based on the same technique, but replacing the experimental values of (F+M) by the assumption M = 1, so that F = R, and the intersection denoted by (●) again enable the final F value to be found.

The experimental results show (table 18) that M is of the order of 1 mole/l. for all R values, while the residual F varies widely.

Derivation of equations (59 and 60) for plasticisation and crosslinking parameters.

Let p be the chance of a fumarate carboxyl having become esterified during polycondensation, and q the chance of a fumarate double bond not having become polymerized during polyaddition. The Flory

"most-probable" distribution of the number fraction Π_n of n-meric condensation chains is:

$$\Pi_n = p^{n-1} (1-p) \qquad (v)$$

with a number average chain length

$$DP_{nc} = 1/(1-p) \qquad (vi)$$

After polyaddition (cross-polymerisation) the distribution of unattached condensation chains, i e. chains all of whose double bonds have escaped polyaddition, is given by

$$\Pi_n' = p^{n-1} (1-p) q^n \qquad (vii)$$

since the fraction of all the original chains of length n is given by (v) and the fraction of these which remain unattached is q^n (because there are n double bonds, each of which has an independent chance q of being unpolymerised). By summation of Π_n' we obtain the fraction of the original chains remaining unattached:

$$\Sigma \Pi_n' = q (1-p) \Sigma (pq)^{n-1} = q (1-p)/(1-pq) \qquad (viii)$$

The concentration (moles per litre) of original condensation chains is given by

$$F_{oc} / DP_{nc} = F_{oc}(1-p) \qquad (ix)$$

Hence the concentration of free condensation chains is

$$\Pi_F = F_{oc} q (1-p)^2 / (1-pq) \qquad (60)$$

To find the concentration of crosslinks, i e. of condensation chain segments lying between couples of polymerised fumarate double bonds (junction points in the network), we first select a fumarate unit F at

random. We require to find the chance that F should be polymerised, and that proceeding from F along the condensation chain in one fixed direction, say downward, we shall eventually encounter another polymerised fumarate double bond. The total contingency of this event is made up of four chances, thus: The chance of F being polymerised is $(1-q)$, that of finding n fumarates below is p^n. There is a chance q^{n-1} that the first $(n-1)$ of these are unpolymerised, and a chance $(1-q)$ that the n^{th} is polymerised. Combining the four chances we find the overall contingency:

$$(1-q)\ p^n\ q^{n-1}(1-q) = p^n q^{n-1}(1-q)^2 \qquad (x)$$

Summing over all values of n we find the fraction Z of all the original fumarate double bonds which have given rise to a proper crosslink as defined i.e. a segment of condensation chain leads downward from them to another junction point:

$$Z = p\ (1-q)^2 / (1-pq) \qquad (xi)$$

Multiplying by the number of moles per litre of original fumarate double bonds, we find the concentration of crosslinks:

$$V = F_{oc}\ p\ (1-q)^2 / (1-pq) \qquad (59)$$

Table 20.

Table of physical properties for resins for fig.2.

Run	Resin	Reaction time mins.	DP_{ne}	DP_n	Density	R.I.
1	A	90	3.43	2.66	-	-
2	B	-	3.75	2.94	1.3507	1.5087
"	C	215	4.88	3.90	-	-
"	D	270	6.04	4.42	-	-
"	E	310	7.38	6.88	1.3618	1.5129
3	F	105	3.78	2.90	1.3475	1.5070
"	G	235	5.73	5.58	1.3534	1.5100
"	H	315	6.68	5.65	1.3508	1.5110
4	J	93	3.46	2.93	1.3556	1.5068
"	K	195	5.25	5.09	1.3616	1.5101
"	L	320	9.32	9.81	1.3642	1.5130
5	N	95	5.05	3.29	1.3568	1.5081
"	P	200	8.61	5.02	1.3612	1.5106

Table 21.

R.I. and specific volume vs. 10^4/ end-group M.W. for fig. 3 and 4.

Resin	Specific volume	R.I.	10^4/M.W.
J	0.7377	1.5068	19.65
K	0.7344	1.5101	13.11
L	0.7330	1.5130	7.46
F	-	1.5070	18.03
G	-	1.5100	12.03
H	-	1.5110	10.03

Table 22.

Tabulation of visco-dilatometer runs.

Run	Feed ratio R	Temp. °C	% MEK cat.	Induction time min.	Gel time t_c min.	% conversion. at G.P.	Rate x 10^5 mole.$l.^{-1}$ $sec.^{-1}$
D.4	1.0	62.0	1.97	4	10	2.34	35.1
D.6	0.67	"	2.11	4	24.5	5.28	32.3
D.8	0.50	"	1.96	2	42.67	9.09	32.0
G.2	1.25	62.0	1.98	2	8.75	2.34	40.0
G.4	1.0	"	2.07	4	16.5	3.51	32.05
G.6	0.80	"	1.97	2	20.5	3.39	24.70
G.8	0.67	"	2.02	2	28.25	4.96	26.20
G.10	0.50	"	2.01	2	31.5	5.69	27.1
G.12	0.50	"	2.09	4	29.0	5.47	28.3
G.14	0.33	"	2.03	4	36.25	7.80	32.2
G.16	0.20	"	1.99	5	53.25	10.82	30.5
G.18	0.10	"	1.97	5	77.0	15.63	30.4
G.20	0.15	"	2.04	5	74.0	15.37	31.2
G.22	1.0	"	1.93	2	15.0	2.93	29.25
G.24	0.67	"	1.99	4	30.5	5.82	28.7
F.2	1.0	62.0	2.09	2	18.5	4.61	37.4
F.4	0.50	"	2.10	5	43.0	11.17	33.9
F.6	0.33	"	1.80	5	67.33	15.97	35.6
F.8	0.20	"	1.98	5	59.33	14.54	36.8
F.10	0.80	"	1.94	5	28.5	7.33	38.6
F.12	0.40	"	2.00	5	57.0	14.51	38.2
F.14	0.50	"	1.98	5	53.0	14.14	40.0
F.16	0.50	"	2.10	5	60.0	17.22	43.0
F.18	1.0	"	2.04	2	17.5	4.69	40.1
F.20	0.33	"	2.01	5	67.0	17.55	39.2
F.22	2.0	"	2.02	2	10.0	4.13	62.0
F.24	0.20	"	2.00	5	92.0	23.55	38.4
F.26	0.25	"	1.98	5	76.0	19.9	39.25

Table 23.

Tabulation of visco-dilatometer runs for rate determination only.

Run	Feed ratio R	Temp. °C	% MEK cat.	Reaction time t mins.	% Conversion at t min.	Rate x 10^5 mole $l.^{-1}$ $sec.^{-1}$
F.28	0.33	72.0	2.09	37	19.94	80.8
F.30	"	82.0	2.03	21	25.4	181.2
F.32	"	52.0	2.08	91	11.06	18.23
F.34	"	52.0	2.06	160	18.64	17.50
F.36	"	72.0	2.04	30	16.70	82.2
F.38	"	32.0	2.04	70	2.02	4.31
F.40	"	42.0	2.01	80	4.31	8.08
F.42	"	67.0	2.02	39	15.62	60.1
F.44	"	57.0	2.02	56	10.35	27.7
F.46	"	62.0	2.04	59	16.02	40.8
M.4	0.0	62.0	2.0	30	6.61	33.05
M.6	"	52.0	2.0	30	3.67	18.3
M.8	"	42.0	2.0	40	2.0	7.55
M.10	"	62.0	1.99	30	7.21	36.0
M.12	"	72.0	1.99	20	8.84	66.4
M.14	"	72.0	1.99	20	8.61	71.8
M.16	"	82.0	2.01	15	13.18	132.1
M.18	"	57.3	2.01	30	4.91	24.5
M.20	"	47.0	2.01	50	3.90	11.7
M.22	"	62.0	0.50	150	19.10	20.1
M.24	"	62.0	0.51	163	19.57	20.0

Table 24.

Details of readings for fig.6, (readings from calibrated scale).

Plug	Time m.	s.	Open	Time m.	s.	Plug	Time m.	s.	Open	Time m.	s.
0.30	1	20	4.0	1	35	1.65	14	40	5.67	15	25
0.40	1	50	4.1	1	5	1.55	15	50	5.0	16	5
0.50	2	25	4.2	2	35	1.50	16	25	4.95	16	40
0.65	3	10	4.35	3	20	1.45	17	10	4.87	17	30
0.80	3	55	4.55	4	25	1.40	17	55	4.82	18	15
0.95	4	40	4.65	5	0	1.35	18	40	4.75	19	0
1.05	5	15	4.75	5	35	1.28	20	0	4.66	20	20
1.26	6	5	4.87	6	20	1.23	21	10	4.60	21	20
1.30	6	40	5.0	7	15	1.18	22	25	4.52	22	45
1.45	7	35	5.10	7	55	1.15	23	15	4.48	23	35
1.55	8	20	5.20	8	40	1.12	24	40	4.43	24	55
1.68	9	10	5.29	9	25	1.09	26	5	4.38	26	20
1.75	9	40	5.35	9	55	1.07	27	20	4.33	27	55
1.85	10	20	5.45	10	40	1.06	28	20	4.31	28	45
1.95	11	0	5.50	11	10	1.05	29	25	4.28	29	50
	Flow reversed.					1.04	31	5	4.24	31	35
1.90	12	0	5.40	12	20	1.035	32	10	4.22	32	20
1.84	12	35	5.34	12	50	1.030	32	45	4.21	33	0
1.78	13	10	5.27	13	30	1.030	33	25	4.19	33	45
1.70	14	5	5.18	14	20	1.030	35	0	4.17	35	15

Table 25

Details of readings for fig.7, (readings from calibrated scale).

Plug	Time m.	s.	Open	Time m.	s.	Plug	Time m.	s.	Open	Time m.	s.
0.7	1	15	4.6	1	25	1.44	38	40	4.47	39	10
1.0	1	35	4.90	1	45	1.40	40	0	4.43	40	20
1.30	1	55	5.25	2	10	1.37	41	50	4.35	42	30
1.70	2	20	5.60	2	30	1.35	43	30	4.32	44	10
	Flow reversed.					1.33	44	50	4.27	45	20
1.80	3	10	5.40	3	25	1.31	46	50	4.22	47	10
1.40	3	45	5.0	3	55		Flow reversed.				
1.10	4	10	4.70	4	20	1.32	48	0	4.21	48	20
0.85	4	30	4.40	4	45	1.34	49	40	4.20	49	55
0.60	5	0	4.15	5	10	1.35	51	10	4.19	51	30
	Flow reversed.					1.36	51	55	4.18	52	10
0.60	5	55	4.40	6	10	1.37	53	20	4.17	53	35
1.10	6	55	4.85	7	5	1.38	54	50	4.15	55	5
1.60	7	50	5.35	8	5	1.385	56	10	4.14	56	25
1.90	8	25	5.65	8	40	1.39	56	40	4.13	57	0
	Late stages.					1.395	58	0	4.12	58	10
1.57	33	50	4.70	34	15	1.40	58	15	4.11	58	30
1.50	36	5	4.59	36	25	1.40	59	5	4.105	59	20
1.47	37	15	4.53	37	45	1.40	60	10	4.09	60	25

Table 26.

Points for theoretical curves in fig.9
(from eqn.(34), $k_t/k_p^2 = 98, r_P = 0.25, r_M = 29$)

R	$\frac{1}{F}$ l.mol.$^{-1}$	t_c sec. resin G.	t_c sec. resin F.
2	0.17	429	731
1.33	0.19	635	1080
1.0	0.22	825	1405
0.67	0.28	1185	2020
0.50	0.33	1529	2600
0.33	0.44	2185	3720
0.25	0.56	2860	4860
0.20	0.67	3505	5970
0.14	0.89	4810	8180

Table 27.

Plot of t_c vs 1/F and R (experimental points) for figs. 9 and 10.

Run	R	1/F l.mol.$^{-1}$	t_c secs. resin F	t_c secs. resin G
F.22	2.0	0.17	600	-
G.2	1.25	0.20	-	525
F.2,18;G.4,22	1.0	0.22	1080	945
F.10;G.6	0.8	0.25	1710	1230
G.8,24	0.67	0.28	-	1760
F.4,14,16;G.10,12	0.5	0.33	3120	1800
F.12	0.4	0.39	3420	-
F.6,20;G.14	0.33	0.44	4020	2175
F.26	0.25	0.56	4560	-
F.24;G.16	0.20	0.67	5520	3195
G.20	0.15	0.85	-	4440

Table 28.

Log gel time vs 10^3/temp.°K for resins N & F (figure 11).

Run	$\log_{10} t_c$		10^3/temp.°K
	resin N	resin F	
F.30	-	1.3222	2.818
F.28	-	1.5682	2.899
F.6&20;N.12,60&62	0.8451	1.8261	2.985
N.14,22,58,24&26	0.9956	-	3.077
N.16 & 28	1.1461	-	3.125
N.18,20&30	1.2900	-	3.175
N.32	1.4393	-	3.225
N.34&36	1.8162	-	3.335

Table 29.

$\log_{10}$ (rate x 10^5) vs. 10^3/temp.°K. for MMA. (figure 12).

Run	$\log_{10}$(rate x 10^5)	10^3/temp.°K
M.16	2.1206	2.816
M.12	1.8222	2.899
M.4 & 10	1.5378	2.986
M.18	1.3892	3.028
M.6	1.2625	3.077
M.20	1.0682	3.125
M.8	0.8779	3.175

Table 30.

$\log_{10}$(rate x 10^5) vs. 10^3/temp.°K. for resins N and F (figure 13).

Run	$\log_{10}$(rate x 10^5)		10^3/temp.°K
	resin N	resin F	
F.30	-	2.2582	2.818
F.28,36	-	1.9112	2.899
F.42	-	1.7789	2.941
N12,60,62;F6,20,46	1.4624	1.5866	2.985
F.44	-	1.4433	3.031
N.14,22,24,26,58; F.32,34	1.0693	1.2519	3.077
N.16,28	0.8899	-	3.125
N.18,20,30;F.40	0.6794	0.9074	3.175
N.32	0.5447	-	3.225
F.38	-	0.6345	3.278
N.34,36	0.1769	-	3.335

Table 31.

% shrinkage P vs. reciprocal molar volume 1/Mv. Nickels & Flowers.[34]

	1/Mv	% shrinkage
Vinyl chloride.	0.0147	34.4
" bromide.	0.01414	28.7
Methacrylonitrile.	0.01193	27.0
MMA	0.00939	21.2
Vinyl acetate.	0.01083	20.9
Styrene	0.00872	14.5
Ethyl methacrylate.	0.00798	17.8
n-Propyl "	0.00704	15.0
n-Butyl "	0.006255	14.3
iso- " "	0.006255	12.9

Table 32.

Densities (gm/ml.) of individual cross-polymer film fragments at 300°K

Film fragment.	Density	Film fragment.	Density
D.1.1	1.2978	B.3.4	1.2539
2	1.2999	5	1.2941
3	1.2911	6	1.2758
4	1.2837	7	1.2627
5	1.2708	C.1.1	1.2562
6	1.2733	C.2.1	1.2470
D.2.1	1.2718	2	1.2429
2	1.2736	3	1.2432
3	1.2748	4	1.2373
4	1.2606	5	1.2365
5	1.2671	6	1.2325
B.1.1	1.2691	7	1.2324
2	1.2667	E.1.1	1.1981
3	1.2648	2	1.1975
4	1.2605	3	1.2033
5	1.2632	4	1.2023
6	1.2699	5	1.2011
7	1.2611	E.2.1	1.1938
8	1.2621	2	1.1973
B.2.1	1.2502	3	1.1980
2	1.2500	4	1.2019
3	1.2529	E.3.1	1.1982
B.3.1	1.2520	2	1.1977
2	1.2522	3	1.2029
3	1.2535	4	1.1940

Table 33.

Details of experimental points for fig.21.

Run	Time mins.	% Conversion	Run	Time mins.	% Conversion
N.20	8.5	0.276	N.40	53	8.16
"	12.5	0.398	"	58	9.11
"	19.5	0.617	"	63.5	10.23
"	24.5	0.813	"	71.5	11.95
"	29.5	1.036	"	79.5	13.96
"	34.5	1.266	N.44	3	0.84
"	44.5	1.752	"	6	1.69
"	64.5	2.887	"	8	2.23
"	84.5	4.287	"	10	2.81
"	114.5	6.727	"	11.5	3.24
"	144.5	9.917	"	13.5	3.80
N.40	10	1.42	"	16	4.68
"	20	3.01	"	18.75	5.59
"	30	4.53	"	20	6.15
"	40	5.75	"	24	7.82
"	44	6.67	"	32	12.04
"	47	7.16	"	36	14.7
"	50.5	7.80			

Table 34.

Detail of kink for run N.26, fig. 22.

Reading cm.	Time mins.	Reading cm.	Time mins.
59.578	15	59.168	21
59.542	15.5	59.125	21.5
59.515	16	59.090	22
59.477	16.5	59.050	22.5
59.447	17	59.011	23
59.378	18	58.970	23.5
59.344	18.5	58.927	24
59.310	19	58.886	24.5
59.245	20	58.852	25

Table 35.

Particulars of polymerised resin discs, figs. 27-30.

Run	Feed ratio	Reaction time hrs.	Density gm./ml.	% Conversion
M.24	0	7	1.1016	63.80
"	"	8.25	1.1579	81.01
"	"	9	1.1571	80.77
"	"	12	1.1773	86.79
"	"	15	1.1817	88.10
M.22	"	7	1.1347	73.7
"	"	10	1.1647	83.05
"	"	18	1.1810	87.89
"	"	24	1.1822	84.14
N.74	0.1	14	1.2130	87.2
N.72	1.75	1	1.2888	19.43
"	"	1.18	1.2970	22.04
"	"	1.5	1.3044	24.54
"	"	1.75	1.3103	26.19
"	"	2.0	1.3094	25.93
"	"	2.5	1.3156	27.84
"	"	3.5	1.3189	28.86
"	"	4.5	1.3200	29.18
"	"	5.5	1.3217	29.71
"	"	7.0	1.3202	29.23
N.70	0.5	2.5	1.1640	23.65
"	"	3.5	1.2499	51.73
"	"	3.75	1.2487	51.40
"	"	4.5	1.2579	54.16
"	"	5	1.2616	55.30
"	"	6	1.2711	58.11
"	"	7	1.2720	58.35
"	"	8	1.2762	59.58
"	"	9	1.2765	59.68
"	"	24	1.2871	62.77
N.68	0.2	4	1.1388	45.57
"	"	5	1.1802	59.14
"	"	6	1.2091	68.04
"	"	8	1.2212	71.66
"	"	9	1.2120	68.93
"	"	10	1.2192	71.08
"	"	12	1.2412	77.48
"	"	15	1.2341	75.45
"	"	18	1.2367	76.20
"	"	24	1.2339	75.40

Table 35 (contd.)

Run	Feed ratio	Reaction time hrs.	Density gm./ml.	% Conversion
N.64	1.0	1.33	1.2356	22.83
"	"	1.67	1.2463	26.32
"	"	2.0	1.2715	34.37
"	"	2.25	1.2787	36.65
"	"	2.50	1.2893	39.89
"	"	3.0	1.2955	41.76
"	"	4	1.3047	44.49
"	"	5	1.3049	44.60
"	"	6	1.3090	45.81
"	"	24	1.3138	47.17
N.62	1.25	1.25	1.2913	30.76
"	"	1.5	1.2943	31.27
"	"	2.0	1.3008	33.67
"	"	3.0	1.3054	35.12
"	"	4	1.3065	35.43
"	"	6.5	1.3094	36.32
"	"	8	1.3124	37.20
"	"	12	1.3100	36.47
"	"	24	1.3125	37.25
"	"	48	1.3106	36.68
